NTNU

Faculty of Engineering Science and Technology
DEPARTMENT OF PETROLEUM ENGINEERING
AND APPLIED GEOPHYSICS

An Experimental Study of Viscous Surfactant Flooding for Enhanced Oil Recovery

Master Thesis by
Olav Selle

Trondheim,
June 2005

NTNU
Norges teknisk-naturvitenskapelige universitet
Studieprogram i Geofag og petroleumsteknologi

Fakultet for ingeniørvitenskap og teknologi

MASTEROPPGAVEN

Kandidatens navn: OLAV SELLE

Oppgavens tittel: AN EXPERIMENTAL STUDY OF VISCOUS SURFACTANT FLOODING FOR ENHANCED OIL RECOVERY

Utfyllende tekst:

1.

2.

Studieretning: PETROLEUM ENGINEERING

Fagområde: RESERVOIR TECHNOLOGY

Tidsrom: 13.01.06 - 09.06.06

……

Faglærer

PREFACE

This Master Thesis has been carried out in cooperation with Statoil ASA. The Master Thesis is the fulfilment of 5 years of university studies. It is a requirement curricula counting for the whole study load in the spring semester of the 5. year for a Masters degree at NTNU. The Master Thesis work is carried out at the Formation Technical Laboratory in the F&T LPT BPL department at Statoil R&D Centre in Trondheim.

I would like to express my thanks to my two teaching supervisors, professor Ole Torsæter at NTNU, and Dr. Hans Kristian Kotlar at Statoil ASA. A project performing laboratory assignments will function at the laboratory's mercy. Most things can and will go wrong, and you need a strong support team to move forward. This project has also seen its share of challenges and I am therefore especially thankful to the whole Formation Technical Laboratory team at the Statoil R&D Centre. A special thanks goes to Laboratory Apprentice Johnny Kvakland Melbø, his optimism and ability to always lend a hand is much appreciated. Finally I would also like to thank all my fellow students at the Department of Petroleum Engineering and Applied Geophysics. Mutual encouragement and professional as well as social discussions has truly enriched my time as a student.

Trondheim, 09.06.2006

Olav Selle

ABSTRACT

This Master Thesis work aims to find a model system combining the positive effects of surfactant and polymer flooding to enhance oil recovery. This report presents the results of 12 core floods performed to enhance recovery of waterflood residual oil. The recovery is enhanced by a viscous surfactant flood consisting of one polymer to increase the viscosity, one surfactant for interfacial tension reduction, and one di-alcohol to function as co-surfactant and for salinity control.

The chemical treatment that gave the best result, gave an additional oil production normalized on OOIP of 20%, improving the oil recovery from 45 to 66% mostly by the means of mobility control. Pure viscosity floods gave an additional recovery of 12 to 13% of OOIP.

Novel technology is used to investigate environmental friendly enhanced oil recovery. A biopolymer made out of microfibrils from wooden material was for the first time ever to my knowledge, attempted used in a core flood to enhance oil recovery.

A viscous surfactant tertiary recovery process may help improve oil recoveries from many marginal oil fields or those that face shut-down due to uneconomic operating costs, but still contain significant amounts of oil.

CONTENT

1 INTRODUCTION

The use of crude oil plays an important role in the world economy today. The International Energy Agency states that petroleum products still will be the world's most important source of energy for the next 30 years. The worlds demand for energy will increase by 50 percent the next 25 years. The production rates of the 100 largest oilfields in the world are all declining from plateau production[1]. When a typical oil reservoir reaches its economic limit after primary and secondary recovery (water flooding) more than two-thirds of the original oil is left in place[2]. The challenge is to develop Enhanced Oil Recovery (EOR) methods that ensure an economical tail end production from these fields.

Waterflooding leaves the residual oil capillary trapped. Surfactant injection can mobilize this residual oil by a strong reduction in the interfacial tension between oil and water as illustrated in **Figure 1**. In the top most part of the figure the droplet is capillary trapped, while it in the bottom part has been mobilized due to a reduction in the interfacial tension (IFT) caused by a surfactant.

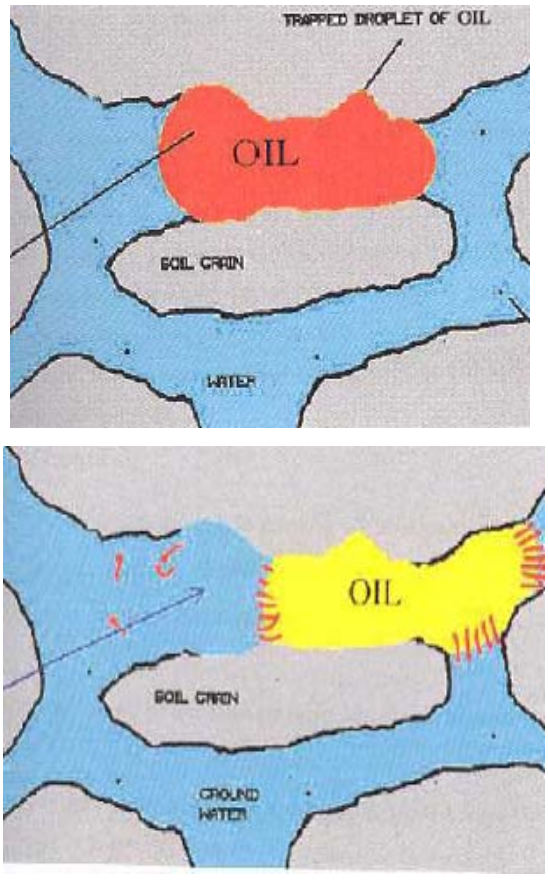

Figure 1. Illustration of capillary trapped droplet, before and after mobilization by surfactants[2].

The use of surfactants, and especially bio-surfactants, can provide a cheap and simple tertiary oil recovery method, especially if a combination of low IFT and viscosity can be obtained. Bio-surfactants can be generated within oil reservoirs by bacteria that grow in saline and anaerobic conditions. Development of a simple surfactant EOR method can be especially beneficial for small fields with high water cuts. Low cost waterfloods and other recovery projects where low oil flow rate is accompanied by high water cuts will by a small increase in oil production easily provide an increase in profitability.

Today's oil price is very high. This gives an increased interest and better economics for EOR-concepts. There is now a trend in the business that companies again are doing research and development on surfactants[3]. Surfactants are traditionally expensive and the handling of large volumes of chemicals offshore is logistically troublesome, so practically only a small portion of the reservoir pore volume can be injected with surfactant solution. Therefore it is important to develop low cost and low concentration surfactants. On the Norwegian Continental Shelf it is a demand from this year on, 2006, to use chemicals that are not harmful to the environment. That means that the environmental properties should be classified as category green or yellow. The utilization of viscous surfactants can be one way to achieve this.

This thesis work aims to find a model system combining the positive effects of surfactant and polymer flooding to enhance oil recovery. McInerney et.al[18, 19] of the University of Oklahoma has a very promising system with bio-surfactants for EOR which has been an inspiration and guidance to this work. To relate the experiments to field conditions, it was decided to work towards the Heidrun Tilje formation offshore Mid-Norway. Heidrun is a heavily faulted sandstone reservoir, where Tilje is a low recovery formation of coastal marine and inter-tidal depositions of low permeabilities averaging less than 100 md[4]. The reservoir is slightly water wetting[5]. Stratigraphic and facies associations for the geology in the Haltenbanken area are attached in **Appendix B.** There is also an ongoing Statoil project aiming at understanding the biodiversity at Heidrun to further explore the possibility of utilizing bio-surfactants. The polymers used in the project are specially designed for the Heidrun Tilje formation water. This project has specially ordered the polymers from the French company SNF Floerger. Literature theory points out positive synergetic effects of short-chained alcohols used in surfactant flooding and the co-surfactant di-alcohols used are chosen according to this.

2 LITERATURE STUDY

2.1 ENHANCED OIL RECOVERY

The third stage of hydrocarbon production where more sophisticated techniques are used is called enhanced oil recovery (EOR). The main disadvantage of all primary oil recovery methods is a decrease in reservoir pressure which leads to the development of a solution gas drive, resulting in low oil production rates and oil recovery. Even a natural water drive is normally not sufficient to maintain pressure, and therefore many fields are supported by water or gas injection. By gas injection one usually means hydrocarbon or not-miscible carbon dioxide injection. Waterflooding, using seawater, has been the most frequently applied technique in the North Sea reservoirs. Often waterflooding is not enough to yield a good recovery, mainly for the following reasons[6]:

- reservoir heterogeneity
- problems related to the well siting and spacing
- unfavourable mobility ratio between the displacing (water, gas) and displaced (oil) fluids

These reasons yields low volumetric sweep efficiency. Other factors leading to insufficient recovery are the displacement efficiency of water and the differences in densities of the displacing (water, gas) and displaced (oil) fluids.

The purpose of EOR is not only to restore formation pressure, but also to improve oil displacement or fluid flow in the reservoir. The three major types of enhanced oil recovery operations are chemical flooding (polymer, surfactant or alkaline floods), miscible displacement (carbon dioxide [CO_2] injection or hydrocarbon injection), and thermal recovery (steamflood or *in-situ* combustion). The optimal application of each type depends on reservoir temperature, pressure, depth, net pay, permeability, residual oil and water saturations, porosity and fluid properties such as oil density and viscosity.

2.2 SURFACTANT FLOODING THEORY

When a surfactant solution has been injected, the trapped oil droplets are mobilized due to a reduction in the interfacial tension (IFT) between oil and water. Due to coalescence of these drops there will be a local increase in oil saturation and an oil bank is generated. The oil bank

will start to flow and mobilize any residual oil in front of the bank. Re-trapping of the oil bank is prevented by the surfactant slug flowing behind. The movement of the oil bank is dependent on the viscosity of the surfactant slug. The interfacial tension, the viscosity and the volume of the surfactant solution behind the oil bank will therefore be of importance for the final residual oil saturation[7].

The oil saturation will be reduced by liberating the capillary-trapped oil. To overcome the capillary forces, the pressure drop across the trapped oil has to be larger than the capillary pressure. A large enough IFT reduction will provide such a pressure drop. A large number of studies have shown that the residual oil saturations correlates to a ratio known as the capillary number, Nc[6]. The capillary number is the dimensionless ratio between the viscous and the capillary forces and has numerous representations. In this report the following will be used,

$$N_C = \frac{u \times \mu}{\sigma}$$

where u is the Darcy velocity, μ the viscosity of the displacing fluid and σ is the interfacial tension between the oil and surfactant solution[8]. A large capillary number means less residual oil. In order to achieve that, both a decrease in the interfacial tension and an increase of the viscosity or the velocity will be beneficial. **Figure 2** shows a typical plot of residual oil saturation as a function of N_C called the Capillary Desaturation Curve (CDC). The CDC's will depend upon pore-size distribution and wettabilities. As seen from **Figure 3** a surfactant flood should perform best in a water-wet reservoir.

The IFT between the oil and water during waterflooding is in the range of 10^1 to 10^0 mN/m. The use of proper surfactant can lower the IFT to 10^{-2} mN/m or less, which increases the capillary number. The capillary number during waterflooding is approximately 10^{-6}. By the use of surfactants lowering the IFT, the Nc can be increased at least two or three orders of magnitude.

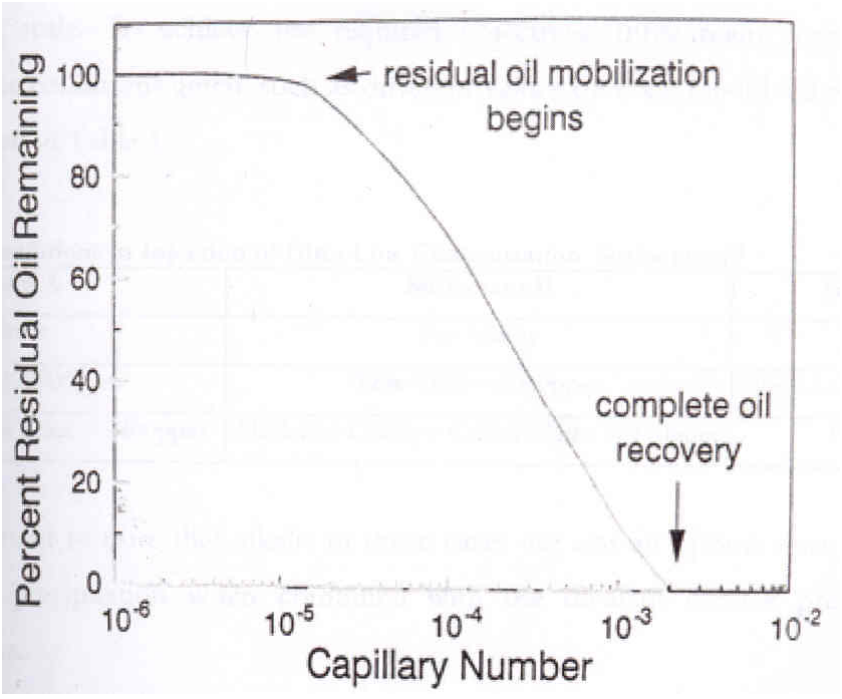

Figure 2. Typical plot of capillary number versus residual oil saturation[6].

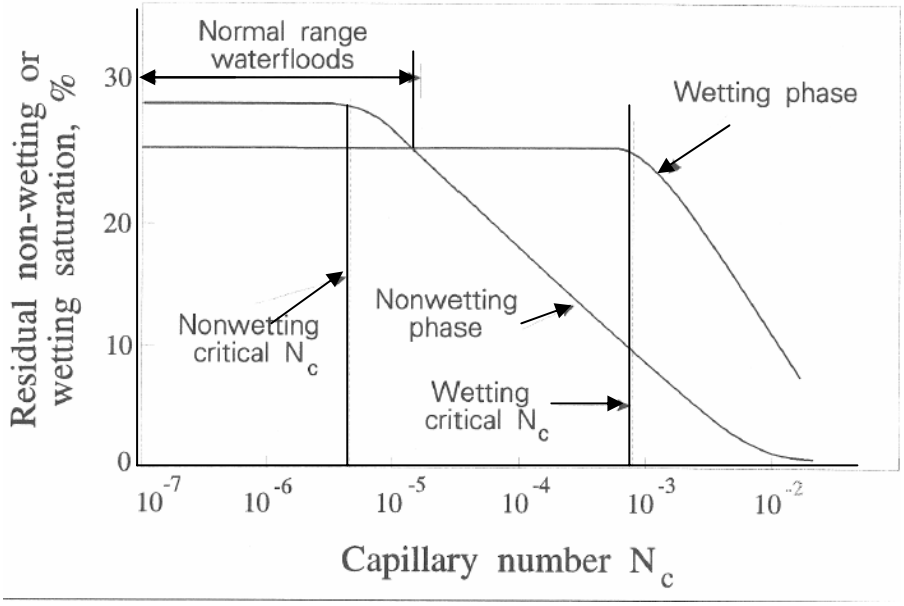

Figure 3. Schematic Capillary Desaturation Curve with respect to wettabilities[9].

2.2.1 Surfactants

The term surfactant is a contraction of "**Surf**ace **act**ive **a**ge**nt**"[10]. Surfactants reduce the interfacial tension between oil and water by adsorbing at the liquid-liquid interface.
They are usually organic compounds that are amphipathic, meaning they contain both hydrophobic groups (their "tails") and hydrophilic groups (their "heads"). Therefore, they are typically soluble in both organic solvents and water. **Figure 4** shows a typical surfactant.

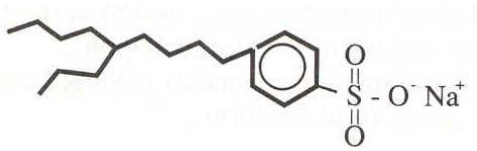

Figure 4. Anionic surfactant[8].

The surfactants will orient on the liquid-liquid interface with the hydrophilic part in the water phase and the hydrophobic part in the oil phase as shown in **Figure 5**. The surfactant will act as a bridging agent making the transition between the two phases less abrupt. Thus the demand for energy to bring a molecule to the interface is reduced, and the systems surface free energy - that is Gibb's free energy, and in principal the same as the interfacial tension - is reduced[11].

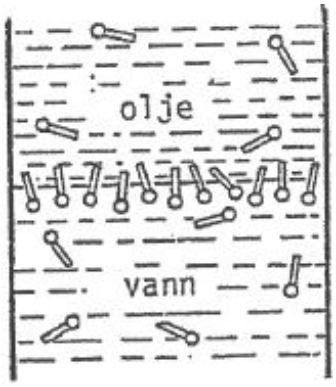

Figure 5. Adsorpsion by surface active agents on the interface between oil and water[11].
Translation of text in figure: "olje" means oil, and "vann" means water.

The ability of surfactants to reduce IFT depends on various factors that have to be met if the surfactant treatment should have an effect. Conditions met during lab tests are often far from those in the reservoir. Salinity and hardness of brine are the most important factors affecting

the surfactants ability to reduce IFT. The other effect of great importance is adsorption of surfactant by the reservoir rock, an effect which is greater at reservoir conditions than observed in the lab[6]. This effect is very much dependent on the surfactant type (chemistry) and the mineralogy of the rock.

The brine salinity controls the type of emulsion phase system generated by a typical surfactant. There are three types of phase systems; II(-), III, II(+). **Figure 6** shows the correlation between brine salinity, interfacial tension and phase system.

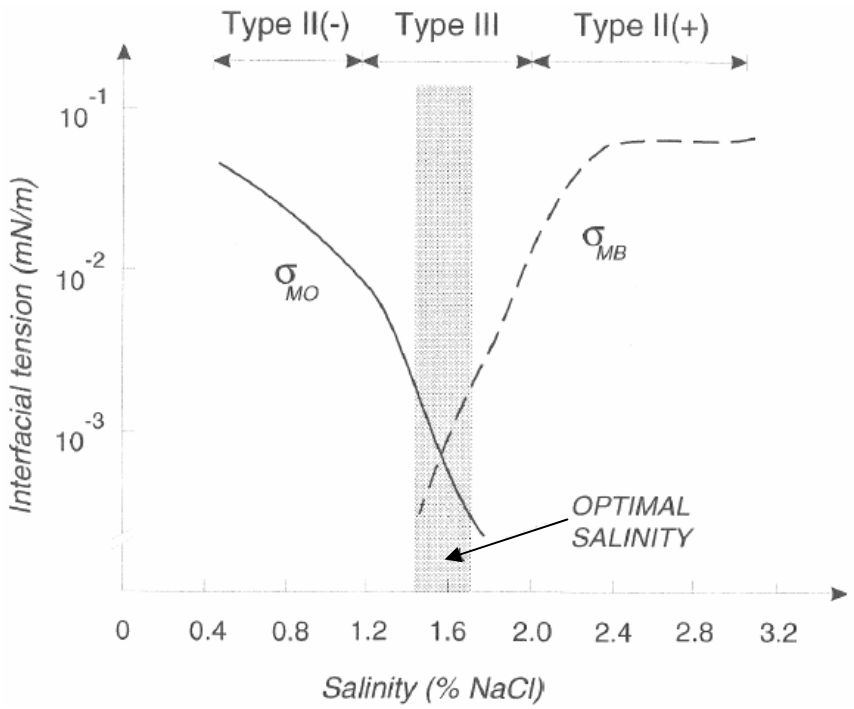

Figure 6. Interfacial tension versus brine salinity[6].

By increasing concentration of surfactant, the formation of micelles will occur when the critical micelle concentration (CMC) is reached. A micelle is a liquid particle (typically droplet-like), stabilized in another liquid by surfactant molecules. In the non-polar interior of such micelles, organic molecules can be solubilized. Since the CMC is small, the surfactant is predominately in micelle form, as opposed to monomers, at nearly all practical concentrations. The most efficient reduction of IFT will occur at the CMC, this is due to the fact that only monomers contribute to the IFT reduction. At CMC point the surfactant monomers presented in the emulsion have the highest possible concentration thus reducing

the IFT most. A further increae in concentration will only result in an increased number of micelles[6,7,8,10].

2.2.2 Type II(-) system

In a II(-) phase system only two phases can form near the oil-brine boundary. At low brine salinity a typical surfactant have a good solubility in the aqueous phase and poor solubility in the oleic phase. Near the interface there will be an excess oil phase and a (water external) emulsion phase containing brine, surfactant and some solubilized oil as shown in **Figure 7.** The solubilized oil is placed inside the micelles.

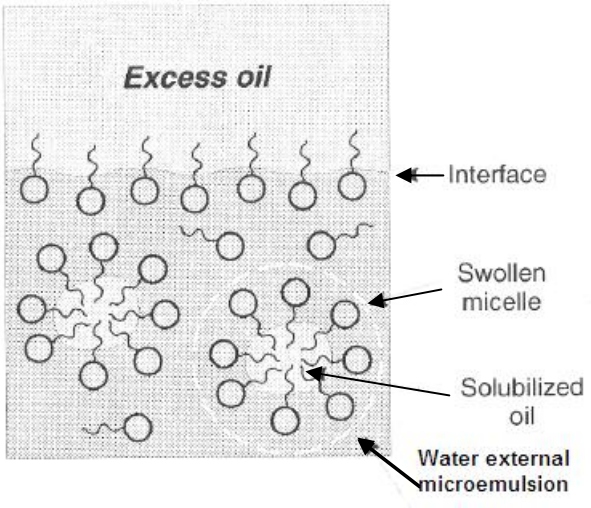

Figure 7. Type II(-) system in surfactant oil-brine environment[6].

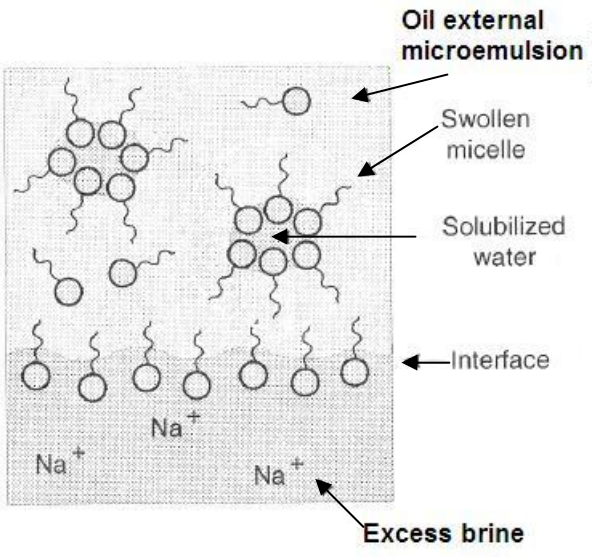

Figure 8. Type II(+) system in surfactant oil-brine environment[6].

2.2.3 Type II(+) system

In a II(+) phase system only two phases can form near the oil-brine boundary. At high brine salinity, electrostatic forces of the brine drastically reduce the surfactant solubility in the aqueous phase. Near the interface there will be an excess brine phase and a (oil external) emulsion phase containing surfactant with some solubilized brine as shown in **Figure 8**.

2.2.4 Type III system

At intermediate salinities a third surfactant-rich phase can form. There will be an excess oil and an excess brine phase, in addition a emulsion phase with equal amounts of solubilized oil and brine in micelles respectively. See **Figure 9** for sketch. The type III system has two IFTs; between the oil and emulsion and between the emulsion and brine as seen in **Figure 6**. This phase environment gives the lowest IFTs and is the most attractive for oil recovery by surfactant flooding[6].

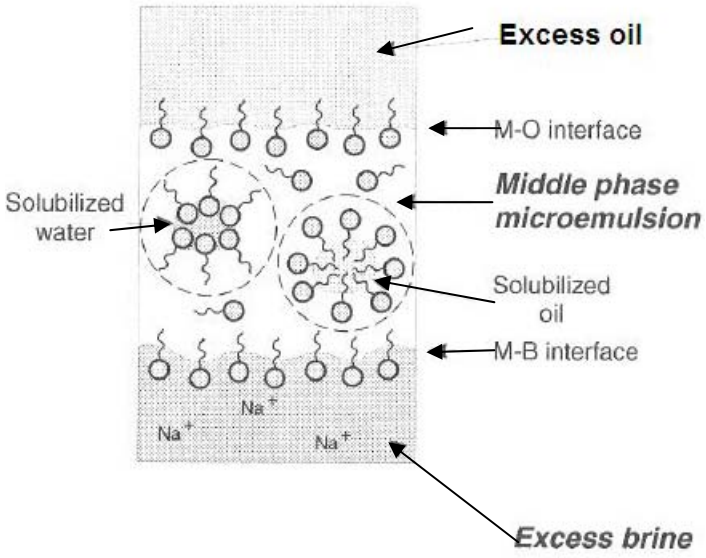

Figure 9. Type III system in surfactant oil-brine environment[6].

2.2.5 Surfactant design

It is possible to design surfactants for specific conditions. Optimal salinity of the surfactant system should be as close to the brine salinity in question as possible. By adjusting the length

and branching of the hydrophobic tail of the surfactant it is possible to achieve efficiency at a certain salinity. The longer the hydrophobic tail, the more of the surfactant molecule will orient in the oleic phase and the system will go from type II(-) to III to II(+). Such an alteration will affect the solubility and the robustness of the system. Compromises have to be made because it is very important that the system is robust, meaning that the III phase region is wide enough for the given reservoir system. Co-surfactants, as short-chained alcohols (C_3-C_5), are often added to enhance solubility and reduce the effect of salinity[8]. Since alcohols too are polar molecules they will also contribute in reducing the IFT.

Surfactants are classified in two ways, by their polarities and by the ratio between the length of their hydrophobic (the same as lipophilic) tail and their hydrophilic head – hydrophilic/lipophilic balance, HLB.

Polar characterization[6,7].

- **anionics** are most used in oil recovery since they are soluble in the aqueous phase, efficiently reduce IFT, relatively resistant to retention, stable and not expensive. In **Figure 4** there is a sketch of an anionic surfactant
- **cationics** have little use due to high adsorption by the anionic surfaces of interstitial clays
- **non-ionics** are mainly used as co-surfactants
- **amphoterics** have not been used in oil recovery

2.2.6 Surfactant retention

Surfactant retention causes a drastic reduction in the concentration of surfactants in solution, and therefore essentially decreases their ability to reduce IFT. Various surfactant retention mechanisms have been identified as: precipitation of negatively charged surfactants and multivalent cations, phase trapping of the surfactant in the oil phase, and adsorption of surfactant on the rock interface. It is today technically possible to prevent loss of surfactants due to precipitation and phase trapping[8]. This is achieved by utilizing salt tolerant surfactants and being confident that changes in parameters (salt, hardness, pressure, temperature, co-surfactant, etc.) influencing phase behaviour only take place within acceptable limits.

Adsorption on the reservoir rock surface is an extremely negative effect, except in the case of oil-wet reservoir rock. Then adsorption will give a positive effect by changing the wettability preference of the rock to less oil-wet, but still surfactant retention will take place. Very often adsorption of surfactants at the solid/liquid interface is initiated by electrostatic interaction between the solid and the surfactant. At reservoir pH-value (about 5) of the brine, most of the reservoir minerals (quartz, kaolinite, etc.) show a net negative charge. In order to lower the adsorption, negatively charged surfactants are usually considered as the main surfactant species of the slug.

Observations yield[8]:

- branching of the surfactant tail has been found to decrease adsorption
- general, anionic surfactants increase adsorption by increased salinity
- decreasing pH will increase the number of positively charged sites on the surface, leading to increased adsorption of negatively charged surfactants
- adsorption of non-ionic surfactants increases as temperature increases
- adsorption of anionic surfactant on oil-wet surface is greater than adsorption on water-wet surface
- the rate and extension of adsorption is a function of the properties of the clay minerals and the oil saturation
- mixtures of anionic and non-ionic surfactants often show increased adsorption compared to a pure anionic surfactant
- mixtures of two different anionic surfactants often show decreased adsorption compared to a pure anionic surfactant

The following scheme is often used today to prevent adsorption and increase the technological effect[6]:

- preflush is used to form the best conditions for the effective reduction of IFT. Even though field experience has shown that preflushes often not are effective in controlling brine salinity and divalent-ion content. Thus, a surfactant flood generally must be designed to tolerate resident brine[7]
- surfactant slug injection to recover residual oil
- polymer slug injection in order to improve sweep efficiency

- taper – injection of polymer slug with a gradually decreasing concentration of the polymer from maximum at the front to zero at the back in order to reduce the effect of unfavourable mobility ratio between the taper and chase water
- chase water is used to move the injected volumes deep into the reservoir

2.3 VISCOUS SURFACTANT FLOODING

2.3.1 Mobility control

During a standard waterflood the sweep efficiency achieved is usually not as good as desired. A fingering effect of the water flooding into the oil bank or surfactant slug as can be seen in **Figure 10** is a usual problem. At the top (a), water is fingering into the oil bank. At the bottom (b) the use of a polymer has reduced the effect of fingering significantly. By avoiding fingering and achieving piston-like displacement the volumetric sweep can be improved.

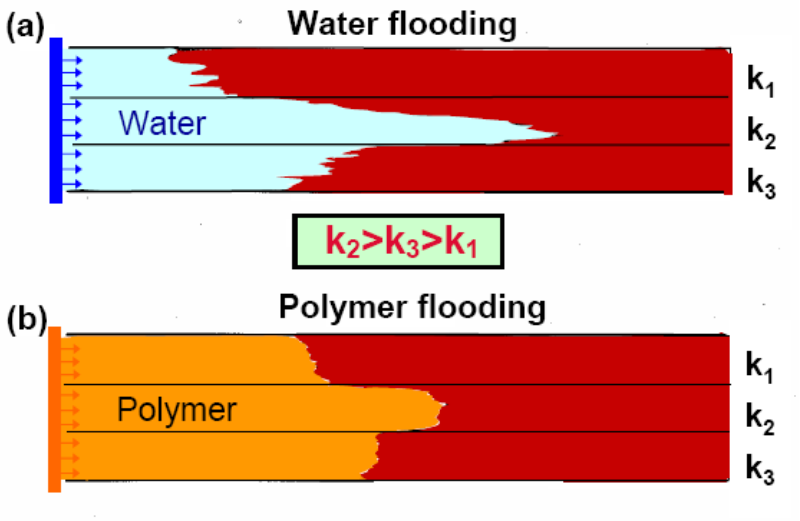

Figure 10. (a) Fingering into the oil bank. (b) Fingering reduced by injection of polymer[12].

Therefore polymer often is added to the surfactant solution to increase its apparent viscosity giving potential to increase both volumetric sweep efficiency and microscopic displacement efficiency.

Polymer is a term used to describe a very long molecule consisting of structural units and repeating units connected by covalent chemical bonds. The term is derived from the Greek words: *polys* meaning *many*, and *meros* meaning *parts*. The key feature that distinguishes

polymers from other molecules is the repetition of many identical, similar, or complementary molecular subunits in these chains. These subunits, the monomers, are small molecules of low to moderate molecular weight, that are linked to each other during a chemical reaction called polymerization[10].

When the residual oil saturation decreases, one should expect an increase in the relative permeability to water, simply because water will flow easier due to less oil. In a surfactant flood, the mobility of the injected solution therefore will increase as IFT and residual oil decreases. The total mobility of oil and water ahead of the surfactant is determined by the oil-bank saturation. It is usually less than the total mobility ahead of the initial waterfront[8]. With the mobility of the displacing phase increasing and the mobility of the displaced phase decreasing, one should expect a large increase in mobility ratio going from water flooding to surfactant flooding. The piston displacement condition states that the mobility ratio between the displacing and displaced fluid must be less or equal to unity to achieve an ideal displacement,

$$M = \frac{\lambda_{displacing}}{\lambda_{displaced}} \leq 1 .$$

Piston displacement condition[13]

Where: $\lambda_{displacing}$ = mobility of the displacing fluid = k'_{rd} / μ_d ,
$\lambda_{displaced\ (oil)}$ = mobility of the displaced fluid = k'_{ro} / μ_o.

The easiest parameter to alter is the viscosity of the displacing fluid, and as seen from the ratio, an increase of displacing fluid viscosity will lower the mobility ratio.

2.3.2 Polymer flooding

During flooding in porous media it is of great importance to have good volumetric sweep efficiency. Polymers to increase viscosity are used as an EOR method either as polymer on its own or in combinations with for example surfactants. Usually, a water soluble polymer is added to the injected water to increase the viscosity. A polymer flood is not intended to

reduce the residual oil saturation, $S_{OR,}$ but is an efficient and quick way to reach S_{OR}. Historically the opinion was that a polymer can only increase the volumetric sweep but not the displacement efficiency[9]. However, field practice has shown that polymer flooding can increase recovery by more than 12% OOIP, and that its production costs are comparable to that of water flooding[14].

Viscosity can be increased by adding mainly two types of polymers[15, 16]:

1. **Polyacrylamides**: are synthetic polymers and their performance depends on the molecular weight and degree of hydrolysis. When partially hydrolyzed, some of the acryl amide is replaced by, or converted into acrylic acid. This tends to increase the viscosity of fresh water, but reduces the viscosity of hard waters. Polyacrylamides can absorb many times its own mass in water while, ionic substances like salt cause the polymer to release some of its waters.

Advantages/disadvantages: They are relatively cheap, develop good viscosities in fresh water, and adsorb on the rock surface to give a long-term permeability reduction. The main disadvantages are their tendency to shear degradation at high flow rates, and their poor performance in high salinity brine.

2. **Biopolymers**: are originated from biological systems. Many of them are products of a bacteria strain. For instance, the most common type is a polysaccharide biopolymer known as Xanthan[20]. Biopolymers used for EOR purposes usually have smaller molecular weight than the polyacrylamides. The biopolymers excellent viscosifying abilities in high saline waters are caused by their great molecular stiffness. However, they have less viscosifying abilities than polyacrylamides in fresh water.

Advantages/disadvantages: They have good viscosifying ability in high salinity water and good resistance to shear degradation. Also, some of them show little retardation on the rock surface and thus more easily propagate into the formation than polyacrylamides. This can reduce the amount of polymer required for a flood.

As a rule of thumb, the higher the polymer molecular weight, the higher the viscosity of the polymer solution, the more permeability is reduced and the better the recovery. But if the molecular weight is too high, the polymer may plug the formation pore space.

Key parameters in polymer flooding:

- mobility ratio
- permeability
- effective porosity
- mobile oil saturation
- initial water saturation
- reservoir depth (temperature)
- depletion stage
- rock minerals
- water salinity

Choosing the correct polymer based on the key parameters above must lead to a polymer that is:

- injectable into the reservoir
- abel to move through the reservoir and provide the required viscosity

On condition of the same amount of polymer injected, the more heterogeneous the reservoir is, the better the displacement results with a polymer slug of high concentration compared to that of low concentration[17]. Polymer stability is subjected to mechanical degradation as well as salinity and temperature. They are also vulnerable to bacterial attack in low-temperature regions of the reservoir, which is up to 90ºC. Because of high salinity and temperature it has been challenging to find good polymers for use offshore Norway.

2.3.3 Viscous surfactant flooding

In earlier formulations of surfactant slugs, polymers were typically not added directly to a surfactant solution. The concern was that dispersion might cause mixing at the surfactant – polymer slug interface. Mixing could effect phase behaviour and IFT negatively, and by that

influence the EOR performance. These effects have been investigated and it is shown that polymer can be added to a surfactant slug under controlled conditions to increase slug viscosity without negatively altering phase behaviour or IFT. However, some anionic surfactants are reported to precipitate in the presence of partially hydrolyzed polyacrylamid[7]. Today polymers are added to the surfactant solution for the purpose of mobility control.

A combination of polymer for mobility control, alcohol for enhanced solubility and reduced effect of salinity, and surfactant to lower the IFT will according to the theory of the previous chapters have a good effect as a tertiary oil recovery method. Such a system utilizing very low surfactant concentrations has been thoroughly studied in the laboratory by McInerney et.al.[19,19]. They have come up with a mixture of a polymer, an alcohol and a bio-surfactant produced by bacteria found *in-situ* in oil reservoirs. This combination is studied in several experiments, both on flooding sand packs and on core floods using Berea sandstone cores. The system recovers between twenty and eighty percent of the residual oil dependent on bio-surfactant concentration. The main mechanism is the IFT reduction provided by the bio-surfactant. It is shown that the bio-surfactant requires a co-surfactant (alcohol) and a viscosity modifier to recover oil from saline environment. By themselves, a combination of alcohol and polymer recovers up to ten percent of residual oil through improved sweep and recovery efficiency. The relationship observed between residual oil recovered and bio-surfactant concentration is approximately linear going down to a minimum concentration of 10-15 ppm bio-surfactant to recover oil by IFT reduction[18, 19]. **Table 1** gives core flood data of relevance to this Master Thesis. The first 8 core flood data are given by McINerney et.al.[19]. The last 4 core flood data are found in "An Experimental Pre-study of Bio-surfactants for Enhanced Oil Recovery"[36].

Table 1. Results from surfactant, polymer and di-alcohol core floods relevant to this Master Thesis.

Core	Kabs	PV	Sor,w	Surfactant	Recovery
	md	cc	%	PV	%
1	108.0	31.5	39.0	1.0	13.8
2	72.0	32.0	35.3	1.0	15.9
3	72.2	32.0	35.6	1.0	8.8
4	68.7	30.0	40.0	1.0	9.6
5	60.9	31.8	39.6	1.0	10.3
6	122.9	32.5	39.4	1.0	13.3

7	103.0	31.0	36.8	2.0	20.2
8	240.0	33.0	36.1	1.0	9.7
1	172	18.4	48.8	-	11.4
2	134	18.2	44.0	-	13.5
3	157	18.2	44.8	-	12.7
4	144	18.2	49.7	2.0	12.3

2.3.4 Environmental friendly viscous surfactant flooding

The focus on environmental friendly chemicals in the industry continues to grow. Offshore chemicals are in Norway under strict regulations by the government. Much research is aimed at finding new effective chemicals to solve production challenges and enhance oil recovery. A growing activity on bio-surfactants to enhance oil recovery is taking place in Trondheim. Bacteria, either injected or *in-situ* the reservoir, can produce surfactants under the right stimuli. As shown by McInerney et.al. certain bacteria can also produce di-alcohols[18]. To obtain what is sometimes referred to as a white system, meaning a complete system entirely consisting of biodegradable environmental friendly ingredients, there is a need for a biopolymer. In the late 80-ties, Statoil was involved in a large project with a biopolymer called Xanthan. It is a polysaccharide secreted by the bacteria *Xanthomonas campestris*. It is an anionic polymer with tolerance for salinity and fair tolerance for hardness ions. Temperature tolerance varies with water-phase components, but starts to degrade around 93 to 121ºC. It is susceptible to bacterial attack and does not tolerate extreme pH[20]. Even though very promising, Xanthan was found not profitable at that time[21].

One of the possible new areas of application for debris from the paper and pulp industry can be biopolymers. Three kinds of polymers are present in wood: cellulose, hemicelluloses and lignin. Cellulose is the framework polymer, comprising 40-50% of wood, whereas hemicelluloses and lignin are the matrix substances present between cellulose microfibrils.

Cellulose microfibrils constitute layers (lamellas) which form the cellulose fibre as can be seen in **Figure 11**. The microfibrils consist of 20-100 cellulose chains organised more or less in parallel. The degree of parallel orientation of the cellulose chains is termed crystallinity. The cellulose chains consist of 5-10 000 glucose monomer units which give the microfibrils a

high aspect ratio (length/diameter =L/D). The microfibrils are 1-50 nm thick and may have an aspect ratio of more than 100.

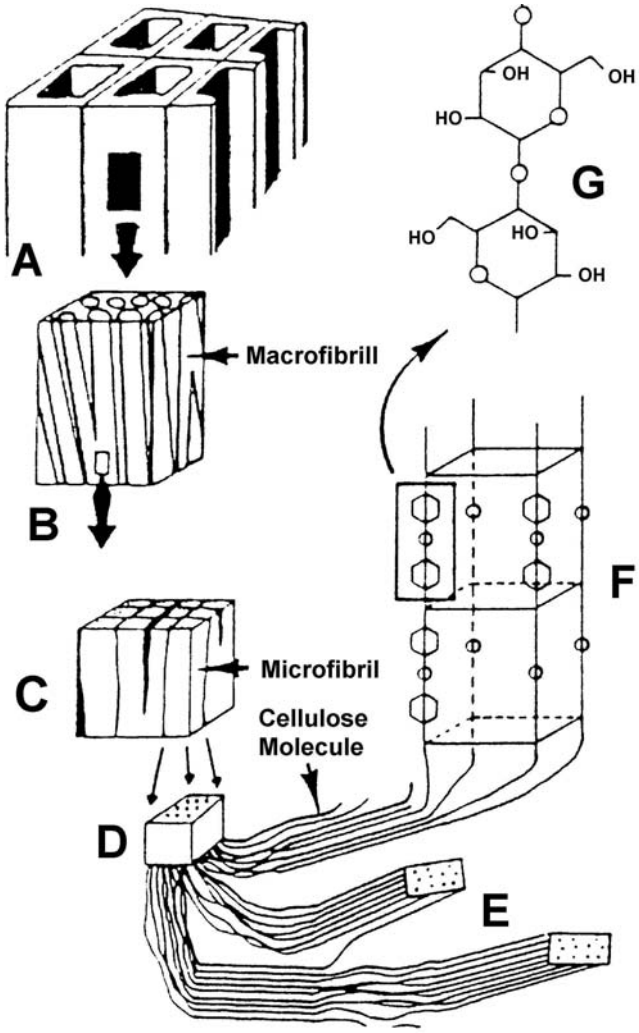

Figure 11. Fibres, microfibrils and polymers are the three structural cellulose components in wood[22].
A: Wood structure, B: Macrofibrils, C: Bundle of microfibrils, D: Single microfibril, E: Crystallite cellulose, F: Crystallite cellulose cell, G: Repeating cellulose unit.

Wood fibres consist of polymers synthesized by nature with many beneficial properties. They are generally strong, hydrophilic, and insoluble in water, stable to chemicals, generally recognized as safe to living creatures, renewable, recyclable, biodegradable, and easily available[22].

Another interesting biopolymer for further investigations called Chitosan is made out of prawn peel.

2.4 LABORATORY PARAMETERS

Standard laboratory parameters as density, viscosity, IFT, water content, porosity and permeability are all concepts that form the working day for reservoir lab personnel. These physical properties are important in understanding the experimental systems and have been vital to this project.

2.4.1 Interfacial tension

Interfacial tension (σ) of fluids results from molecular properties occurring at the surface or interface. The energy barrier produced by interfacial tension prevents one liquid from becoming emulsified into the other. The dimension of interfacial tension is mN/m. In this report interfacial tensions are measured by to different instruments. The KSV Sigma 701 Tensiometer applies the ring method and was performed at Statoil R&D Centre Laboratories. The measuring range is 0-500 mN/m and the resolution is 1 μN[23]. However it is stated from Statoil laboratory personnel that readings under 10 mN/m are influenced by a high uncertainty. The pedant drop method is also applied with the KSV Cam 200 goniometer, performed at the Department of Petroleum Engineering and Applied Geophysics Laboratory at NTNU. The measuring range is 0.01 - 999 mN/m, and the inaccuracy is $\pm$ 0.01 mN/m[24].

Measuring principle ring method (Du Noüy method):

To measure the interfacial tension, a platinum ring is placed in the interface between the two test liquids. The force necessary to break the interfacial film with the ring is recorded. This is though an apparent value and has to be corrected by a correction factor.

Measuring principle pedant drop method:

One can determine the interfacial tension optically from measurements of the shape of a pendant drop of one fluid, formed in the other fluid. Pictures of the drop are taken, and the IFT is calculated based on the drop geometry.

2.4.2 Viscosity

Viscosity (μ) is defined as the internal resistance of fluid to flow. It varies with pressure and temperature, rather sensitive to changes in temperature, but relatively insensitive to pressure until rather high pressures have been attained. The dimension of dynamic viscosity is Pas = $Ns/m^2 = 10^3$ cp. The viscosity is often measured as kinematic viscosity (ν), the ratio of $\mu/\rho = \nu$. Oil viscosity is measured by both by a SVM 3000 Anton Paar viscometer and a Paar Physica UDS 200 Rheometer. The various water and polymer viscosities are measured by a capillary viscometer, the SVM 3000 Anton Paar viscometer and the Paar Physica UDS 200 Rheometer.

Measuring principle Ubbelohde capillary viscometer from SCHOTT-GERÄTE:
The viscosity is found by measuring the time it takes the sample to flow through a given capillary tube. The viscosity is then calculated by the following formula[25];

$$\mu = \rho * (t - y) * K ,$$

where ρ is the density, t is the flow time, y is the correction in time inherent in the Hagenbach Correction Factor and K is the Ubbelohde specific constant. The liquid temperature is kept constant by immersing the glass capillary tube in a temperature-controlled water bath. Temperature is regulated by HART Temperature Controller 2100 and measured by HART Tweener 1675. During previous testing, test results show that the bath holds a stable temperature within ± 0.04°C[26, 27].

Measuring principle SVM 3000 viscometer from Anton Paar:
The measuring cell is in principle a tube fitted with a magnet inside. When the tube starts to rotate, the sensors register the frictional forces under which the tube is influenced by the fluid. This is recalculated into dynamic viscosity. The SVM 3000 has a measuring range of 0.2–20000 mPas, reproducibility of ± 0.35% and repeatability of 0.1%. The temperature range is –56 to 100°C, temperature accuracy of ± 0.02°C and the test volume is approximately 2.5 cm^3.

Measuring principle Paar Physica UDS 200 Rheometer:
UDS stands for Universal Dynamic Spectrometer. The Paar Physica UDS 200 is a rotational rheometer that can be used to measure shear viscosity, viscoelastic functions, creep, and yield stress of materials using different geometries such as cone-and-plate, parallel-plate, and

concentric cylinder. Tests can be performed under controlled "shear rate" (0.0001 to 5000 1/s, geometry dependent) or controlled "stress" (0.002 mNm - 150 mNm). Where shear rate is the gradient of the velocity vector perpendicular to the flow. Temperature is controlled between room temperature and 300ºC[28]. When utilizing the correct measuring geometries the UDS 200 can operate in a viscosity range of $0.5*10^{-3}$ to $8.5*10^{8}$ Pas[29]. The Paar Physica UDS 200 can be used with several different measuring geometries. The measuring geometry used is called double-gap. This geometry limits the effect of turbulence for low-viscosity samples sheared at high rates. The double-gap utilizes a rotor which is shaped like an inverted cup which fits over a cylinder centred on the bottom cup as shown in **Figure 12**[30].

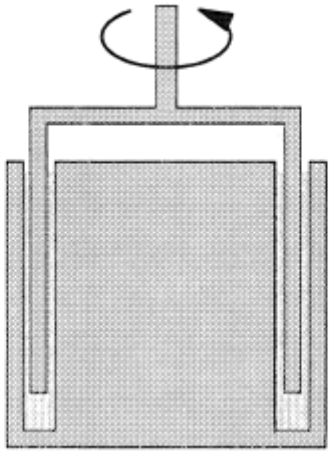

Figure 12. Schematic diagram of double-gap concentric cylinder geometry[31]

2.4.3 Permeability

Permeability (k) is a property of the porous medium and it is a measure for the capacity of the medium to transmit fluids. The dimension of permeability is Darcy (D), or m^2 ($\approx 10^{12}$ D) in the SI system. Permeability is governed by Darcy's law,

$$\frac{q}{A} = u = \frac{k}{\mu}\frac{\Delta P}{L},$$

where q is volumetric rate, A cross-sectional area, u flow velocity, k permeability, μ fluid viscosity, ΔP pressure gradient in the distance L. In this report permeabilities are based upon measurements of ΔP during flooding.

Measuring principle:

A core is placed in a core holder similar to the one shown in **Figure 13**. Confining pressure of 50 bara is applied on the rubber sleeve and formation water is flooded through the core at different rates while measuring the corresponding ΔP. This yields the permeability:

$$k = \frac{q \times \mu}{A} \frac{L}{\Delta P}.$$

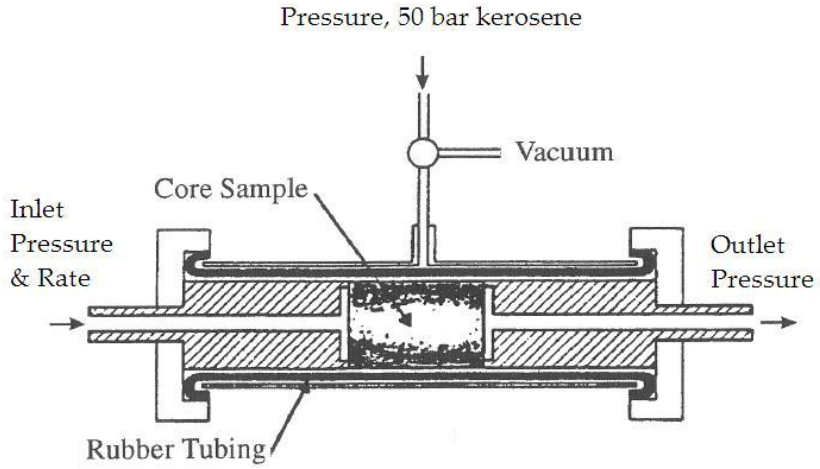

Figure 13. Schematic diagram of core holder, sketch modified to fit with conditions[32]

2.4.4 Porosity

Porosity is a measure of storage capacity of a reservoir, defined as the ratio of pore volume to bulk volume

$$\varphi = \frac{Vp}{Vb},$$

where φ is the porosity measured as a fraction or in percent, Vp the pore volume and Vb the bulk volume. The porosity measured is the effective porosity, the ratio of interconnected void spaces to the bulk volume. In this report porosity is measured by the helium technique, which employs Boyle's law, solved for the unknown volume V_2,

$$V_2 = V_{ref}\left(\frac{P_1}{P_3} - 1)\right).$$

Measuring principle:

The helium gas in the reference cell isothermally expands into a sample cell. After expansion, the resultant equilibrium pressure is measured. The pressure measuring inaccuracy is ± 0.01%[33]. The Helium porosity apparatus is shown schematically in **Figure 14**

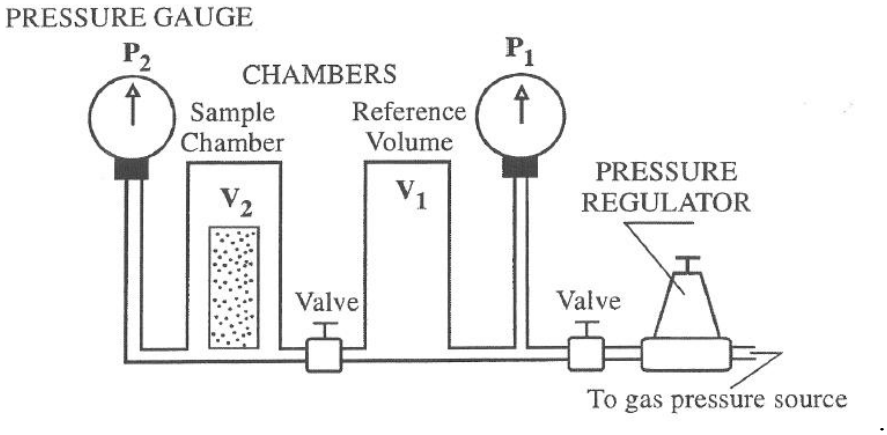

Figure 14. Schematic diagram of helium porosimeter apparatus[32]

2.4.5 Density

Density (ρ) is defined as the mass of the fluid per unit volume. In general, it varies with pressure and temperature. The dimension of density is kg/m^3. In this report measured densities are measured with the ANTON PAAR density meter DMA 48. The DMA 48 has a measuring range of 0–3 g/cm^3, accuracy of ± 0.1 mg/cm^3, temperature range of –10 to 70°C, temperature accuracy of 0.1°C and the test volume is approximately 0.7 cm^3.[34]

Measuring principle:

The DMA 48 density meter determines density on fluids and gas by measuring the vibration frequency. The sample is injected into a u-tube that oscillates, and the density is determined from the effect the sample substance has on the frequent. When the u-tube is full, the oscillating volume will be the same each time.

2.4.6 Water in oil content

The water content in oil can be determined by a Mettler Toledo DL31 Karl Fisher titrator. Karl Fisher titration is one of the most often used methods for water content determination. The sample is solved in an appropriate solvent and is titrated with a special Karl Fisher reagent to the end point. Methanol is used as solvent. The relative standard deviation (srel) is expressed from the variations of successive measurements of the same sample. Assuming optimum control and the best possible amount of sample, the values presented in **Figure 15** can be obtained for this parameter under repeatability conditions[35].

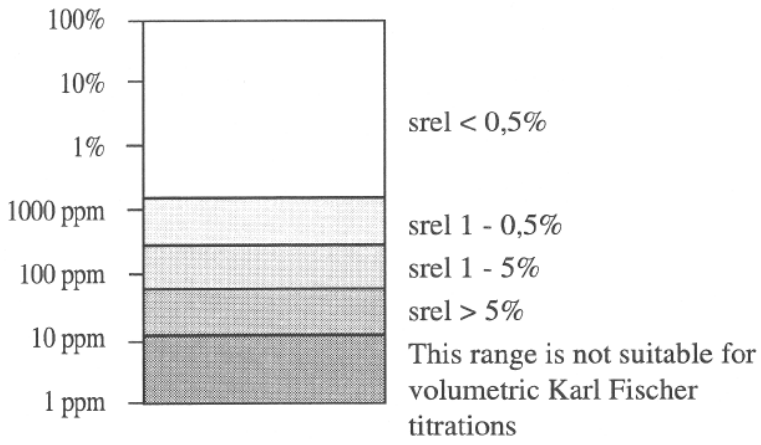

Figure 15. Relative standard deviation for different water contents[35]

3 EXPERIMENTAL WORK

3.1 APPARATUS

The apparatus used for the experiments is called “Fløммerigg 3-518” and can be seen in **Figure 16**. It was build during summer 2005 as a simple apparatus without differential pressure measurement and confining pressure for core material. The purpose of the rig was to flood 6 sand packs simultaneously in a compact mobile apparatus.

Figure 16. Picture of “Fløммerigg 3-518”

Statoil has a very comprehensive policy regarding HSE which involves all activities in the company. All apparatuses in Statoil laboratories are under the subject of HSE surveillance. More information about HSE and the safety measures of "Fløммerigg 3-518" can be found in **Appendix A.**

The apparatus was further modified during the work with the project thesis "An experimental pre-study of bio-surfactants for enhanced oil recovery"[36] autumn 2005, to contain a confining pressure system. The confining pressure system is shown in the lower left hand corner of the picture in **Figure 17**

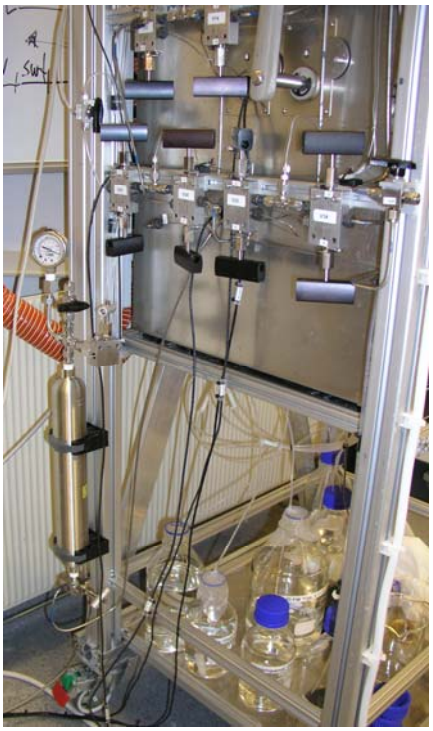

Figure 17. Picture of confining pressure system and some valves

Modifications were also done to the piping system so that differential pressure readings were made possible. The drawback is that the transmitter is not placed close to the core inlet and outlet, but it still gives a good indication of the pressure drop over the core. Permeabilities can be calculated by the differential pressure measurements. Even though the permeability issue is not essential for this study, it is a benefit to know if, and how, the permeability has been altered by the treatment. For the current connection diagram, please view **Appendix C**.

3.1.1 Core holder

The core holder used is the ProLight Ti-690-30 by Proserv A/S. It is applicable up to 690 barg at 65ºC. Maximum core diameter is 40 mm and the maximum core length is 95 mm. The sleeve used is a moulded Fluor-Carbon rubber called Viton of 70-75 shore. The o-rings used at the internal inlet piping are also Viton of 80 shore. The sketch in **Appendix D** shows a core holder construction like the ProLight Ti-690-30. The picture in **Appendix E** shows the dismounted core holder with all components. **Figure 18** shows the core holder completely mounted in the heating cabinet, whereas **Figure 19** shows the sleeve, a core and the two inner end pieces before mounting.

Figure 18. Picture of core holder completely mounted in heating cabinet.

Figure 19. Picture of the sleeve, a core and the two inner end pieces.

3.1.2 Components

All valves and pressure transmitters are made in acid resistant steel, while all piping is manufactured in Hast C-276 and 316SS. This ensures that the apparatus is resistant against corrosion at temperatures up to 200ºC. Swagelok pressure balancing valves with a range up to 20.6 bara are used as back pressure valves. Pressure, temperature and weight are logged with the Labview logging system. **Appendix F** presents an outline of the components used in the apparatus.

3.2 THE EXPERIMENTS

3.2.1 Core flooding

The experiments were designed to fit Heidrun Tilje semi-conditions. This includes synthetic Tilje formation water and authentic Tilje crude oil from well number A-48. Two different batches of crude oil were used, the first sampled in October 2005 and the second was sampled in February 2006. **Appendix G** displays details regarding the oil, and in **Appendix H** the brine recipe is attached. The temperature will not be reservoir temperature of 85ºC but will be performed at 70ºC. This because we have chosen to use one of the experiments from last years project thesis[36] in the experiment matrix, and need the same temperature of the new experiments to utilize the data. The core floods will be performed with a back pressure of 15 bars. The core material is Berea sandstone plugs of approximately 75 mm length and 1.5" diameter. The estimated permeability is said to be 500 md from the supplier. The chemical injection rate is chosen to be 0.2 ml/min which corresponds to a typical reservoir frontal advance rate of 1 ft/day.

Two different kinds of treatments were tested. The main focus was on a system composed of one polymer to increase the viscosity, one surfactant for interfacial tension reduction, and one di-alcohol to function as co-surfactant and for salinity control. 12 experiments were conducted with this treatment. 10 of these experiments enter into an experiment design described in detail in Chapter 3.4 Experimental Design. Three polymers specially accommodated with the high salinity of the Heidrun Tilje brine were obtained from the French company SNF Floerger. All three were hard to dissolve in formation water, but one was easier than the others. The growth of bacteria was apparent quite fast in the other two polymers, whereas the

easy solved one survived much longer. At the same time it provided the best viscosity profile. The polymer chosen is a high molecular weight linear polyacrylamide, with a 5 to 7% hydrolysed entities in mole (Na acrylate). It is not considered hazardous to the environment, but concerning the biodegradability there is a risk of getting a substitution warning[37]. Hence, it would probably be environmentally classified as a red chemical. The di-alcohol and surfactant are chosen on background of experience from the project thesis "An Experimental Pre-study of Bio-surfactants for Enhanced Oil Recovery, NTNU, December 2005"[36]. Regarding the environmental concerns for using the di-alcohol and the surfactant, none of them are considered hazardous to health. The di-alcohol is naturally occurring as a volatile constituent of sweet corn, fermented soybean curds, whole and ground grains, and in rotten mussels. The correct environmental test regarding toxicity, biodegradation and bioaccumulations is not performed. But the bioaccumulation of the di-alcohol is estimated and found non-bio accumulative. The chemicals need further environmental testing to verify if they are applicable for field operations in Norway.

The second treatment utilizes microfibrils based on various waste products from the paper and pulp industry. These microfibril particles will function as a biomaterial viscosity enhancer. One experiment was initiated, but could not be performed with this treatment.

3.2.2 Compatibility and emulsion testing

Compatibility and emulsion testing were performed to investigate if the viscous surfactant system could be used for core flooding and injection offshore. The emulsion stability of the various combinations of the system was also investigated. If there should be any sign of a third phase supporting a theory of the di-alcohol forming a slip-phase it would be of great interest. 12 selected combinations of the system were tested. A mixture of 50:50 chemical solution and crude oil, typically 10 ml total, were shaken by hand in graduated tubes for two minutes. At given time intervals from 5 seconds to 5 minutes, a reading of the free "water phase" was taken. **Table 2** gives the test setup. Visual observation of any incompatibility was also performed.

Table 2. Compatibility test experiment matrix

	Chemical composition
1	Distilled water
2	HDFW Tilje
3	HDFW Tilje + 2000ppm polymer
4	HDFW Tilje + 2000ppm polymer + 10mM di-alcohol
5	HDFW Tilje + 2000ppm polymer + 10mM di-alcohol + 20ppm surfactant
6	HDFW Tilje + 2000ppm polymer + 20ppm surfactant
7	HDFW Tilje + 1500ppm polymer
8	HDFW Tilje + 1000ppm polymer
9	HDFW Tilje + 10mM di-alcohol
10	HDFW Tilje + 10ppm surfactant
11	HDFW Tilje + 20ppm surfactant
12	HDFW Tilje + 10mM di-alcohol + 20ppm surfactant

3.3 MULTIVARIATE DATA ANALYSIS

Multivariate data analysis considers multiple variables simultaneously. One approach is called chemometrics. The word "chemometrics" was invented in 1972 by Svante Wold. A possible definition of chemometrics is: Chemometrics uses mathematical, statistical and artificial intelligence methods to[38]:

- design or select optimal experimental procedures
- provide maximum chemical information by analysing chemical data
- obtain knowledge about chemical systems

Multivariate data analysis systems usually provide the following advantages:

- fast analysis of data
- easy to use
- can be used to understand complex relationships
- can provide selective information from non-selective data
- provides diagnostics to access the accuracy of derived information
- can be done cheaply

By taking advantage of the power in multivariate data analysis software you can gain information about the effects of your variables. In this thesis there are three variables that

each varies between a high and a low value. Two response factors, oil recovery and residual oil in place are provided for the software. Applying a full factorial design in addition to one centre point experiment will give enough information to analyse the data for effects of the variables that are positive or negative correlated for the two response factors. The so-called centre point corresponds to the experiment in which all experiment variables are precisely at their mean value. When response measurements are costly, one often chooses to use only such centre points to determine the analytical inaccuracy. In addition the centre point gives an indication of the interactions of the variables. A way to improve the precision of the measurements is to increase the number of replicates.

The multivariate data analysis software MODDE is used to build the experimental design as described in Chapter 3.4. After conducting the experiments, MODDE is used to analyze the results by multiple linear regression (MLR). MLR is the most widely used multivariate regression method. But there are some weaknesses with MLR worth taking into consideration. MLR has severe problems when the variables are linearly dependent. The MLR prediction solution is inherently unstable due to numerical properties in the linearly dependent data sets[39]. This should not be a subject in this case due to highly independent variables; polymer, di-alcohol and surfactant.

3.4 EXPERIMENTAL DESIGN

3.4.1 Viscous surfactant flooding

The main chemical treatment consists of three different components. Variations between one high and one low value of these components will yield a full factorial design of 2^3, that is 8, different experiments. Adding one experiment with centre values finishes the experiment design matrix. The multivariate data analysis software MODDE is used to help construct the experiment design. In addition to the experiment matrix by MODDE, replica experiments were conducted to ensure validity of data. In **Table 3** all experiments included in the multivariate data analysis work is presented. In addition to the experiments performed during this Master Thesis, one previous experiment (marked 2*) performed during the project thesis work "An experimental pre-study of bio-surfactants for enhanced oil recovery"[36] is included

to fulfil the experiment matrix. Numbers listed as experiment design numbers, are the number given for the experiment by the MODDE software. The internal experiment numbers are chronological with the experiments performed.

Table 3. Core flood experiment matrix

Experiment design number	Internal experiment number	Polymer	Di-alcohol	Surfactant	Comment
		ppm	ppm	ppm	
1	3	1000	0	0	
2	7	2000	0	0	
3	2*	1000	10	0	Experiment conducted autumn 2005
4	8	2000	10	0	
5	4	1000	0	20	
6	9	2000	0	20	
7	1	1000	10	20	
7	2				Replica of experiment 7
7	5				Replica of experiment 7
8	10	2000	10	20	
9	6	1500	5	10	

After analyzing the results of the design matrix it was decided to perform two more experiments as displayed in **Table 4**. One with a lower concentration of polymer, no surfactant and a higher concentration of di-alcohol because results of the previous experiments indicate that it might be a favourable combination. The second extra experiment is another replicate of design experiment number 7, only this time with an chemical injection of 1/3 pore volume instead of two, simply because that is the largest realistic volume to use in an actual field trial. Studies have shown that slug sizes smaller than 7% PV have not been successful, while slug sizes between 7 and 33% PV have been successful[15].

Table 4. Extra experiments

Internal experiment number	Polymer	Di-alcohol	Surfactant	Comment
	ppm	ppm	ppm	
11	500	40	10	2 PV chemical injection
12	1000	10	20	1/3 PV chemical injection

3.4.2 Microfibril flooding

For the first time in history to my knowledge, a microfibril solution is used in a core flood. The objective was to investigate the possibilities for this environmental friendly viscosity enhancer for enhanced oil recovery. The microfibril particles will function as a biomaterial viscosity enhancer. A 1-2% microfibril solution can be seen in **Figure 20.** This treatment includes only the viscosity modifier, no surfactants. The microfibril solution used in the core flood was a dilution of 0.5%. The experiment procedure used is the same as for the other chemical treatments, and can be found in **Table 5** and **Appendix I**.

Figure 20. Microfibril solution

3.5 EXPERIMENT PROCEDURE

All experiments were performed in the same way according to the main points stated below:

- assemble the core holder
- evacuate the core
- saturate the core with brine
- flow brine to achieve Sw = 1.0
- flow oil to achieve Swi
- flow brine to achieve near Sor conditions
- flow chemical solution to reduce Sor further
- flow brine as post-flush to produce out mobilized oil

Detailed flooding procedure is attached in **Appendix I**. A simplified flooding scheme is displayed in **Table 5**.

Table 5. Flooding scheme

Saturation brine		Flooding to Swi		Flooding to Sor		Chemical injection		Post-flush	
PV	Rate [ml/min]	PV	Rate [ml/min]	PV	Rate [ml/min]	PV	Rate [ml/min]	PV	Rate [ml/min]
1	By vacuum	1	0.5	1		2	0.2	4	Increasing rate
		9	Increasing rate	7	Increasing rate			4	Decreasing rate

4 RESULTS

4.1 LITERATURE

Based on the literature studied during this project it is evident that a system of combined surfactant and polymer flooding could be very promising in terms of enhanced oil recovery. Surfactant flooding in the Heidrun Tilje reservoir should in theory perform satisfactory since the reservoir is slightly water-wet and the most optimal conditions for surfactant flooding will be achieved under water-wet conditions. The salinity of the Heidrun Tilje formation at approximately 55.000 TDS or 5.7 wt% is clearly in the type II(+) phase system region indicating that the emulsion formed will be an oil external phase containing solubilized brine inside the micelles. Surfactant retention is crucial to the surfactants ability to reduce IFT. Net negatively charged surfactants also tolerant to the resident brine seem to be the best alternative to prevent surfactant retention. The best volumetric sweep efficiency is achieved when the displacing fluid viscosity is increased. Choosing a biopolymer would in general terms give better compatibility with high salinity waters. Because of the high salinity and temperature, it has been challenging to find good polymers for use offshore Norway. The biopolymer Xanthan was a good candidate but turned out to be too expensive in the late 80-ties. A combination of a polymer and a surfactant flood has the potential of providing an increase in both volumetric sweep efficiency and microscopic displacement efficiency. Laboratory experiments with systems combining polymers for mobility control, di-alcohol for enhanced solubility and reduced effect of salinity, and surfactant to lower the IFT has shown very good results.

4.2 EXPERIMENTAL

The experimental results are presented mainly in tables and figures. Larger figures are found in the appendices. All systems are based on Heidrun Tilje formation water even though this is not denoted in all tables and figures to save space.

4.2.1 Fluid properties

The different viscosities measured are presented in **Table 6**. One viscosity is correlated by using a Statoil laboratory internal spreadsheet. Plot of shear and temperature scans are found in **Appendix J.**

Table 6. Measured viscosities of Heidrun (HD) crude oil and formation water (FW), and various additions of polymer

System	Viscosity [mPa-s = cP]		Measuring method
	1bar	15 bar	
HD crude, current, 20C	41.5	-	T-scan, rheometer
HD crude, current, 70C	8.8	-	T-scan, rheometer
HD crude, previous, 20C	49.8	-	SVM 3000 viscometer, Anton Paar
HD crude, previous, 70C	7.1	-	SVM 3000 viscometer, Anton Paar
HD FW @ 20C	1.0	-	Ubbelohde capillary viscometer
HD FW @ 70C	-	0.5	Correlated
500ppm @ 20C	2.0	-	T-scan, rheometer
500ppm @ 20C, 100[1/s]	2.2	-	Shear scan, rheometer
500ppm @ 70C	1.9	-	T-scan, rheometer
1000ppm @ 20C, new	2.5	-	T-scan, rheometer
1000ppm @ 70C, new	1.3	-	T-scan, rheometer
1000ppm @ 20C, old	4.2	-	SVM 3000 viscometer, Anton Paar
1000ppm @ 70C, old	1.6	-	SVM 3000 viscometer, Anton Paar
1000ppm @ 20C, 100[1/s]	3.0	-	T-scan, rheometer
1000ppm @ 70C, 100[1/s]	2.4	-	T-scan, rheometer
1000ppm @ 20C, 100[1/s]	5.2	-	Shear scan, rheometer
1000ppm @ 80C, 100[1/s]	1.9	-	Shear scan, rheometer
1500ppm @ 20C	4.7	-	T-scan, rheometer
1500ppm @ 20C, 100[1/s]	6.6	-	Shear scan, rheometer
1500ppm @ 70C	2.4	-	T-scan, rheometer
2000ppm @ 20C	5.5	-	T-scan, rheometer
2000ppm @ 20C, 100[1/s]	8.3	-	Shear scan, rheometer
2000ppm @ 70C	2.9	-	T-scan, rheometer

The different densities measured are presented in **Table 7**. Density at 70ºC is also correlated by spreadsheets used at Statoil laboratories.

Table 7. Measured densities of Heidrun (HD) crude oil and formation water (FW), and various additions of polymer

System	Density [g/cm3]		Measuring method
	1bar	15 bar	
HD crude, current, 20C	0.915	-	DMA 48, Anton Paar
HD crude, current, 70C	0.883	-	DMA 48, Anton Paar
HD crude, previous, 20C	0.913	-	DMA 48, Anton Paar
HD crude, previous, 70C	0.880	-	DMA 48, Anton Paar
HD FW @ 20C	1.036	-	DMA 48, Anton Paar

HD FW @ 70C	1.019		DMA 48, Anton Paar
HD FW @ 70C	1.014	1.014	Correlated
500ppm @ 20C	1.037	-	DMA 48, Anton Paar
500ppm @ 70C	1.016	-	DMA 48, Anton Paar
1000ppm @ 20C	1.014	-	DMA 48, Anton Paar
1000ppm @ 70C	1.016	-	DMA 48, Anton Paar
1500ppm @ 20C	1.030	-	DMA 48, Anton Paar
1500ppm @ 70C	1.012	-	DMA 48, Anton Paar
2000ppm @ 20C	1.038	-	DMA 48, Anton Paar
2000ppm @ 70C	1.012	-	DMA 48, Anton Paar

The different IFT's measured are presented in **Table 8**. Measurement methods used are ring tensiometer and pendant drop. The IFT value given in **Table 8** is the end point value of that specific measurement. These values can not be used until seen in comparison with other values and trends in a plot. IFT plots are found in **Appendix K**.

Table 8. Interfacial tensions.

System	Parallel	IFT mN/m	Measuring method
HD FW Tilje, previous oil	1	22.7	Ring tensiometer
HD FW Tilje, previous oil	2	19.2	Ring tensiometer
HD FW Tilje, current oil	1	26.7	Ring tensiometer
HD FW Tilje, current oil	2	26.6	Ring tensiometer
HD FW Tilje, current oil	3	25.3	Pendant drop
10ppm surfactant	1	8.6	Pendant drop
20ppm surfactant	1	7.7	Pendant drop
40ppm surfactant	1	6.9	Pendant drop
200ppm surfactant	1	5.7	Pendant drop
10mM di-alcohol	1	27.0	Ring tensiometer
10mM di-alcohol	2	26.8	Ring tensiometer
20mM di-alcohol	1	26.4	Ring tensiometer
20mM di-alcohol	2	26.0	Ring tensiometer
40mM di-alcohol	1	26.7	Ring tensiometer
40mM di-alcohol	2	26.0	Ring tensiometer
40mM di-alcohol	3	26.0	Ring tensiometer
200mM di-alcohol	1	24.7	Ring tensiometer
200mM di-alcohol	2	24.9	Ring tensiometer
200mM di-alcohol	3	25.8	Ring tensiometer
10mM di-alcohol, 20ppm surfactant	1	6.5	Pendant drop
10mM di-alcohol, 20ppm surfactant	2	8.4	Pendant drop
10mM di-alcohol, 20ppm surfactant - previous oil	1	5.7	Pendant drop
10mM di-alcohol, 20ppm surfactant - previous oil	2	5.7	Pendant drop
10mM di-alcohol, 20ppm surfactant - previous oil	3	5.7	Pendant drop
500ppm polymer, 40mM di-alcohol, 10ppm surfactant	1	8.4	Pendant drop
1000ppm polymer, 10mM di-alcohol, 20ppm surfactant	1	8.0	Pendant drop
2000ppm polymer, 10mM di-alcohol, 20ppm surfactant	1	7.0	Pendant drop
2000ppm polymer	1	20.3	Ring tensiometer
2000ppm polymer	2	20.3	Ring tensiometer
2000ppm polymer, 10mM di-alcohol	1	19.6	Ring tensiometer
2000ppm polymer, 10mM di-alcohol	2	19.6	Ring tensiometer
2000ppm polymer, 20ppm surfactant	1	6.9	Pendant drop

Water in oil content for Heidrun Tilje is measured for both the previous and the current batch of crude oil. The results are found in **Table 9**.

Table 9. Measured water in oil content of three parallels.

Type of crude oil	Water in oil content		
	1	2	3
	ppm	ppm	ppm
Previous batch	3700	3600	3700
Current batch	120	90	90

The mobility ratios are calculated based on two different types of viscosity measurements as can be seen in **Figure 21** and as a table in **Appendix L**. Mobility ratios marked by 1000 [1/s] are calculated based on a viscosity measured at a shear rate of 1000 [1/s], and mobility ratios marked by 100 [1/s] are calculated based on a viscosity measured at a shear rate of 100 [1/s]. The first five experiments listed used another batch of crude oil, and therefore displays a different ratio than the rest. The mobility ratio is significantly reduced due to the chemical treatment.

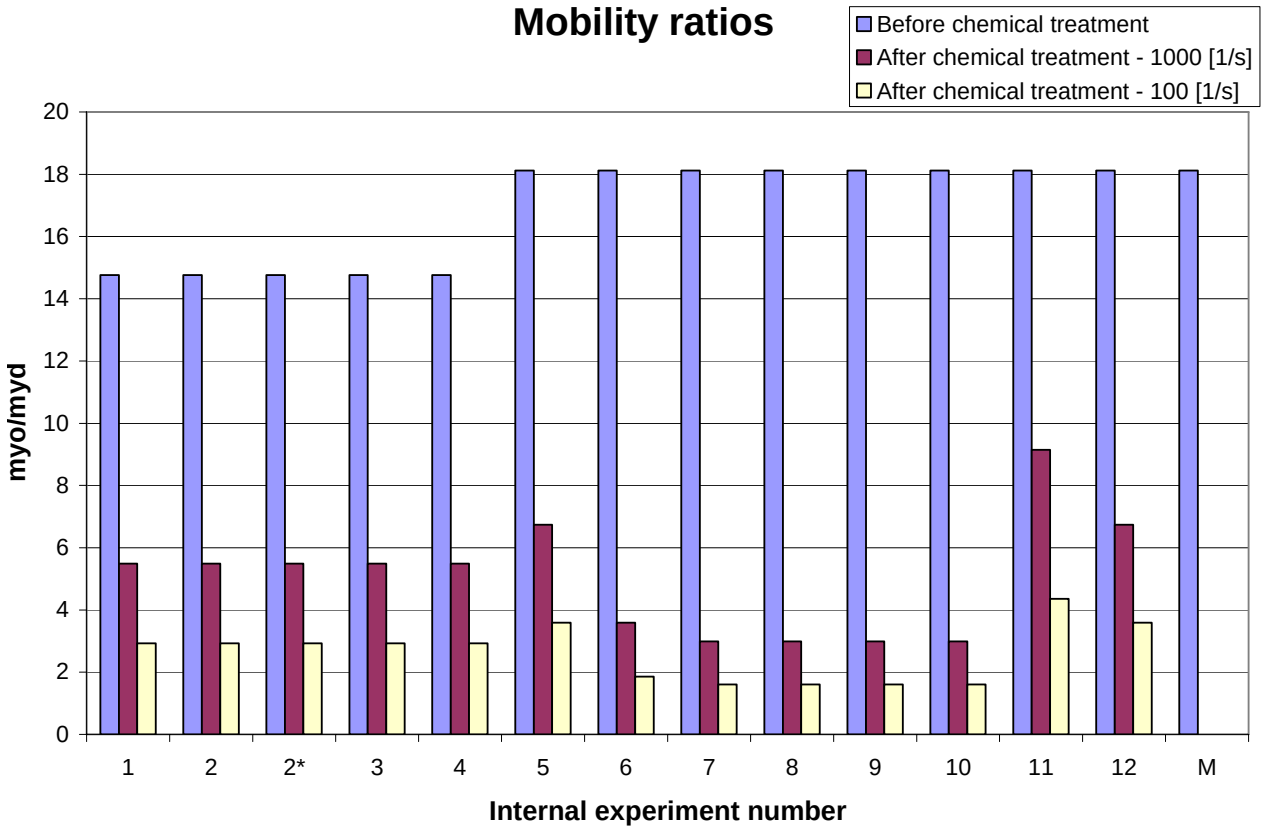

Figure 21. Calculated mobility ratios from two different viscosity measurements

4.2.2 Compatibility and emulsion testing

In addition to the 12 emulsion tests, several replica parallels were performed to verify the data. A plot of the various chemical solutions versus separation times can be found in **Figure 22**. The data are presented in table format in **Appendix M**.

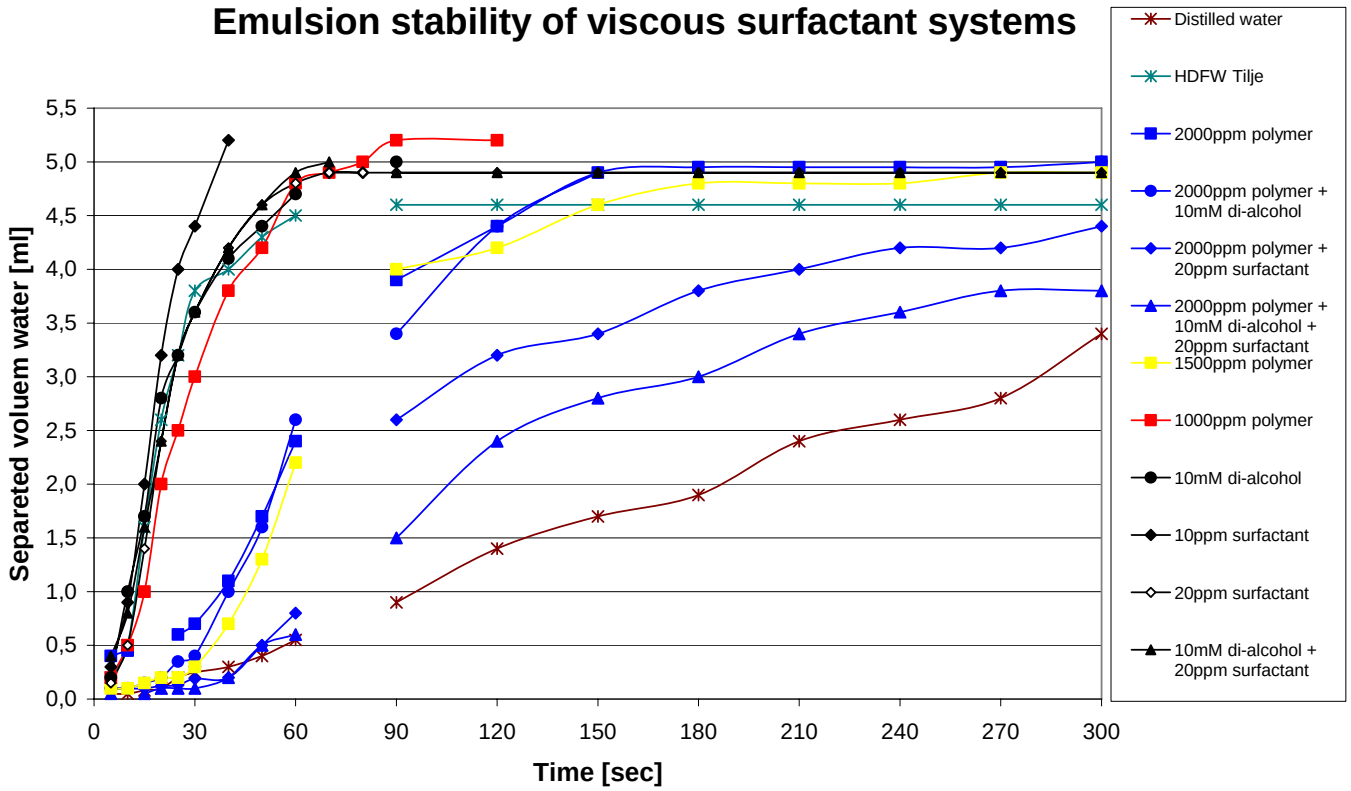

Figure 22. Separation time, compatibility tests.

No precipitation, clouding or colour difference were observed. The emulsion stability is low. pH of the 1000 ppm polymer, 10 mM di-alcohol, 20 ppm surfactant solution is measured to 6.65. The compatibility test concludes that the various viscous surfactant treatments with respect to compatibility issues can be applied for core flooding and used offshore. However there is one special issue to be aware of. The polymer is not easy to solve. It takes time, and the easiest way was found to be as follows:

- do not make batches smaller than 1 litre
- weigh out the correct amount and place it in a large test tube
- add formation water little by little under constant stirring to let the polymer granules soak up and hydrolyse slowly
- transfer the solution to a 1 litre bottle and continue to add small amounts of formation water while stirring with a magnetic stirrer
- leave to stir over night or until the polymer is completely solved

4.2.3 Rock properties

The core plug porosities and measures are presented in **Appendix N.** Core plug porosities can also be found in **Table 10**.

Permeabilites calculated with Darcy's equation are also presented in **Table 10**. These values include an additional pressure loss term from pressure loss in tubing, and are not a correct permeability representation. That is because the transmitters are not placed close to the core inlet and outlet. But they will still give a good indication of the performance of the system as the main interest is the relative changes in permeability. The plots giving the permeabilities are found in **Appendix Q**.

Table 10. Core flood porosities and permeabilities.

Core flood	Porosity	Absolute k	k @ Swi	k @ Sor,w	k @ Sor,c
	%	[md]	[md]	[md]	[md]
1	22,7	176	165	24	16
2	22,7	150	176	37	15
2*	22,4	134	168	**	21
3	22,5	178	158	35	14
4	22,3	160	150	26	15
5	23,6	183	188	40	18
6	23,5	90	214	33	16
7	23,6	214	170	35	15
8	23,9	216	218	45	17
9	23,7	125	220	42	16
10	23,9	159	180	68	20
M	23,4	191	108	37	***
11	21,9	80	90	11	6
12	23,6	170	214	40	19

** One of the pressure transmitters started malfunctioning. No pressure data from this part of the experiment
*** Experiment terminated, piping blocked by microfibril particles

4.2.4 Viscous surfactant flooding

Presented in **Table 11** and **Figure 23** you find saturations and recoveries achieved after core flooding normalized against original oil in place (OOIP). For saturations and recoveries achieved after core flooding as water and oil saturations please view **Appendix O**.

The chemical treatment giving the best result consists of the low polymer, the high di-alcohol and the high surfactant content. It gave an additional oil production normalized on OOIP of 20%, improving the recovery from 45 to 66%.

Table 21. Oil recovery and saturation results normalized against OOIP

Chemical treatment	Internal Experiment Number	OOIP	Initial recovery - Oil produced by water		Remaining oil after water production		Additional oil production by chemical		Remaining oil after chemical production		Final recovery
		[ml]	[ml]	%	[ml]	%	[ml]	%	[ml]	%	%
Centre experiment	6	14.8	6.3	42	8.5	58	2.4	**16**	6.1	41	**59**
Low polymer, low di-alcohol, high surfactant	4	12.8	6.3	49	6.5	51	1.7	**13**	4.8	38	**62**
Low polymer, low di-alcohol, low surfactant	3	14.3	6.1	43	8.2	58	1.9	**13**	6.3	44	**56**
Low polymer, high di-alcohol, low surfactant	2*	13.1	5.1	39	8.0	61	2.5	**19**	5.6	42	**58**
Low polymer, high di-alcohol, high surfactant	1	12.8	5.8	45	7.0	55	2.6	**20**	4.4	35	**66**
Low polymer, high di-alcohol, high surfactant	2	13.8	6.5	47	7.3	53	1.8	**13**	5.5	40	**60**
Low polymer, high di-alcohol, high surfactant	5	15.3	6.8	44	8.5	56	1.9	**12**	6.6	43	**57**
High polymer, low di-alcohol, high surfactant	9	15.0	6.0	40	9.0	60	1.4	**10**	7.6	50	**50**
High polymer, low di-alcohol, low surfactant	7	14.8	6.3	42	8.5	58	1.8	**12**	6.8	46	**54**
High polymer, high di-alcohol, low surfactant	8	15.3	6.8	44	8.5	56	2.2	**14**	6.3	41	**59**
High polymer, high di-alcohol, high surfactant	10	15.5	7.8	50	7.8	50	1.5	**10**	6.3	40	**60**
500ppm polymer, 40mM di-alcohol, 10ppm surfactant	11	13.8	5.8	42	8.0	58	1.0	**7**	7.0	51	**49**
1/3 PV: Low polymer, high di-alcohol, high surfactant	12	15.3	6.8	44	8.5	56	0.8	**5**	7.8	51	**49**

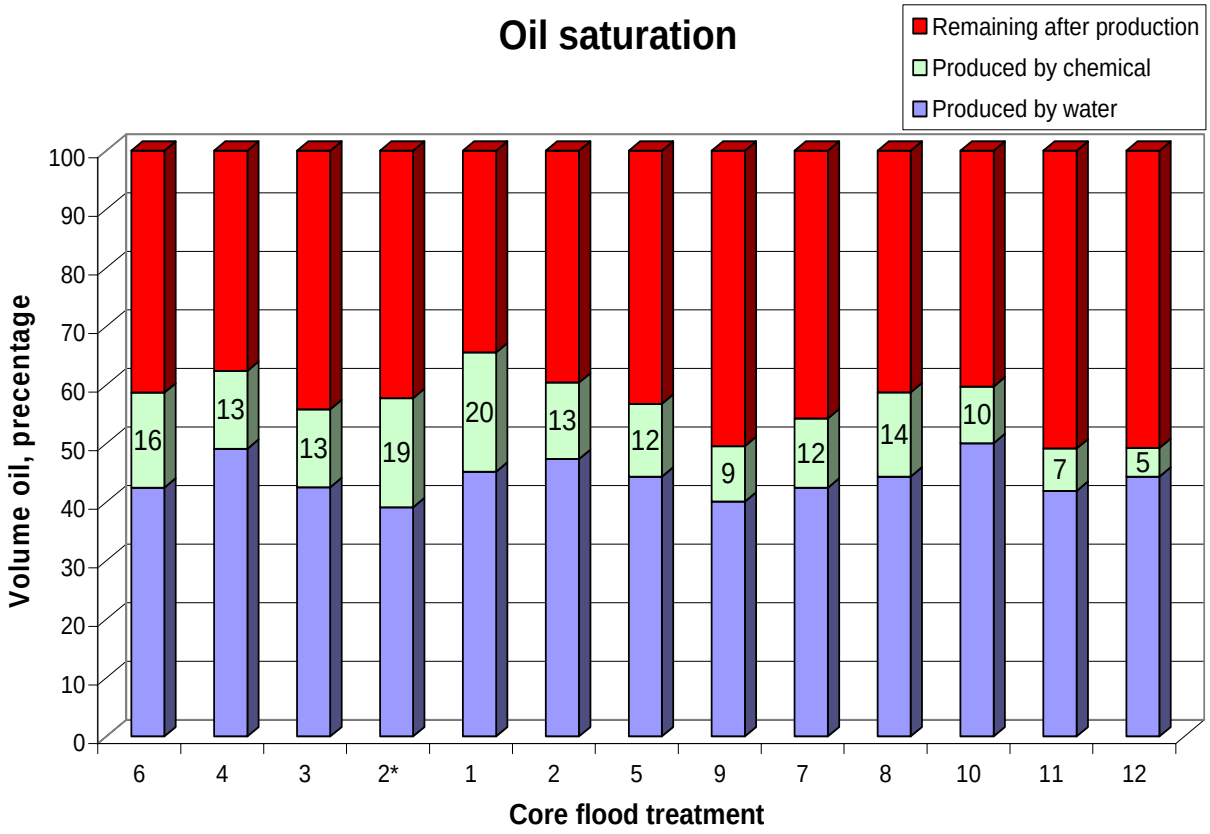

Figure 23. Saturations and recoveries normalized against OOIP.

The different experiments are presented in experiment design sequence, but labelled by internal experiment number as follows: 6: centre experiment, 4: low polymer, low di-alcohol, high surfactant, 3: low polymer, low di-alcohol, low surfactant, 2*: low polymer, high di-alcohol, low surfactant, 1: low polymer, high di-alcohol, high surfactant, 2: low polymer, high di-alcohol, high surfactant, 5: low polymer, high di-alcohol, high surfactant, 9: high polymer, low di-alcohol, high surfactant, 7: high polymer, low di-alcohol, low surfactant, 8: high polymer, high di-alcohol, low surfactant, 10: high polymer, high di-alcohol, high surfactant, 11: 500ppm polymer, 40mM di-alcohol, 10ppm surfactant, 12: 1/3PV with 1000ppm polymer, 10mM di-alcohol, 20ppm surfactant.

The different capillary numbers calculated are presented in **Figure 24** as well as in **Table 12.**

A full-scale version of **Figure 24** can be found in **Appendix P**.

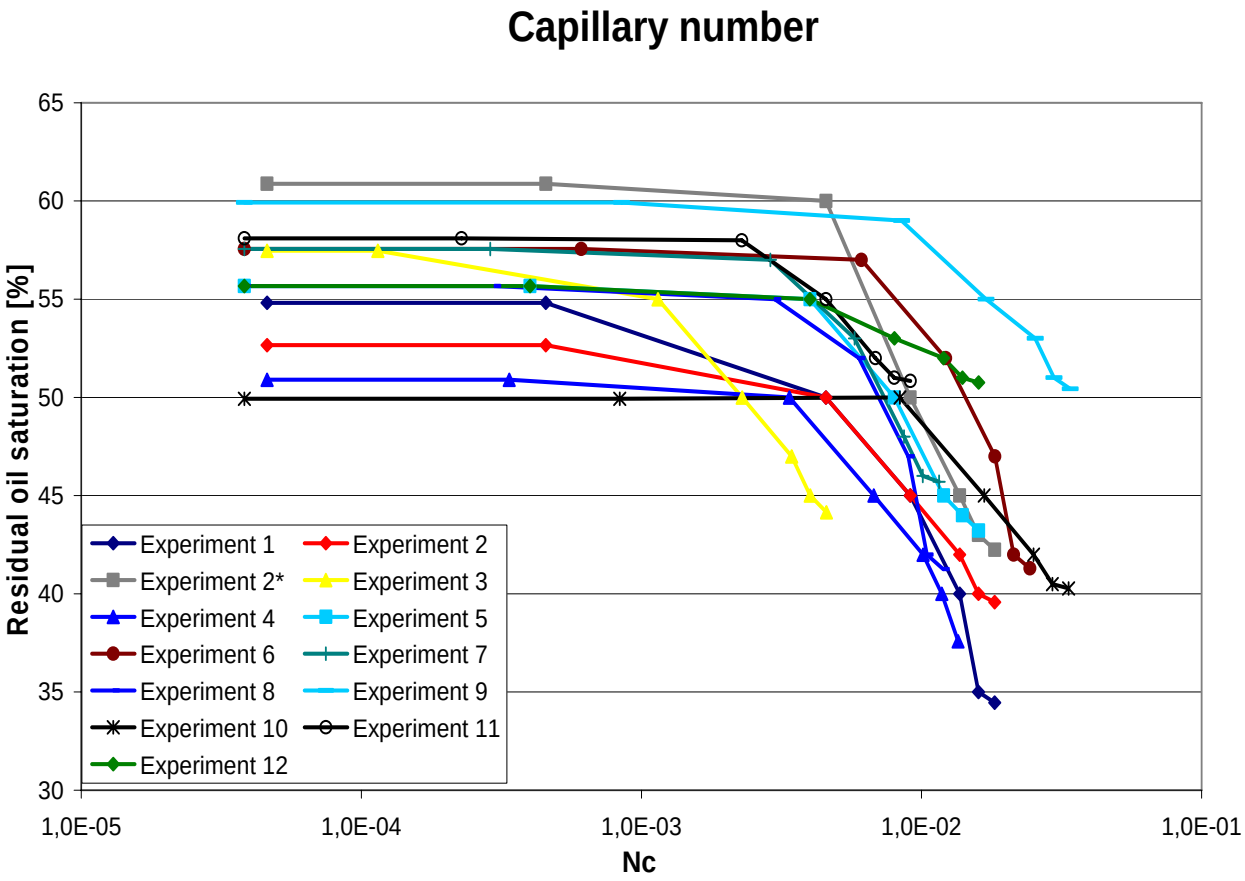

Figure 24. Capillary number plotted against residual oil saturation

Table 32. Capillary number.

Internal experiment number	Nc	
	before chemical injection	after chemical injection
1	4.61E-05	1.82E-02
2	4.61E-05	1.82E-02
2*	4.61E-05	1.82E-02
3	4.61E-05	4.85E-03
4	4.61E-05	1.35E-02
5	3.82E-05	1.60E-02
6	3.82E-05	2.44E-02
7	3.82E-05	1.15E-02
8	3.82E-05	1.20E-02
9	3.82E-05	3.40E-02
10	3.82E-05	3.35E-02
11	3.82E-05	9.12E-03
12	3.82E-05	1.60E-02

4.2.5 Microfibril flooding

The experiment with the microfibril flooding system could not be performed. The microfibril particles did not stay in solution for a long enough period of time, and large amounts separated out in the pump. This resulted in a blockage of the piping and a pressure build up. Finally it was decided to terminate the experiment.

5 DISCUSSION

5.1 LITERATURE

Surfactant retention is one of the most important parameters for field scale success with surfactant flooding. This thesis work has chosen to focus on surfactants that yield little theoretical retention. If one were to investigate it, one could measure the concentrations of surfactant by chemical analysis of water samples before and after the core flood. If the surfactant used in this work were to be field tested, specific surfactant retention measurements need to be conducted.

For field trials one need treatments that can provide both volumetric sweep efficiency and microscopic displacement efficiency. A combination of a polymer and a surfactant flood has the potential of providing an increase in both factors. The microscopic displacement efficiency is investigated at the laboratory in similar tests that this thesis work describes. The volumetric sweep efficiency can not be verified without reservoir simulations and field trials.

It was stated that a polymer flood is not intended to reduce the residual oil saturation, $S_{OR,}$ but is an efficient and quick way to reach S_{OR}. But there are field examples that polymer flooding can increase recovery by more than 12% OOIP. This concurs with my results where pure polymer flooding increases recovery between 12 and 13% OOIP.

McInerney et.al. reports that the main mechanism of their success full EOR method is the IFT reduction provided by the bio-surfactant. That is not the case with the results presented in this report. The main mechanism of EOR is the increased viscosity provided by the polymer.

Other than the issues mentioned, there is no contradictory information found in the literature reviewed for this Master Thesis.

5.2 EXPERIMENTAL

5.2.1 Fluid properties

Viscosity measurements are used as input for mobility ratio and capillary number calculations. The instrument accuracy is not given. The Fluid Department performing the rheometer work does no operate with a given accuracy. They run reference oil measurements, and if the measurement concurs with the reference they are satisfied. There are performed two exactly similar measurements of 1000 ppm polymer. The two curves match almost perfectly for most of the measurement. Therefore an inaccuracy of 0.1 cP is assumed, reporting measurements with one decimal place. The largest source of error is if you choose the wrong capillary viscometer or the wrong measuring geometry for the UDS 200. Viscosity measurements are also very temperature dependent. The choice of the correct shear rate has great influence for the resulting viscosities. All viscosity measurements with the UDS 200 were done by the Fluid Department at Statoil R&D Centre.

Viscosity measurements are performed on both filtrated and un-filtrated 1000 ppm of polymer. As seen in **Figure 25** they do not differ significantly either at 20 or 80ºC, and it is assumed that all polymers are completely solved when used in experiments and measurements.

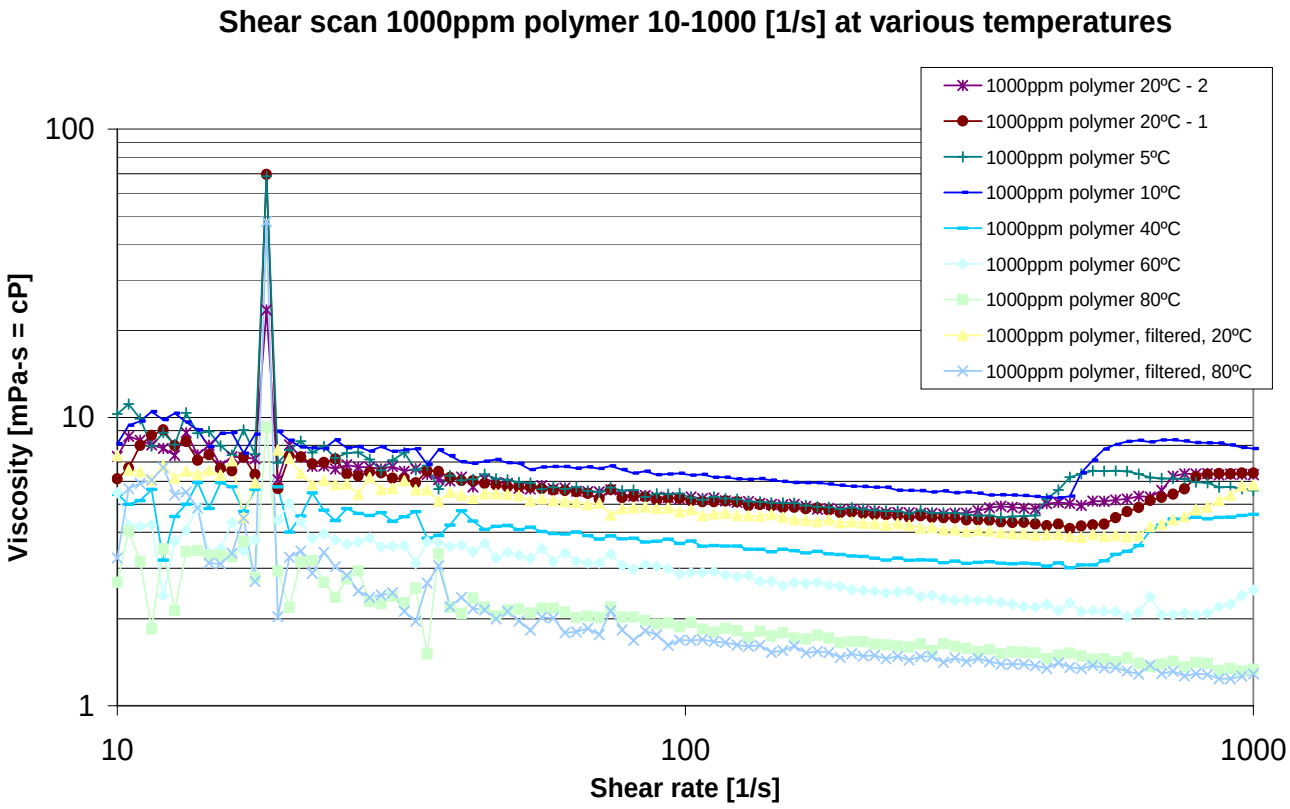

Figure 25. Shear scan of 1000 ppm polymer at various temperatures

As seen from **Figure 25** and **Appendix J** the polymer displays a weak shear thinning effect, whereas the crude oil has a pure Newtonian behaviour. Because of limited time and access to the rheometer it was decided to concentrate a more thorough investigation of the 1000 ppm polymer solution. The 500 and 2000 ppm samples are shear thinning. All 1000 ppm samples displayed at first a shear thinning effect, but when closing up to 1000 [1/s] a shear thickening effect was observed. This effect is also seen in the 1500 ppm sample. There is an effect called "Dilatant Peek" that agrees with these observations. There are two possible explanations for this shear thickening effect[40]:

1. Some times high concentrated dispersions can display shear thickening effects at relatively high shear rates (around 1000 [1/s])
2. Some low viscous fluids can when applying a rotating inner cylinder at high shear rates go from laminar to turbulent flow.

After recommendation from teaching supervisor, the temperature scans should be performed either at the shear rate where the solution displayed Newtonian behaviour or at a shear rate of 1000 [1/s]. This shear rate is very high and will not represent a plausible shear either during

the core flood or in the reservoir. On the other hand, it could be reasonable for the shear rate experienced by the solution when injected in a well. A shear rate of 100 [1/s] seems more appropriate for a core flood. For the 1000 ppm solutions, temperature scans were also performed at different shear rates. At a temperature scan with constant shear rate of 100 [1/s], the reduction of viscosity with temperature is not as large as the corresponding reduction at a temperature scan with constant shear rate of 1000 [1/s]. Also, performing shear scans at a given temperature and making a reading at shear rate equals 100 [1/s], yields generally higher viscosities than a temperature scan reading at the same given temperature at a constant shear rate of 100 [1/s]. This is simply because of the measurement program. In a temperature scan the temperature increases with 12.5ºC/hr. There is not enough time for the temperature in the solution to adjust to the specific temperature given by the program and thus the viscosity differs.

As seen in **Table 6,** viscosities measured at the SVM 3000 viscometer by Anton Paar do not concur with the average results of the rheometer. Interesting though, the results achieved with a shear scan at 100 [1/s] concurs almost with the viscometer results. This is probably due to the shear rate being so low that the polymer shows approximately Newtonian behaviour.

Regarding the crude oil viscosities, the first crude oil batch displays a higher viscosity at 20ºC and a lower one at 70ºC than the second batch. This is probably due to different measuring techniques. The first batch being measured with the SVM 3000 viscometer by Anton Paar and the second batch measured with the rheometer. But other measurements as density, IFT and water in oil content also support the fact that the two batches show slightly different fluid properties.

Density measurements are used as input for software to IFT measurements and to calculate dynamic viscosity when measuring by both capillary viscometer and SVM 3000 viscometer. The instrument accuracy is ± 0.1 mg/cm^3. The largest source of error is if there is air in the instrument. If the instrument is not properly cleaned, it is also a large source of error. Three parallel density measurements are performed for each sample. Measurements are reported with three decimal places to take any sources of error into account. I always use clean and air free apparatuses.

Interfacial tension measurements are used in capillary number calculations. The instrument inaccuracy is ± 0.01 mN/m for the pendant drop and 1μN for the ring tensiometer. The largest source of error is cleaning. Small traces of chemical substances or dirt will have great influence on the ring tensiometer. I always performed the measurements with properly cleaned instrument. The pendant drop method is for example dependent on air free systems not causing the size of the drop to change during the measurement. Measurements are reported with one decimal place to take any sources of error into account.

For the base case measurement of Heidrun Tilje formation water versus Heidrun Tilje crude oil, the two different IFT methods yields concurring results verifying that the value found is correct. Referral information also confirms this[5, 41]. We can also conclude that the results of the two methods can be compared when in an appropriate IFT range according to instrument specifications in Chapter 2.4.1. Adding di-alcohol to the formation water causes some, but very little IFT reduction. Adding surfactant causes far greater reduction. Measuring surfactant concentrations of 10, 20, 40 and 200 ppm indicates that the CMC concentration is somewhere between 40 and 200 ppm. At increasing concentrations of polymer the IFT seems to decrease, even though the surfactant itself is not very surface active. This might be due to some small surface active properties or impurities in the polymer. It is also possible to picture that the viscosity would influence the ring tensiometer measuring method so that the sample would "let go of the ring" easier when under influence of gravity. Even though, the reduction at increasing polymer concentration is also evident by the pendant drop method.

It is important to keep in mind when reading **Table 8** that all values reported are end-point readings. Some of the parallel measurements are done to verify other measurements and are stopped at an earlier time as long as the trend is confirmed as concurring. **Appendix K** shows the different IFT plots.

The water in oil content is used to investigate the possible differences between the two batches of crude oil. The instrument accuracy is 0.5 – 1% at 1000 ppm level, and 1 – 5% at 100 ppm level. The largest source of error is the amount of sample, which is quite easy to control. Three parallels of water in oil content measurements are performed for each sample. Measurements reported are rounded to the nearest 10 to take any sources of error into account. The water in oil content differs significantly between the two batches, the first batch

carrying an average of 3650 ppm water, whereas the second one has approximately 105 ppm. These differences in water in oil content will influence the emulsion stability properties and the viscosity of the two crude oil batches.

The mobility ratios are used to express the change in saturation and viscosity after a chemical treatment. Calculations are reported with one decimal place to take any sources of error into account. To be able to calculate the mobility ratios, the displacing and displaced end-point relative permeabilities were assumed to be equal and constant. This is in reality not true. One should expect the relative permeability to water to increase during chemical injection giving a higher value for the mobility ratio after chemical flooding, than those estimated in **Figure 21** and **Appendix L**. Two different mobility ratios were calculated based on two different viscosities measured at different shear rates. Based on the different viscosities measured at a shear rate of 100 versus 1000 [1/s] and the trend for the 1000 ppm solution, the values given in **Appendix L** for mobility ratio based on viscosity from shear rate of 100 [1/s] is not a measured value. The value is adjusted using the value of 20ºC from a temperature scan at 1000 [1/s], as it seems to fit a plausible trend. As seen from **Figure 21** a significant reduction is achieved, especially with the 2000 ppm polymer systems reaching a mobility ratio of 1.61. This is very good, almost satisfying the ideal displacement condition of 1 or less. This would indicate that the 2000 ppm polymer experiments would yield a higher recovery than the ones with higher mobility ratios. This is not the case. Probably due to the effect of end-point relative permeabilities that are not taken into consideration in this mobility ratio calculation.

5.2.2 Compatibility and emulsion testing

It is a necessity to verify that the chemical systems are compatible with the formation fluids and other oil field chemicals in use. The compatibility test conclusion is important because a negative result will rule out the specific system tested.

The more viscous solutions of 1500 and 2000 ppm of polymer did all use significantly longer time than the more less viscous ones to separate, probably caused by viscous effects at the interface. The 1000 ppm solution gave results similar to the ones with no polymer addition, having separation times of approximately 1 minute. It seams though that the separation is not effected by viscosities up till 2.5 mPas. But one has to have in mind that the compatibility

tests are quite coarse tests, not producing “high accuracy results”. The test concludes with a low emulsion stability of the various systems. This is supported by observing the emulsion effluent produced during the core floods. It ranges from coarse to fine during production, but it is mostly separated shortly after production is stopped.

The pH of 6.65 measured in the chemical system ensures that there will be no corrosion issues to consider if this specific chemical treatment were to be injected in a well.

5.2.3 Rock properties

The porosity measurement gives us the pore volume of the core. All saturation estimates depend on it. The pressure measuring accuracy is ± 0.01% of the measured pressure in bara. This gives a porosity measured in percent accuracy of ± 0.014. The largest source of error is the pressure measurement. One should also have in mind that the porosity is measured by Helium molecules that are smaller than the water and oil molecules introduced to the core later on. Meaning that the given porosity is higher than the porosity the later fluids would experience.

Permeability measurements are used as a way of monitoring the influence of fluids to the core during flooding. The pressure transmitter accuracy is 0.001 bar. The largest source of error is the noise in the measurements caused by the long distance between the pressure transmitters and the core inlet / outlet. Core flood permeabilites reported are rounded to the nearest integer to take any sources of error into account.

The “Fløммerigg 3-518” was not constructed to handle differential pressure measurements. Absolute permeability measurements are not essential for this Master Thesis. However, an estimate of the relative change in permeability by the various treatments was. Some alterations to the rig were done[36], leaving one pressure transmitter placed on each side of the core, but not placed close to the core inlet and outlet. Even though, they still give a good indication of the pressure drop over the core.

The core material permeabilities were indicated to be 500md air permeability by the supplier. Permeability measurements give arithmetic average absolute brine permeability slightly above

170md for all core plugs. Brine permeability is in reality always less than air. As seen from **Figure 26** the permeability in core flood number 1 is reduced to approximately 16 md after chemical injection. The respective permeability values are revealed as the slope of the lines in **Figure 26**. The absolute permeability is reduced to 24 md at Sorw, then further to 16 md at Sorc. This is a general effect in all core floods performed. When increasing the rate gradually up to ten times maximum rate used for permeability measurements, finally reaching 80 ml/min, a lot of emulsion is produced. For all core floods a new permeability measurement then gives values larger than those of the permeability measurement performed after Sor,w is accomplished as shown in **Figure 26**. Similar plots as the one in **Figure 26** are made by routine for all core floods and can be found in **Appendix Q**.

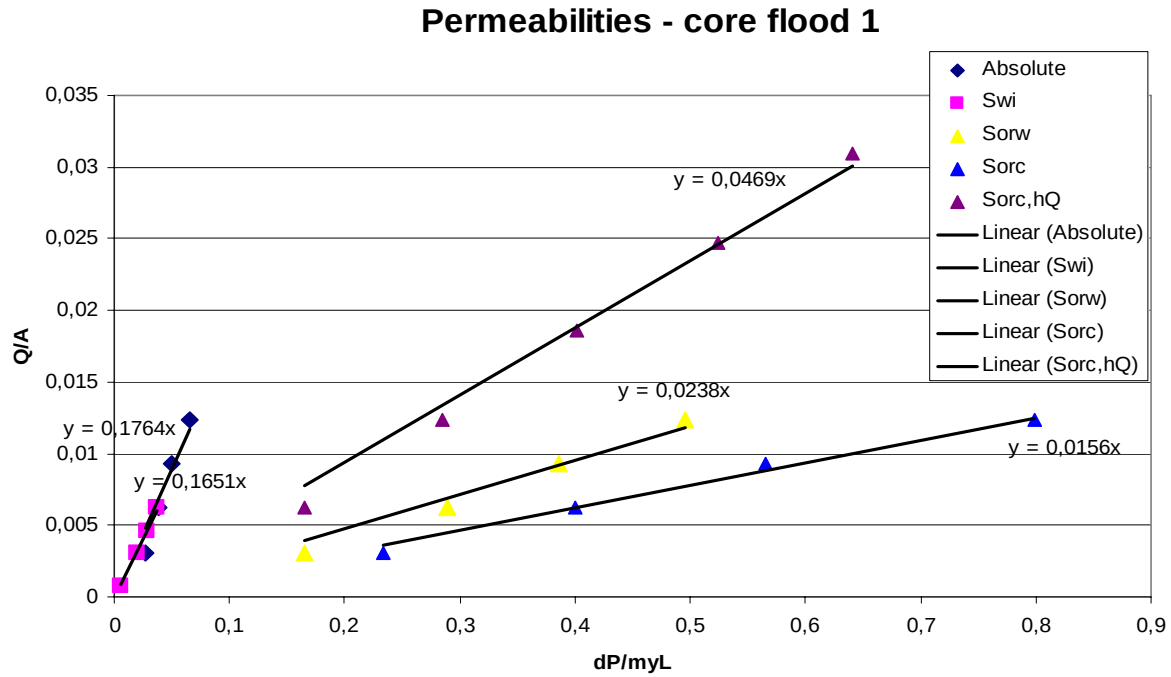

Figure 26. Permeabilities of core flood 1.

5.2.4 Viscous surfactant flooding

Viscous surfactant floodings are used to find the most favourable system for EOR by a combination of polymer, di-alcohol and surfactant. The produced volumes are read of the graded 25 ml cylinder and graded 10 ml tube with an accuracy of respectively ± 0.38 and ± 0.05 ml. The largest source of error for reporting the correct volumes produced is the formation of emulsion in the effluent. Most of that emulsion is not accounted for since it when

produced will sink down from the effluent pipe in the graded tube and diverge out in the water basin below. In addition, with these small volumes, erroneous readings would influence the results highly. Some oil may also get stuck in valves and pipe bends on the way from the core outlet to the production assembly. This oil might eventually be produced, but you never know if that volume adds on to a "good" or "bad" chemical treatment. With the equipment available it is hard to make better saturations determinations.

Another source of error is the change of crude oil batch after experiment number 4. As pointed out earlier in this report the two different batches of crude oil, coming from the same well, sampled in the same manner, show different physical properties. The core material used after experiment 4 was also of another Berea bar. But they were both from the same supplier, purchased within four months of each other so they are probably from the same block, holding mostly the same properties. Even though porosity measurements states that all plugs from the newest bar had 1% higher porosity than the first one. It is also worth taking into consideration that the core material used are Berea sandstone cores that are strongly water wetting compared to the Heidrun Tilje reservoir that is slightly water wetting. How this difference in water wetting would affect recovery need further investigation past the objective of this Master Thesis.

For some experiments between 0.5 and 2.5 ml gas, or most likely air, was produced after chemical injection. It was chosen to work as it did not influence the experiments because the back pressure was 15 bara and the air present would not be free air inside the core at that pressure. All piping is made of acid resistant steel so it was not possible to see if there was any air or gas present before the back pressure valves. The extra production of air was probably dissolved in the formation water, the chemical treatment or the oil. Dummy testing with the upside down placed graded tubing used for collecting of the produced volumes after chemical treatment was performed. It was found that when placing such a graded tube in ordinary distilled water, 0.1 ml of air had evaporated from the water after 3 hours. After 3 days almost 0.4 ml of air had evaporated. But this could only answer for some of the air. After this test, the distilled water used for the production container arrangements always was evacuated. Evacuation routines for formation water and chemical solutions were also stepped up. A vacuum pump was used, and the formation water was evacuated before each new step in the procedure. The oil could not be evacuated because it is impossible to know what

compounds that will be dragged out of it. The pump solvent change program used to change between formation water and chemical treatment goes at a high rate. With some of the very viscous chemical solutions a lot of air was dragged out during the solvent change. Specific caution was applied to the pump, and it was operated to make sure all free air was removed from the system before injection to the core started. After taking these precautions the air production was not an issue. At some occasion's small amounts was produced with the highest viscosity solutions. It was very hard to evacuate to satisfaction, due to the high viscosity.

The best additional recovery of all the experiments was achieved on the first experiment with the chemical composition of low polymer, high di-alcohol and high surfactant. Two replica experiments were conducted during the period to try to verify these good results. But they did not fulfil the expectations. The additional oil production in percentage ranged between 20 and 12 of OOIP for the same chemical treatment. The least recovery of those came out as a number seven when ranged from best to least according to additional oil production of OOIP as can be seen in **Table 13**. All four experiments with the same chemical composition are marked with green shading. The second and third best recovery results of respectively 19% of OOIP with low polymer, high di-alcohol, low surfactant and 16% of OOIP being the centre experiment, contributes little to see a trend in the results. The accuracy of the STOOIP is ± 0.38 ml. Together with the accuracy of the graded tube used for the effluent after the treatment, the accuracy of the additional recovery is ± 3%.

Table 43. Oil recovery results normalized against OOIP ranged after additional recovery

Chemical treatment	Internal experiment number	STOOIP	Initial recovery	Additional recovery	Final recovery
		[ml]	%	%	%
Low polymer, high di-alcohol, high surfactant	1	12.8	45	**20**	66
Low polymer, high di-alcohol, low surfactant	2*	13.1	39	**19**	58
Centre experiment	6	14.8	43	**16**	59
High polymer, high di-alcohol, low surfactant	8	15.3	44	**14**	59
Low polymer, low di-alcohol, low surfactant	3	14.3	43	**13**	56
Low polymer, low di-alcohol, high surfactant	4	12.8	49	**13**	62
Low polymer, high di-alcohol, high surfactant	2	13.8	47	**13**	60

Low polymer, high di-alcohol, high surfactant	5	15.3	44	**12**	57
High polymer, low di-alcohol, low surfactant	7	14.8	43	**12**	54
High polymer, high di-alcohol, high surfactant	10	15.5	50	**10**	60
High polymer, low di-alcohol, high surfactant	9	15.0	40	**10**	50
500ppm polymer, 40mM di-alcohol, 10ppm surfactant	11	13.8	42	**7**	49
1/3 PV: Low polymer, high di-alcohol, high surfactant	12	15.3	44	**5**	49

The capillary numbers presents a theoretical connection between residual oil saturation and the capillary number ratio consisting of the viscosity, IFT and darcy velocisty. The accuracy of the calculations depends on the accuracy of the measurements done. Measurements are reported with one decimal place to take any sources of error into account. The capillary numbers are reduced by two to three orders of magnitude concurring with literature on the subject, although the recovery achieved is smaller than the theoretically expected one. The calculations have taken the change in crude oil batch into consideration. Experiment 1, 2 and 2* have used a IFT value of the correct chemical treatment without the 1000 ppm polymer measured against the first batch of crude oil. Experiment 4 used a value from the correct chemical treatment without the 1000 ppm polymer measured against the second batch of crude oil. The IFT value of 1000 ppm polymer with 10 mM di-alcohol and 20 ppm surfactant was terminated at an early stage, and by following the curve patterns it is plausible that it would have ended at 6.5 mN/m, which is the value used. For the centre experiment using a 1500 ppm polymer solution, no IFT measurements are performed. Based on the other results, an IFT of 8.0 mN/m is assumed and used for the capillary number calculations.

When applying statistical models it is important to know if the model represents the data in a content way. The model fit tells how well we are able to mathematically reproduce the measured data. A quantitative measure of the goodness of fit is given by the parameter R^2 (= the explained variation). The problem with goodness of fit is that with sufficiently many free parameters in the model, R^2 can be made arbitrarily close to the maximal value of one (1.0). More important than fit, however, is the predictive ability of the model. This can be estimated by how accurately we can predict the X-data, either internally via existing data or externally through the use of an independent validation set of observations. The predictive power of a

model is summarized by the goodness of prediction parameter Q^2. The R^2 and Q^2 parameters display entirely different behaviour as the model complexity increases. The goodness of fit, R^2, varies between 0 and 1, where 1 means a perfectly fitting model and 0 no fit at all. R^2 is inflationary and approaches unity as a model complexity increases. Hence, it is not sufficient to have a high R^2. The goodness of prediction, Q^2, on the other hand, is less inflationary and will not automatically come close to 1 with increasing model complexity. This provided that Q^2 is correctly estimated[42].

Hence, a valid model means that it predicts much better than chance. In addition, it should have model parameters with little bias, that is, the model parameters should have the correct sign and be large for important variables and small for unimportant variables. Finally, it should be consistent with fundamental chemical, technical and engineering knowledge.

Figure 27 gives a picture of the goodness of fit for our statistical model. R^2 is only at 0.6 meaning that only 60% of the data variation for recovery of OIP is explained. This is not good. A Q^2 of 0.065 is not either. The model validity though seems good, but the reproducibility is negative in respect to recovery of OIP confirming that the data is poorly reproduced by the model.

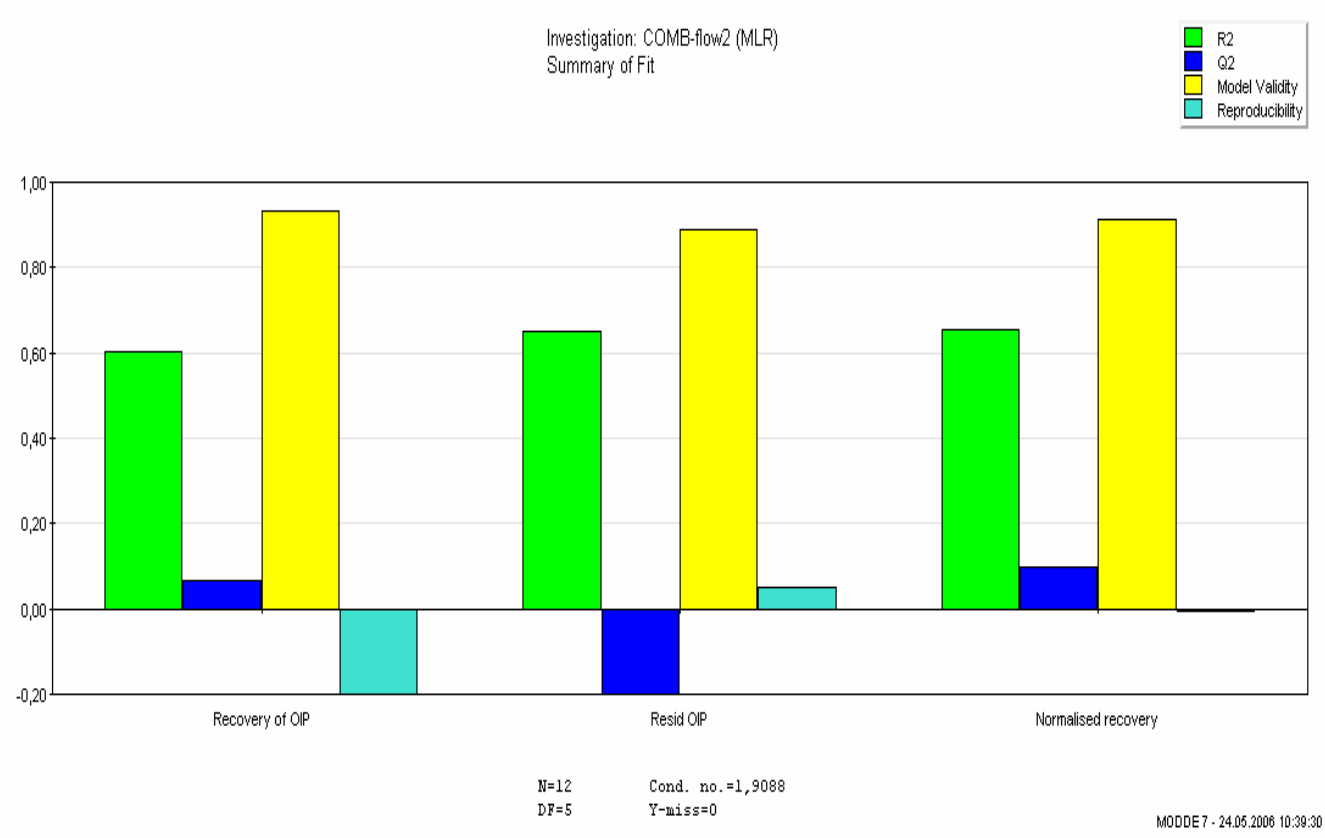

Figure 27. Goodness of statistical model fit.

The residuals in a statistical model are the deviations between the real data and the model. If all residuals in **Figure 28** would locate along a straight line, the statistical model would represent a good fit with the experiment data. As seen in **Figure 28**, two possible straight lines are drawn, neither locating all the residuals along their side. Another confirmation of the bad model fit.

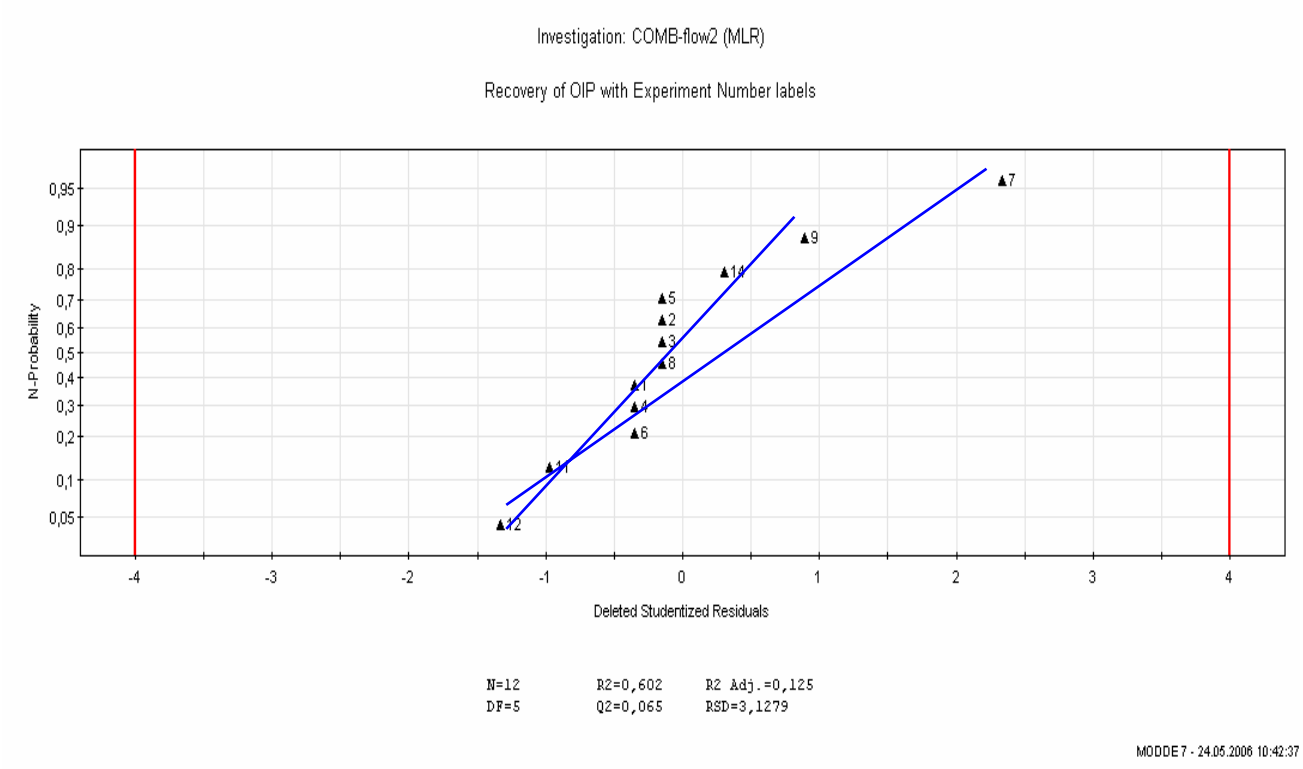

Figure 28. Fit of statistical model by residuals

Outliers are interferents and erroneous measurements. In **Figure 29** the outliers of the plot are marked with circles. The straight blue line symbolizes where they should be. Experiment 7 and 9 are the outliers above the blue line. They are both 2000 ppm polymer experiments, and differ only slightly from experiment number 10 in terms of additional oil recovery. But both experiments had lower initial recovery, and thus also a lower final recovery. Experiment number 11 and 12 making up the second outlier cluster are the two extra experiments. Number 12 is just 1/3 PV of chemical and number 11 has only 500 ppm polymer. They both give lower additional and final recovery than the other core floods. But worth to notice is that they both perform very similar in terms of recovery.

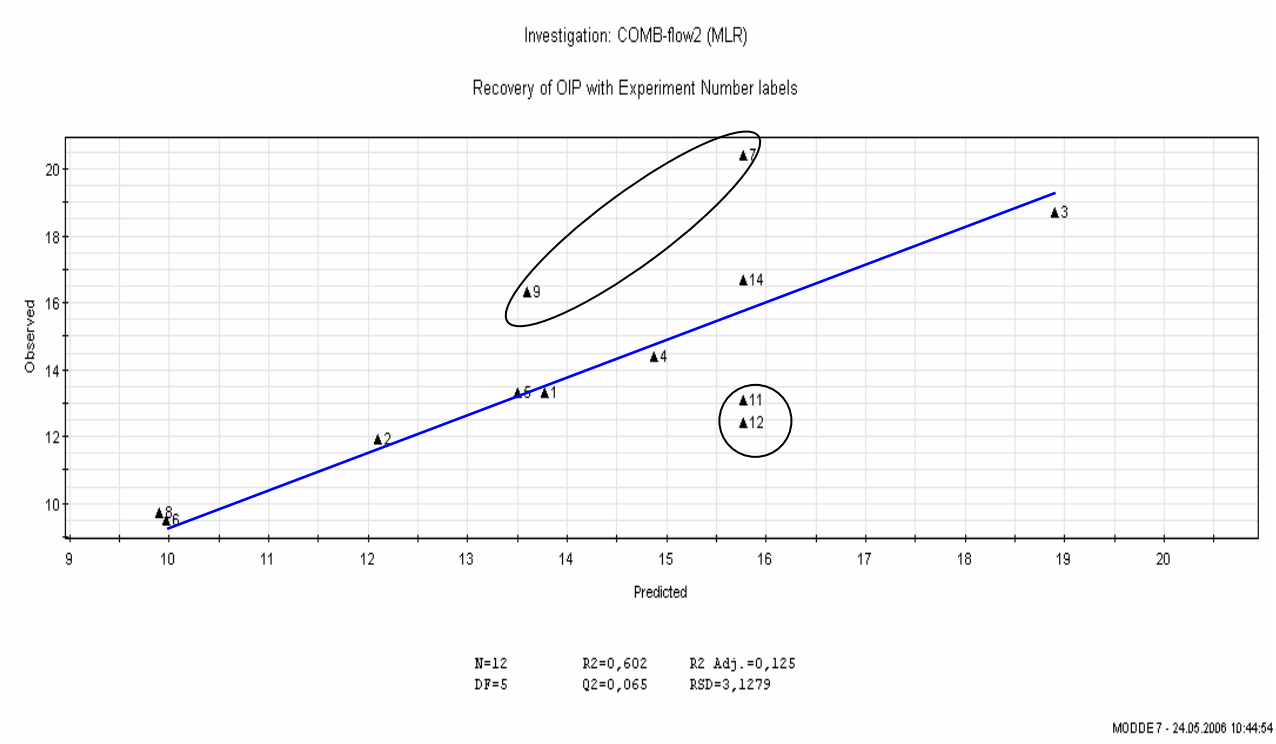

Figure 29. Outlier plot

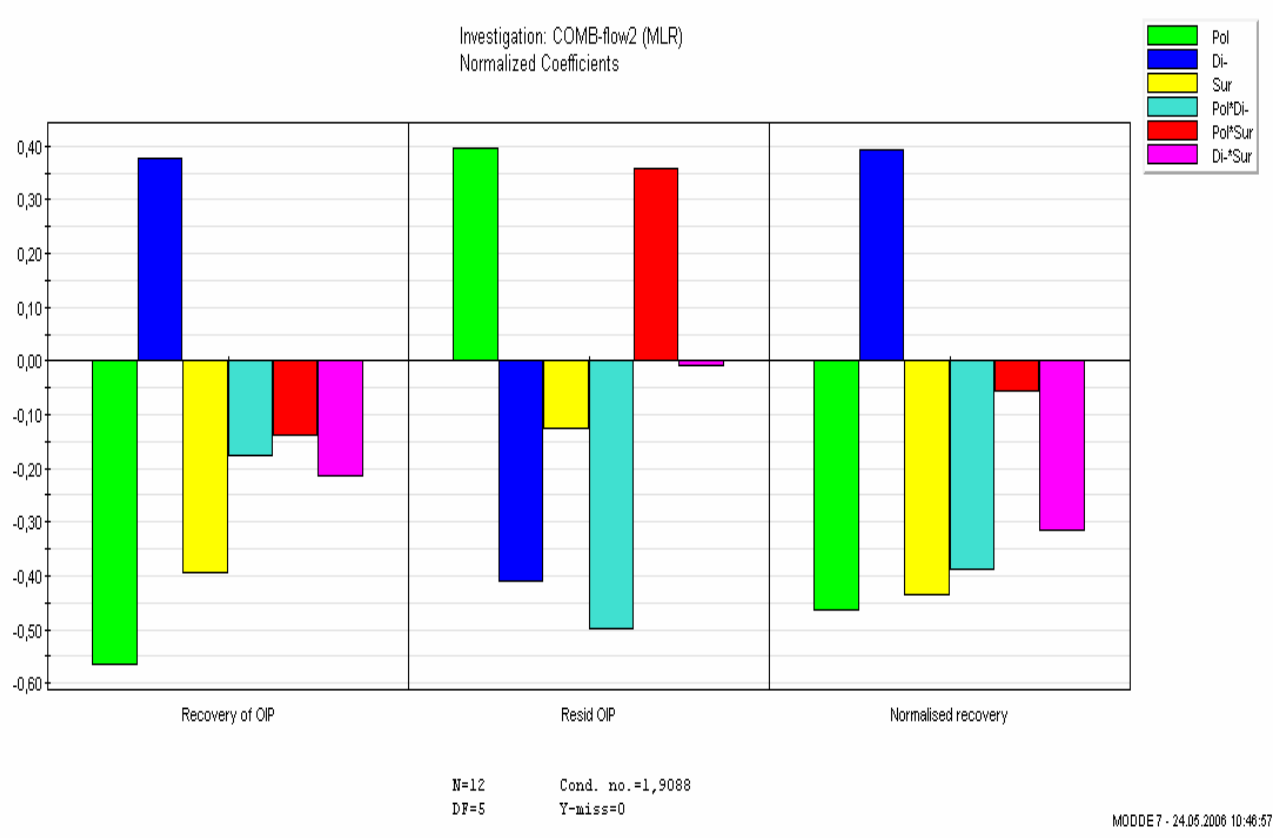

Figure 30. The different variables effect on the response factors

As seen from **Figure 30** the only positively correlated variable for the recovery of OIP response factor is the di-alcohol. A lot of additional oil is produced, so if it was not for the di-alcohol, there would be no doubt that the whole model is not correct. The effect of the polymer is strongly negatively correlated for recovery of OIP. Yet we know that the experiments with pure polymer treatments had an additional recovery of 12 to 13% of OOIP. Indulging MODDE's request for a lower polymer concentration to optimize the recovery still yielded poorer recovery confirming that the statistical model is incorrect.

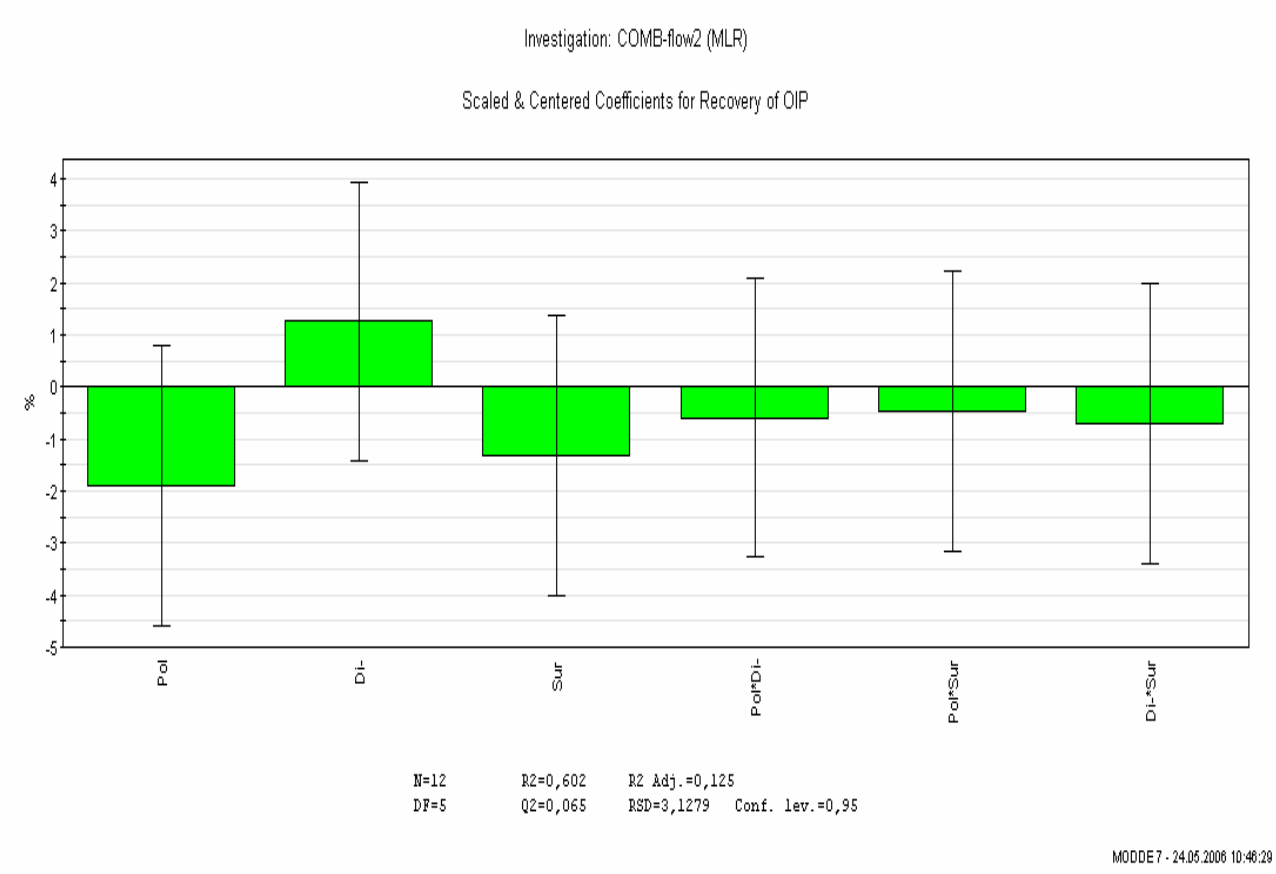

Figure 31. Standard deviations of the effects for recovery of OIP.

The standard deviations are represented by the vertical lines in **Figure 31.** The standard deviations are large, but with this kind of uncertainty all effects might have a positive correlation. To reduce the standard deviation one should perform more experiments as well as more replicate experiments.

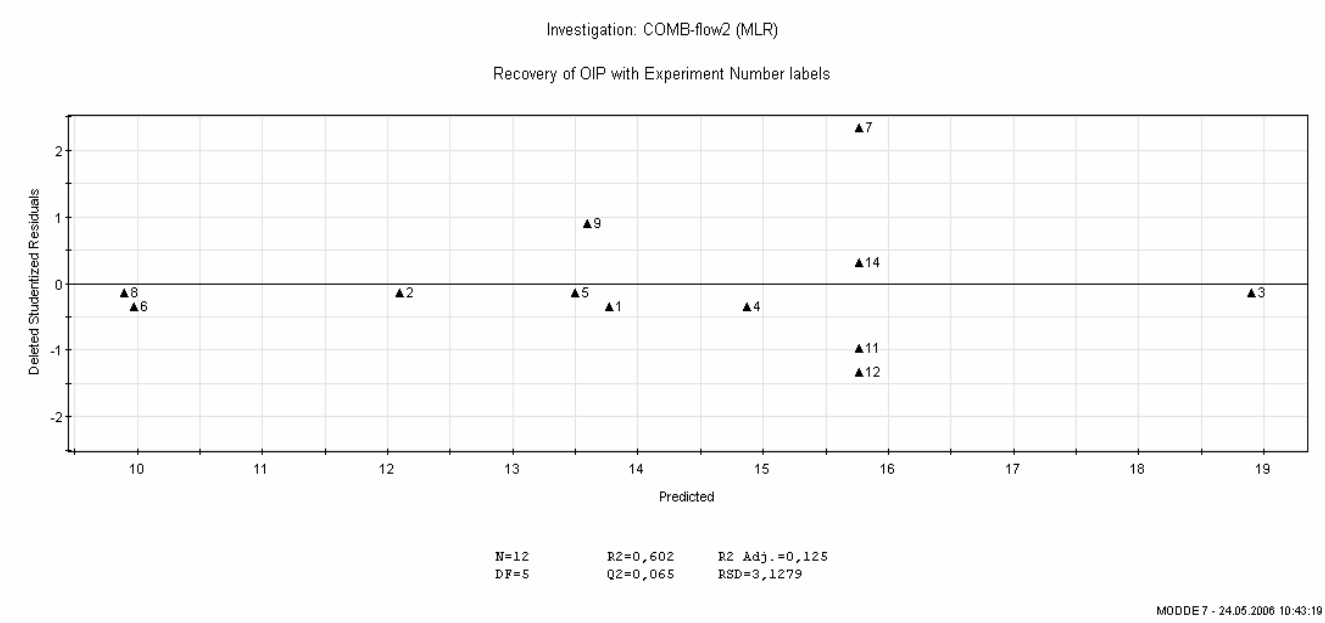

Figure 32. Residuals

Figure 32 shows the residuals, which are unevenly distributed. That is one of the characteristics of a good statistical model.

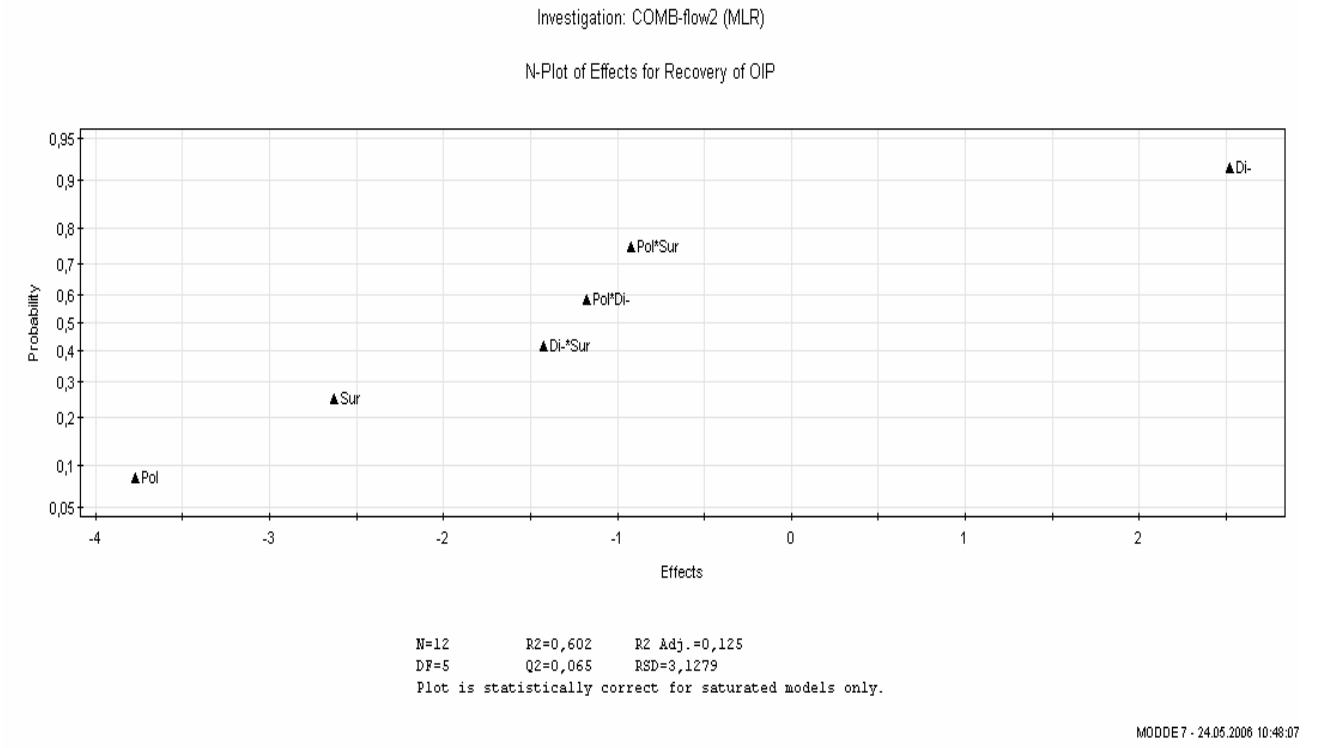

Figure 33. Effect versus probability

The probability for di-alcohol to have a positive influence on the recovery of OIP is 90 % as seen in **Figure 33**. All the other effects are likely to influence the recovery of OIP in a negative respect. We know that the polymer has a significant positive effect to the recovery of OIP. This is another proof of lack of fit in the statistical model.

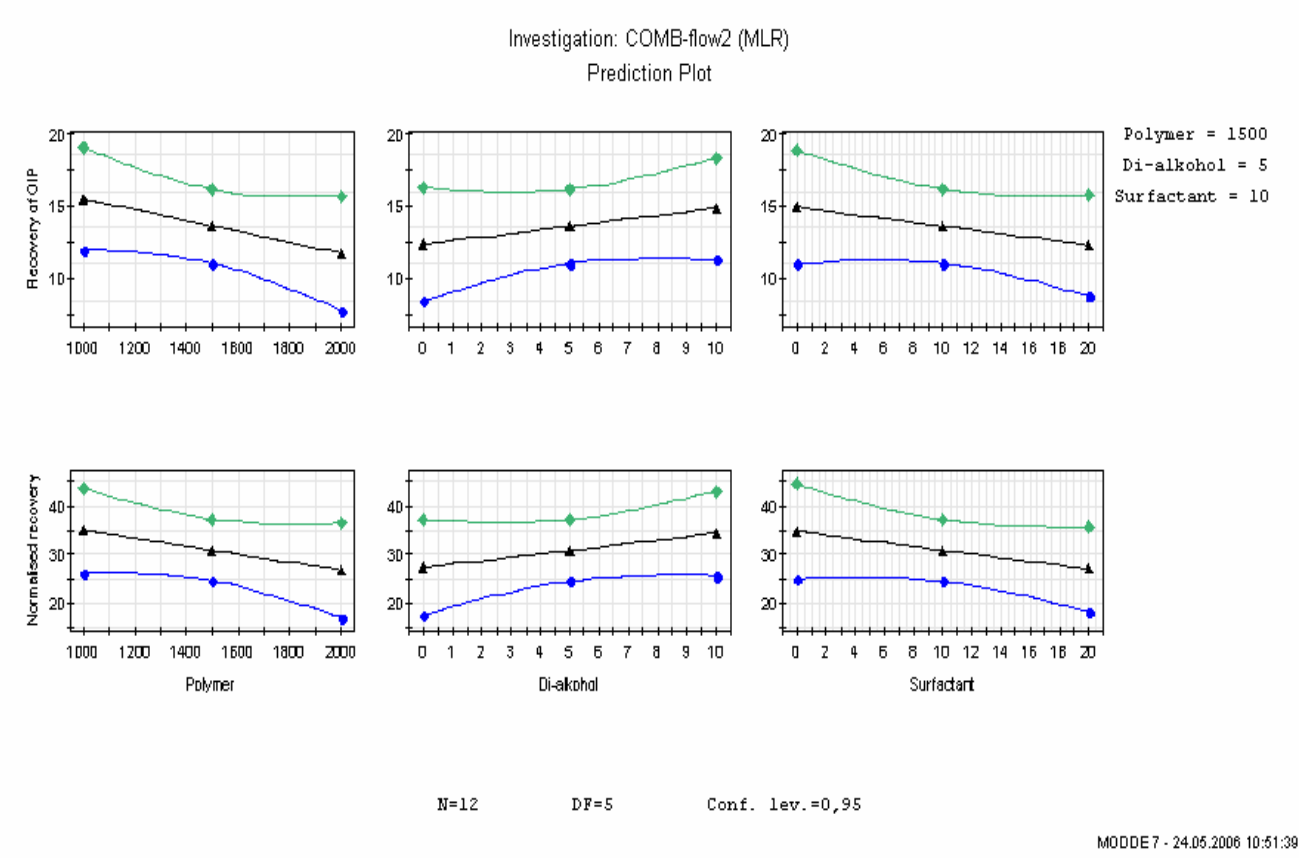

Figure 34. Prediction plot

As seen in **Figure 34** the di-alcohol is the only variable that shows a positive trend for increasing concentration. The upper and lower curves in each plot are the boundary values, while the one in the middle is the average.

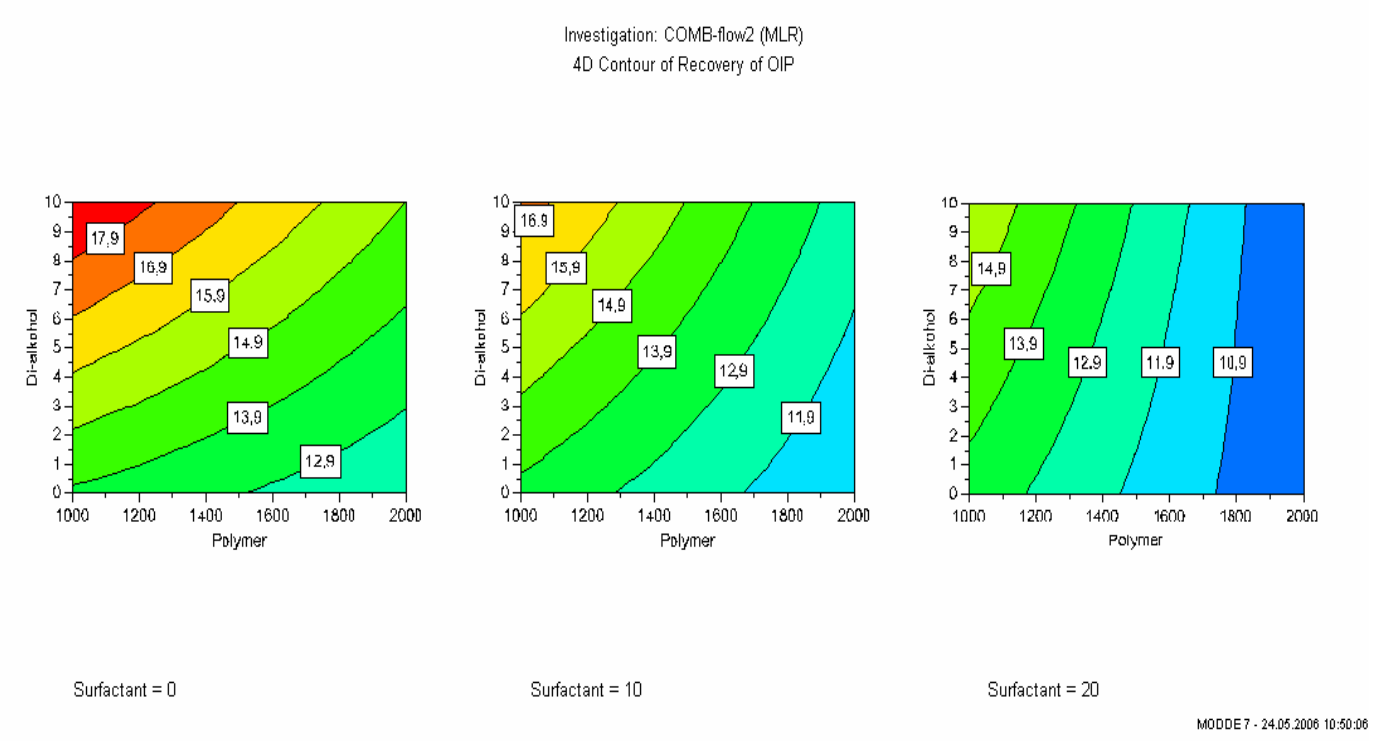

Figure 35. Contour plot of recovery of OIP

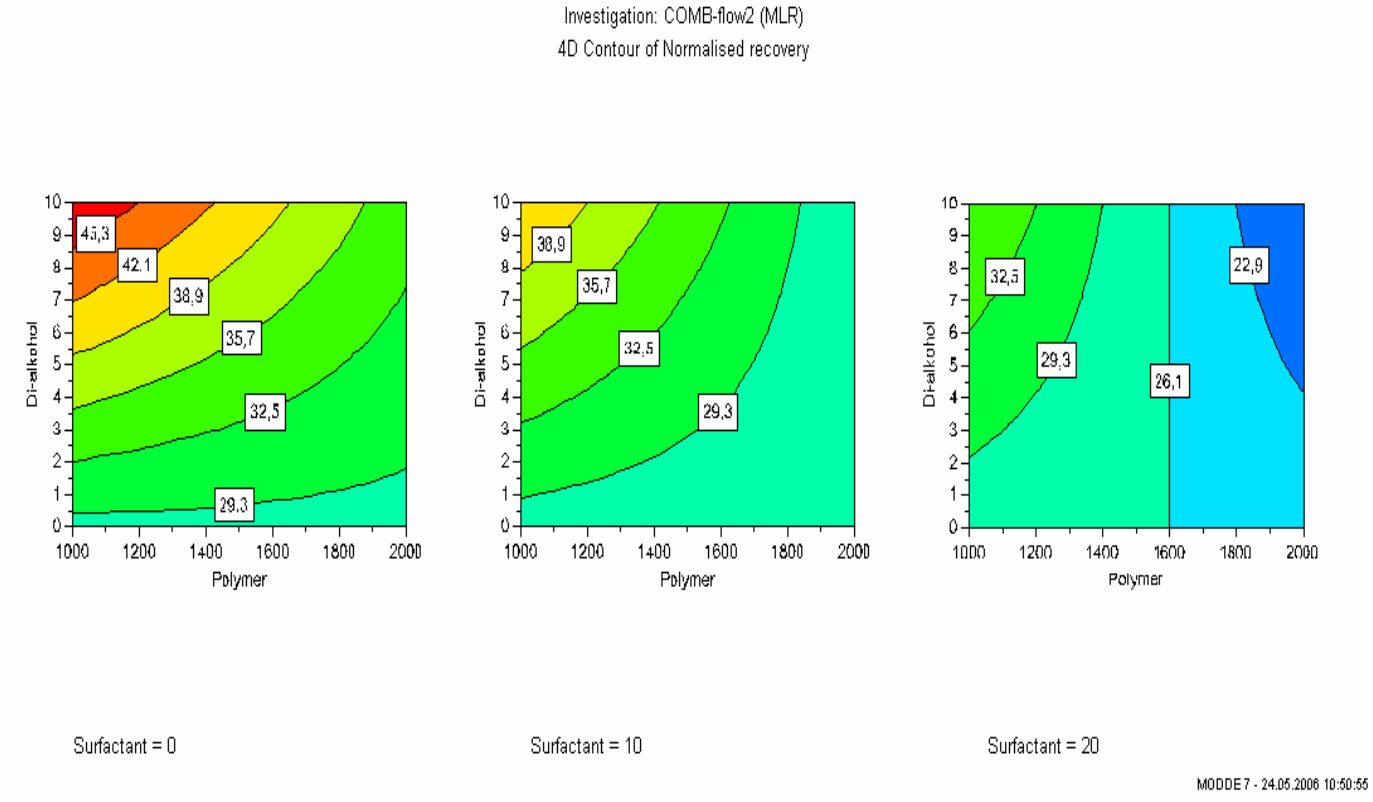

Figure 36. Contour plot of normalised recovery

Figure 34 and **36** displays contour plots of di-alcohol versus polymer concentration at different surfactant concentrations. The recovery achieved is reported in the squares on each curve. The curves in the plots represent the interaction effects between the di-alcohol and the polymer. If all curves were parallel one would have a well described statistical model, but these curves tells us that there are undescribed interaction effects present. The best recovery for all surfactant concentration is achieved with maximum di-alcohol concentration and minimum polymer concentration. Nevertheless, the data will be too scarce to say anything about interaction effects between the various variables.

Our choice of variables has been crucial to the statistical model. The low value of both di-alcohol and surfactant were chosen to be 0, while the polymer low value was 1000. By doing so the polymer contribution evaluated is between 1000 and 2000 ppm. The results presented by the model saying that to increase the polymer concentration from 1000 to 2000 ppm does not influence the recovery of OIP in a positive way is probably correct. To increase the polymer from 0 to 1000 ppm though, do as we know contribute with a very positive effect. Internal experiment number 11 was performed with a chemical treatment of 500 ppm polymer. It gave poorer results than the 1000 ppm polymer experiments indicating that a level of 1000 ppm polymer seem optimal. The effect of surfactant is negatively correlated in the model. This is strange. It could be that the inaccuracy in the process of adding the surfactant is too great. Although IFT measurements of increasing concentration of surfactant show that the IFT is reduced according to the increased concentration. The conclusion of the statistical analysis must be that the statistical design did not give a good model to describe the observed results. Therefore, the statistical model is considered incorrect.

To perform a cost / benefit evaluation of the system for the Heidrun Tilje formation would be of great interest, especially when considering the history with Xanthan. There is enough data in this report to perform such an analysis, but I was not able to get any real offers from suppliers regarding bulk prizes. It is recommended that such an evaluation is performed before further laboratory activities are initiated.

5.2.5 Microfibril flooding

The experiment with the microfibril flooding system could not be performed due to the microfibril particles separating out in the pump. This resulted in a blockage of the piping and a pressure build up. The separation of the microfibrils in the pump is shown in **Figure 37.** Finally it was decided to terminate the experiment. Pictures of the core after microfibrill flooding are found in **Figure 38.** A picture of the blockage in the core holder inlet is found in **Figure 39**.

Figure 37. Pictures of the pump cylinder under microfibrill flooding. At the top the microfibrils have separated out of solution. In the bottom picture a microfibril-cake has formed blocking the outlet.

Figure 38. Pictures of the core after microfibrill flooding

Figure 39. Pictures of the core holder inlet after microfibrill flooding. Microfibrils has blocked two of the inlet pipes.

Correspondence with the Paper and Fibre Research Institute, PFI in retrospect has revealed that they also have observed that the microfibrils might deposit at the bottom if the solution is diluted. The microfibrils make a network keeping them stable and by that manage to stay in dispersion. When diluted over a critical overlap concentration, the network collapse and the microfibrils deposit at the bottom.

6 CONCLUSIONS

- Viscous surfactant flooding has managed to increase recovery of OOIP with between 7 to 20%. A 1/3 PV injection gives additional recovery of 5% of OOIP. Total recoveries achieved ranged from 49 to 66 % of OOIP.
- Pure viscosity floods give additional recovery of 12 to 13% of OOIP. The di-alcohol has shown good effect through the statistical model. Yet the pure results of the core floods are not uniform enough to say anything about the effect of di-alcohol and surfactant.
- It is not a problem to use the viscous surfactant system in field operations concerning compatibility. The chemicals need further environmental tests to verify if they are applicable in field operations.
- The MODDE software did not work well enough. The statistical modelling failed because of too narrow variable value area for the polymer and generally too few experiments to take advantage of the power of this data analysis method.
- Microfibril particles used as a viscosity enhancer is not recommended when in the specific diluted solution as in this work.

7 RECOMMENDATIONS

- Perform cost / benefit analysis to verify if this is a feasible EOR method before further laboratory investigations are initiated.
- Perform the correct environmental tests on the chemicals to verify if they are applicable for field operations in Norway before further laboratory investigations are initiated.
- Perform more experiments to further investigate the effect of the different variables.
- Perform experiments closer to reservoir temperature and pressure.
- Perform reservoir simulations to further investigate the volumetric sweep efficiency of the viscous surfactant system.

8 NOMENCLATURE

A	Cross-sectional area
CDC	Capillary desaturation curve
CMC	Critical micelle concentration
EOR	Enhanced oil recovery
Hast C-276	Hastelloy C-276, an alloy
HD	Heidrun
HD FW	Heidrun formation water
HLB	hydrophilic/lipophilic balance
HSE	Health, safety and environment
IFT	Interfacial tension
k	Permeability
k'_{rd}	End point relative permeability of displacing fluid
k'_{ro}	End point relative permeability of oil
L	Distance
M	Mobility ratio
MLR	Multiple linear regression
N_C	Capillary number
OIP	Oil in place
OOIP	Original oil in place
PV	Pore volume
P	Pressure
ΔP	Pressure difference
q	Volumetric rate
STOOIP	Standard original oil in place
TDS	Total dissolved solids
u	Darcy velocity, of displacing fluid
Vb	Bulk volume
Vp	Pore volume
wt%	Weight percent

Greek letters

μ	Viscosity, dynamic
μ_d	Viscosity of displacing fluid
μ_o	Viscosity of oil
ν	Viscosity, kinematic
σ	Interfacial tension
φ	Porosity

9 LIST OF TABLES

10 LIST OF FIGURES

11 LIST OF REFERENCES

[1] Stensen, A.J.: "Olje og gass fortsatt viktigst," Teknisk Ukeblad (December 2005); Nr 35.

[2] Bravo, J.: "Evaluation of Water Assisted Improved Oil Recovery Methods," Master thesis, NTNU, 2005.

[3] Oral information from Professor Ole Torsæter, Department of Petroleum Engineering and Applied Geophysics, NTNU, fall 2005.

[4] Pedersen, R.L.: "Teksturell og mineralogisk karakterisering av sandsteinsprøver fra Haltenbanken; innvirkning på finstoffmobilisering og tetting av gruspakker," Project thesis, NTNU, Jan. 2005.

[5] Oral information from Specialist Hans Kristian Kotlar, Department of F&T LPT BPL, Statoil, fall 2005.

[6] Ursin, J.R., Zolotukhin, A.B.: "Introduction to Petroleum Reservoir Engineering", Høyskoleforlaget AS, 2000.

[7] Green, D.W., Willhite, G.P.: "Enhanced Oil Recovery", SPE Textbook Series, 1998, 2003.

[8] Kleppe, J., Skjæveland, S.M.: "SPOR Monograph – Recent Advances in Improved Oil Recovery Methods for North Sea Sandstone Reservoirs," Norwegian Petroleum Directorate, 1992.

[9] Lake, L.W.: "Enhanced Oil Recovery," Prentice Hall, 1989.

[10] http://en.wikipedia.org/

[11] Mørk, P.C.: "Overflate og kolloidkjemi – grunnleggende prinsipper og teorier," NTNU, 2001.

[12] PowerPoint presentation by René Tarbary, IFP, January 2006.

[13] Dake, L.P.: "Developments in Petroleum Science 8 – Fundamentals of Reservoir Engineering," Elsevier Science B.V., 1978.

[14] Denim, W., Qun, L., Xiaohong, G., Yan, W.: "The Engineering and Technical Aspects of Polymer Flooding in Daquing Oil Field", paper SPE 64722 presented at the Int. Conference and Exhibition held in Beijing, China, November 2-6 1998

[15] Du, Y., Guan, L.: "Field-Scale Polymer Flooding: Lessons Learnt and Experiences Gained During Past40 Years", paper SPE 91787 presented at the SPE Int. Conference held in Puebla, Mexico, November 8-9 2004.

[16] Needham, R.B., Doe, P.H.: "Polymer Flooding Review," paper SPE 17140, SPE Distinguished Author Series, December 1987.

[17] Wang, D., et.al.: "Application Results and Understanding of Several Problems of Industrial Scale Polymer Flooding in Daquing Oil Field," paper SPE 50928 presented at the SPE Int. Conference and Exhibition held in Beijing, China, November 2-6 1998.

[18] McInerney M.J., et.al.: "Development of Bio-surfactant Based Microbial Enhanced Oil Recovery Procedure," paper SPE 89473 presented at the 2004 SPE/DOE Fourteenth Symposium on Improved Oil Recovery, Tulsa, April 17-21 2004.

[19] McInerney M.J., et.al.: "Tertiary Oil Recovery with Microbial Biosurfactant Treatment of Low-Permeability Berea Sandstone Cores," paper SPE 94213 presented at the 2005 SPE Production and Operations Symposium, Oklahoma City, April 17-19 2005.

[20] Schlumberger Oilfield Glossary: http://www.glossary.oilfield.slb.com/Display.cfm?Term=XC%20polymer

[21] Oral information from Department Manager Birgitte Schilling, F&T LPT, Statoil, spring 2006.

[22] E-mail correspondence with Senior Research Scientist Kristin Syverud, Paper and Fibre Research Institute PFI, spring 2006.

[23] KSV Sigma 701 Tensiometer operations manual.

[24] http://www.ksvltd.com/content/index

[25] Anton Paar SVM 3000 operations manual.

[26] Viscositymeter bath, operations manual Statoil laboratory.

[27] Selle, O.: Density and viscosity measurements, summer 2001, Statoil R&D Centre.

[28] http://www.erc.ufl.edu/facility/equipment.asp?n=43

[29] Technical specifications Paar Physica UDS 200 Rheometer, Jan Schaffer at Dipl.ing Houm AS.

[30] http://www.foodproductdesign.com/archive/1992/0992QA.html

[31] http://iehmtu.edata-center.com/toc/chapt_v/ch22s71.html

[32] Torsæter, O., Abtahi, M.: "Experimental reservoir engineering laboratory work book," NTNU, 2003.

[33] Helium porosimeter, operations manual Statoil laboratory.

[34] Anton Paar DMA 48 operations manual.

[35] Mettler Toledo ML31 operations manual.

[36] Selle, O.: "An Experimental Pre-study of Bio-surfactants for Enhanced Oil Recovery, NTNU, December 2005.

[37] E-mail correspondence with J. Kieffer, SNF Floerger, spring 2006.

[38] Alsberg, B.K.: Lecture notes in "Basic Chemometrics, SIK3049".

[39] Esbensen, K.H.: "Mulitivariate Data Analysis – In Practice," CAMO ASA, 2001.

[40] E-mail correnspondance with Anne Rossbach Hammer, Statoil R&D Centre, spring 2006.

[41] Whitson, C.H.: "Petroleum Engineering Fluid Properties Data Book," NTNU, 1994.

[42] Erikson, L., Johansson, E., Kettaneh-Wold, N., Wold, S.: "Multi- and Megavariate Data Analysis. Principles and Applications", Umetrics AB, 2001.

12 APPENDIX

A HEALTH, SAFETY AND ENVIRONMENT (HSE) ISSUES

Statoil has a very comprehensive policy regarding HSE which involves all activities in the company. All apparatuses in Statoil laboratories are under the subject of HSE surveillance. In addition there is an "Equipment card" following the apparatus that states the maximum conditions for the apparatus in addition to special elements of danger associated with the specific apparatus. "Fløммerigg 3-518" was not classified for a confining pressure system, as well as the use of crude oil and toluene. HSE analysis was performed and the certification altered. Working with pressure equipment will in most cases represent some element of danger. To go through a training document for flooding apparatuses and pressure equipment is mandatory for all personnel working with new and unfamiliar equipment at Statoil Formation Technical Laboratory. All persons authorized to operate the apparatus will be listed in the "Equipment card".

"Fløммerigg 3-518" is equipped with several safety measures. The back pressure valves are adjusted to 15 bara (maximum 20.6 bara). The back pressure need as a minimum to be as high as the vapour pressure of water at 170 ºC, that is 7.9 bara. To ensure that there is no gas trapped in the water phase a back pressure of 15 bara is chosen. A back pressure valve will bleed off the pressure exceeding the chosen pressure limit. The various tubing in the apparatus will not experience a higher pressure than the back pressure as long as none of the valves towards the pump is closed. The pumps also got maximum pressure regulators at a maximum of 30 bara. In front of the pump cylinders (of glass) there are installed polycarbonate covers to reduce the size of a potential explosion. The apparatus also have an emergency power switch, in case of incidents that demands instant shut-down of the system. In addition to these measures a ventilation pipe is installed in the heating cabinet in case of heating of volatile compounds.

B STRATIGRAPHIC AND FACIES ASSOCIATIONS FOR GEOLOGY IN THE HALTENBANKEN AREA

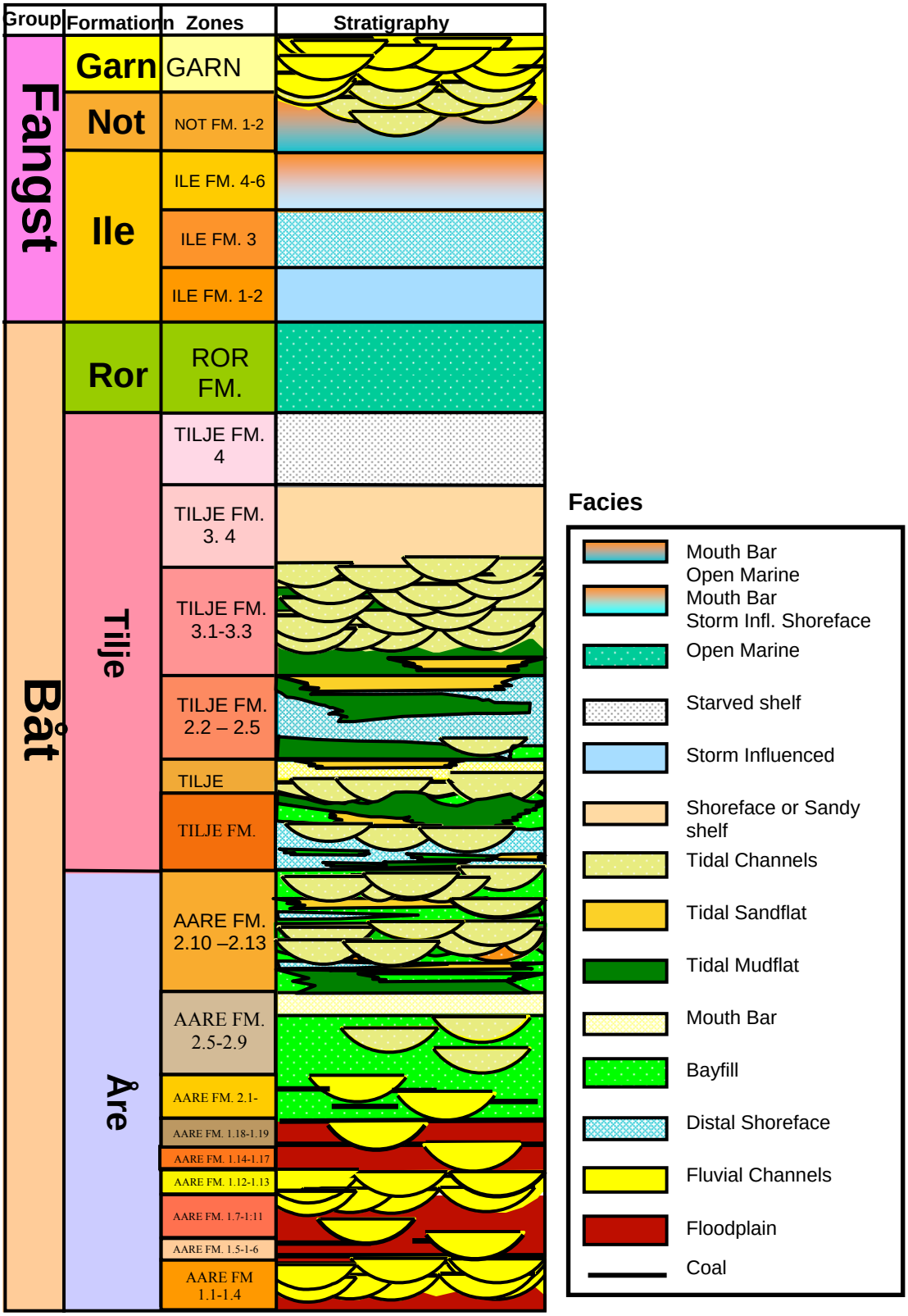

C CONNECTION DIAGRAM, CURRENT

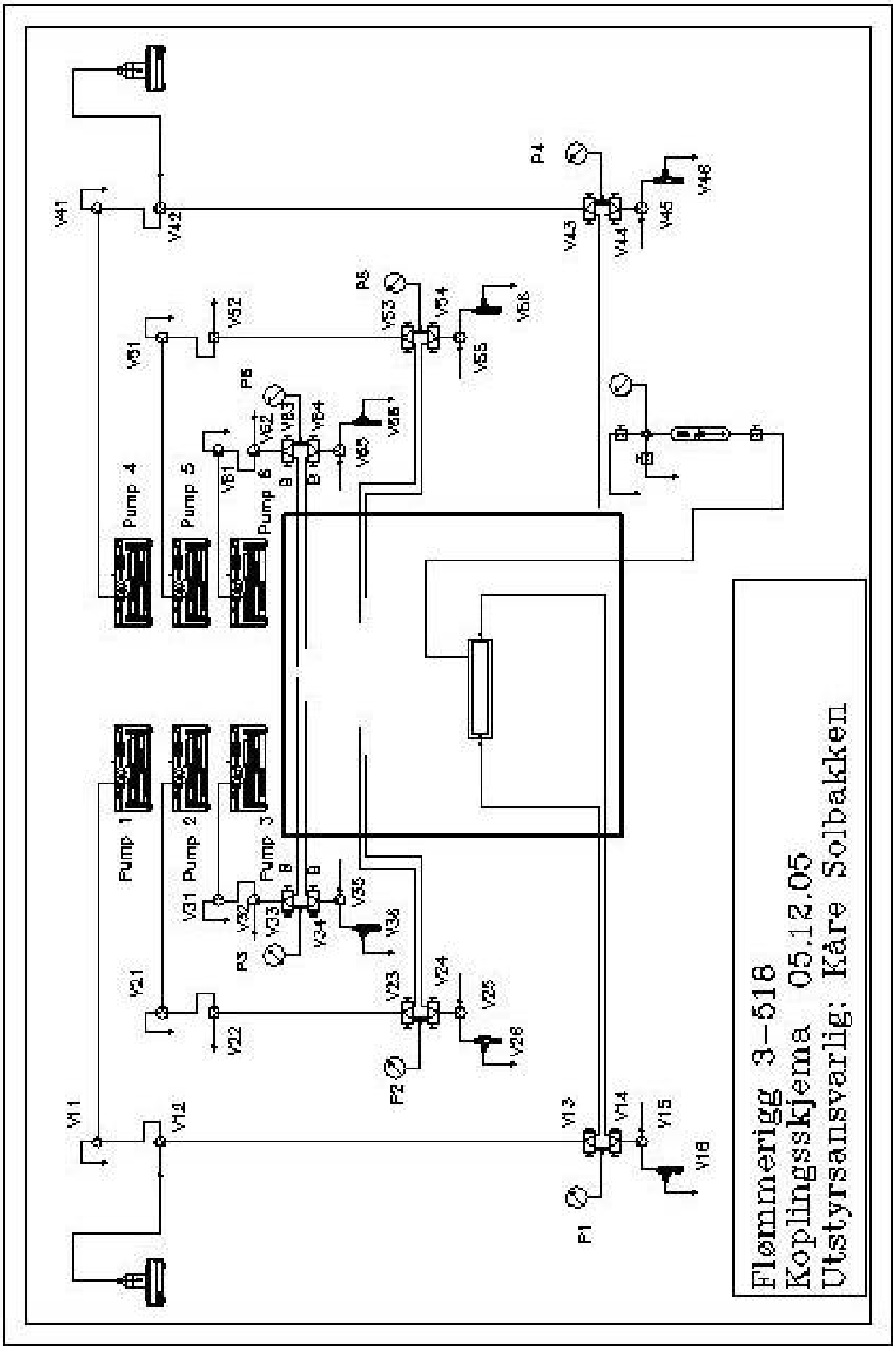

D SKETCH OF CORE HOLDER

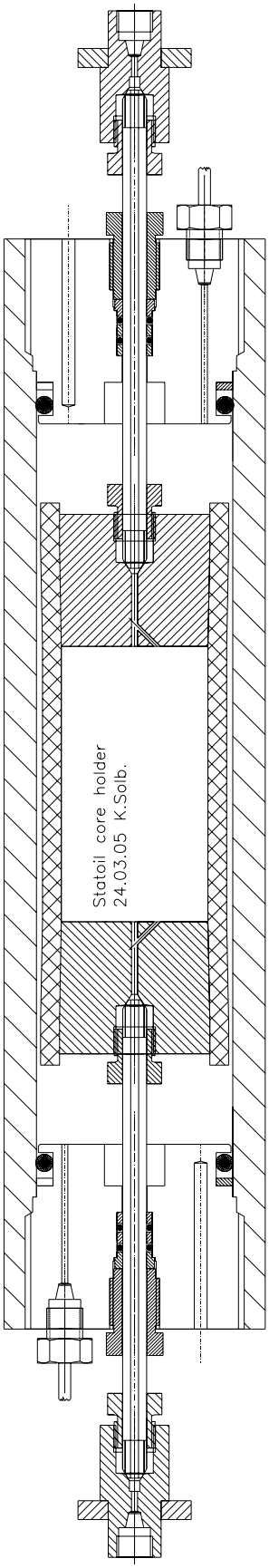

E DISMOUNTED CORE HOLDER WITH ALL COMPONENTS

F OUTLINE OF COMPONENTS USED IN THE APPARATUS

Equipment

Equipment name	*Manufacturer*	*Name in rig*	*Mod nr.*	*Technical data*	*Accuracy*
Pharmacia pump	Pharmacia	Q2	P500, oil	Q: 0-499 cc/hr, P: 0-30 bara	
Pharmacia pump	Pharmacia	Q3	P500, water	Q: 0-499 cc/hr, P: 0-30 bara	
Pharmacia pump	Pharmacia	Q1	P6000, water	Q: 0-99.9 cc/min, P: 0-20 bara	
Heating cabinet	Memmert	Varmeskap	ULP 400	Temp 20 ºC – 200 ºC	
Weight	Mettler-Toledo	Vekt 1	PG5002-S	0 – 5100 grams	0,01 gram
Pressure transmitter	Keller	P1 – P6	LEO 3	0 – 30 bara	0,001 bar
Pressure flask			316L-HDF4-500	V: 500 ml, P: 1800psi = 124 bar	
Temperature transmitter		XX-HPT-1	PT-100	Temp 20 ºC – 200 ºC	0,001 ºC

Valves

Manufacturer	*Modell*	*Dim*	*Material*	*Max working P*	*Conditions [ºC]*	*Comment*
Autoclave	10V2085	1/8”	SS 316	1100 psi = 758 bar	450 ºF = 232 ºC	Reg stem, 3 way
Autoclave	201B-8813	1/8”	SS 316	10150 psi = 700 bar	450 ºF = 232 ºC	Reg stem, 3 way
Swagelok	SS-42S4	¼”	SS 316	2500 psi = 172 bar	65 ºC	Ball valve, 3way
Swagelok	SS-41XS2	1/8”	SS 316	172 bar	65 ºC	Ball valve, 3way
Swagelok	SSRL3S4	¼”	SS 316		20 ºC	Applicable up to 20,6 bar

Piping

Label	*O.D. [”]*	*I.D. [mm]*	*Material*	*Max working P*
Black	1/4”	1,23	SS 316	7500 psi = 517 bar
Blue	1/8”	1,4	Hast C-276	11000 psi = 758 bar
Black	1/8”	1,6	SS 316	11000 psi = 758 bar
Blue	1/16”	1,05	Hast C-276	500 bar
Unmarked	1/8”	1,65	Teflon	26 bar
Unmarked	1/16”	0,76	Teflon	26 bar

G HEIDRUN TILJE CRUDE OIL – SAMPLING AND COMPOSITION

The crude oil sample was taken from the flowline of well A-48. This is an Upper-Tilje well with no water cut. The sample was taken after chemical dosage was stopped so that the oil should contain no additives as scale-treatment, phase-treatment and so on. The possibility of some chemical content is present. Because the test-separator is not working optimally at low water-cuts, it is also possible that the oil could contain some water, though less than 1 %.

Composition and oil data

Well		**A-48**
DST no.		
Sample		**SEP**
Laboratory		**CoreLab**
Perf. top	*m TVD MSL*	2393,7
Perf. bottom	*m TVD MSL*	2455,5
Average depth	*m TVD MSL*	2424,6
GOC depth	*m TVD MSL*	2305,5
Depth below GOC	*m TVD MSL*	119,1
OWC depth	*m TVD MSL*	
Depth above OWC	*m TVD MSL*	
Formation		T3.2-3.4
Segment		I
Tres	*C*	85
Pres	*Bara*	240
Psat	*Bara*	208
Undersaturation	*Bara*	32
Density@bubble point	*kg/m3*	829,3
Viscosity@bubble point	*mPas*	2,632
From SPLIT factors:		
Rs	*Sm3/Sm3*	62,5
Bo@Pres	*m3/Sm3*	
Bo@Psat	*m3/Sm3*	1,178
Density STO	*kg/M3*	927,8
Density STO	*API*	20,90
From sep test experiments:		
Rs	*Sm3/Sm3*	
Bo@Pres	*m3/Sm3*	
Bo@Psat	*m3/Sm3*	
Density STO	*kg/M3*	
Density STO	*API*	

Composition	*mole %*	
N2		***0,160***
CO2		***0,820***
C1		***42,130***
C2		***1,820***
C3		***0,400***
i-C4		***0,170***
n-C4		***0,180***
i-C5		***0,140***
n-C5		***0,060***
C6		***0,290***
C7		***1,320***
C8		***1,830***
C9		***1,400***
C10+		***49,290***
Mole weights	*g/mole*	
C6		***83,140***
C7		***91,490***
C8		***106,330***
C9		***119,930***
C10+		***314,010***
Density	*g/cm3*	
C6		***0,675***
C7		***0,753***
C8		***0,766***
C9		***0,777***
C10+		***0,933***

Bold: Corrected as shown in PVT report

H RECIPE HEIDRUN TILJE SYNTHETIC FORMATION WATER

Salt	Amount of salt [g/5l]	Component	Concentration [mg/l]
NaCl	247,96	Na^+	19510
KCl	5,2	K^+	545
$CaCl_2 * 2\ H_2O$	18,71	Ca^{2+}	1020
$Mg_2Cl * 6\ H_2O$	11,08	Mg^{2+}	265
$SrCl_2 * 6\ H_2O$	2,21	Sr2+	145
$BaCl_2 * 2\ H_2O$	2,52	Ba2+	285
		Cl^-	33190

The brine is filtered with a 0.45 µm Cellulose-Nitrate filter, and evacuated before the pH is adjusted to 5.9.

I DETAILED FLOODING PROCEDURE

Flooding procedure in details

	Action	Extras	Comment
Preparation for evacuation of core holder			
1	Turn V12 to Reservoir		
2	Turn V11 to Waste		
3	Close V13 B		
4	Close V14 B		
5	Open V13 A		
6	Open V14 A		
7	Turn V15 to Vakuum	Connect syringe to V15	
8	Pump FW towards Reservoir		Produce to reservoir
9	Close V12. and bleed out at P-transmitter		
10	Check V11 to Waste		
11	Turn V12 to V11		
12	Start pump 1		Pump medium: FW
13	Solvent change		
14	Solvent change function stops automatically		Pump 1 is 100% filled with FW, as well as to V11
15	Turn V11 to V12		
16	Turn V15 to V16		
17	Start pump 1		Produce out at V16
18	Open V13 B		
19	Bleed out at V13b		
20	Close V13 B		
21	Bleed out at P-transmitter		
22	Stop pump 1		
23	Turn V15 to Vakuum		
24	Close V13 A + V14 A		
25	Open V14 B		
26	Pump isopropanol in from V15 and out V14b	Injection by syringe	Isopropanol collected in container
27	Disconnect V13b from V13		
28	Dry V13b and V15 (and out) with pressurized air		
29	Connect V14b to core holder outlet		
30	Bleed out and connect sleeve pressure pipe		
31	Connect V13b and coil to core holder inlet		1/16" Coil, labelled PL1
32	Disconnect syringe from V15		
Evacuation of core holder			
1	Connect vakuum pump to V15		
2	Start vakuum pump		Check for vakuum-tight system
3	Evakuate untill good vakuum is acheived		
4	Close V15		
5	Shut-down vacuum pump		
Saturation of core			
1	Close V14 B		
2	Turn V12 to Reservoir		Reservoir placed on weight
3	Open V13 B		
Heating of core			
1	Turn V12 to V11		
2	Disconnect V14b from core holder outlet		
3	Connect V34b to core holder outlet	Core holder placed in angle	
4	Open V34 B and V13A		Check V34 A and V35 open
5	Switch on heating cabinet @ 70°C		Check V34 A and V35 open
6	Start pump 1		Low rate: 1 cc/min while heating
Permeability measurments			
1	Adjust rate of pump 1 according to plan	C-H angle removed before start	Check for leakage, pressure tight system
2	Stop pump 1		
3	Close V12 + V35		Check for leakage, pressure tight system
Oil flooding to Swi			
1	Bleed oil with pump 2 out of transition pipe V23 B - V13		Pump medium: HD Tilje crude oil
2	Connect transition pipe from system 2 till 1		
3	Arrange production container system		
4	Start pump 2		Rates according to plan
5	Stop pump 2		
6	Close V21 + V22		
7	Disconnect transition pipe from system 2 till 1		
FW flooding to Sor			
1	Change production container system		Pump medium: FW
2	Open V12 + V35		
3	Start pump 1		Rates according to plan
4	Stop pump 1		According to plan
5	Close V12, V35		
Chemical injection			
1	Change production container system		
2	Solvent change, turn S1 from A to B.		Pump medium: Chemical solution
3	Solvent change function stops automatically		Pump 1 is 100% filled with chemical solution, as well as to V11
4	Start pump 1		
5	Stop pump 1		Pumpe 1 is stopped when 2PV's of chemical solution is in the pipe
6	Solvent change		Pump medium: FW
7	Solvent change function stops automatically		Pump 1 is 100% filled with FW, as well as to V11
8	Start pump 1		Continues injection with FW displacement
Post flush			
1	Pump 1 is running		Post flush start when 2PV of chemical has been injected into the c
2	Stop pump 1		
3	Close V12		
4	Shut-down heating cabinet		

J VISCOSITIES

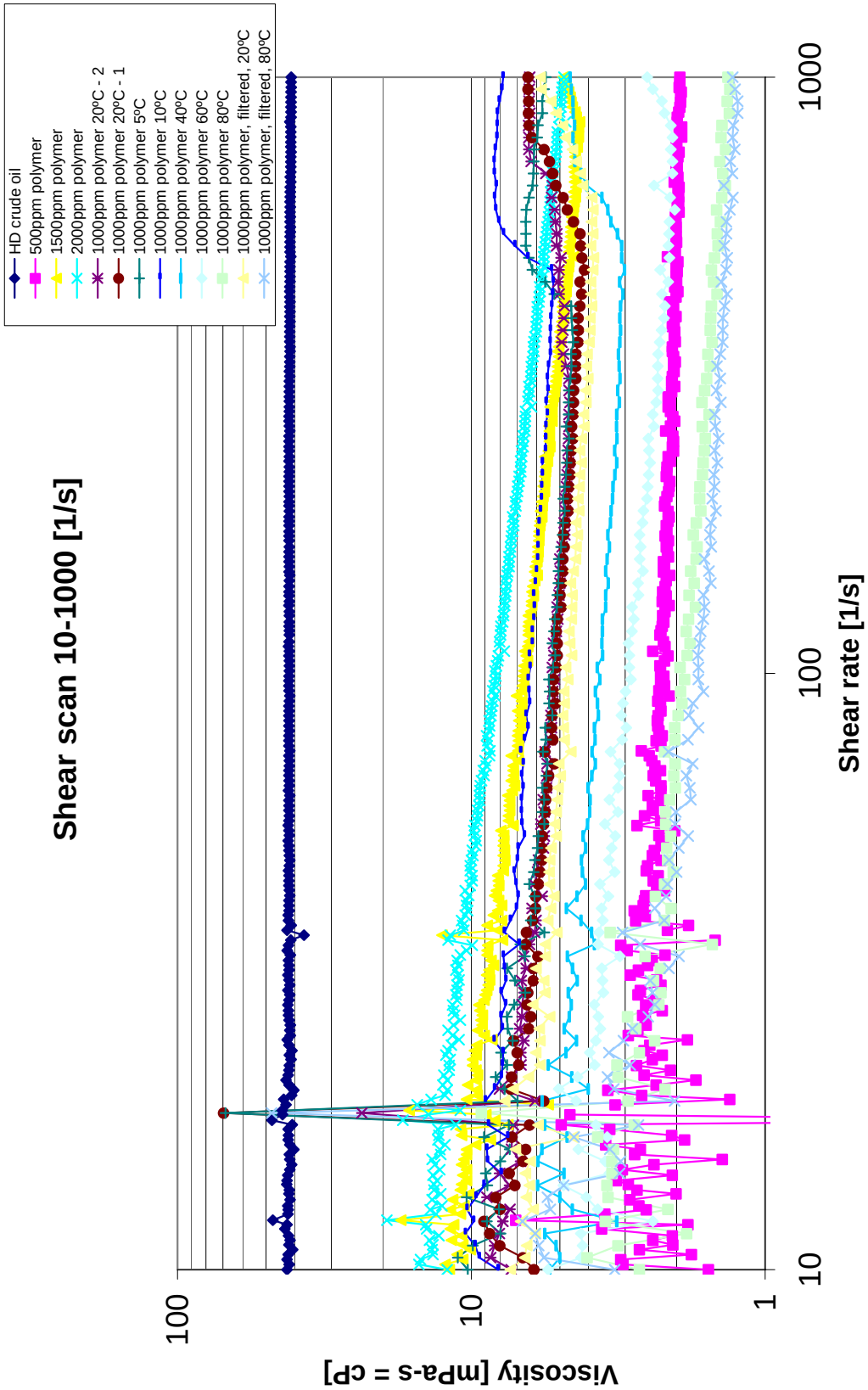

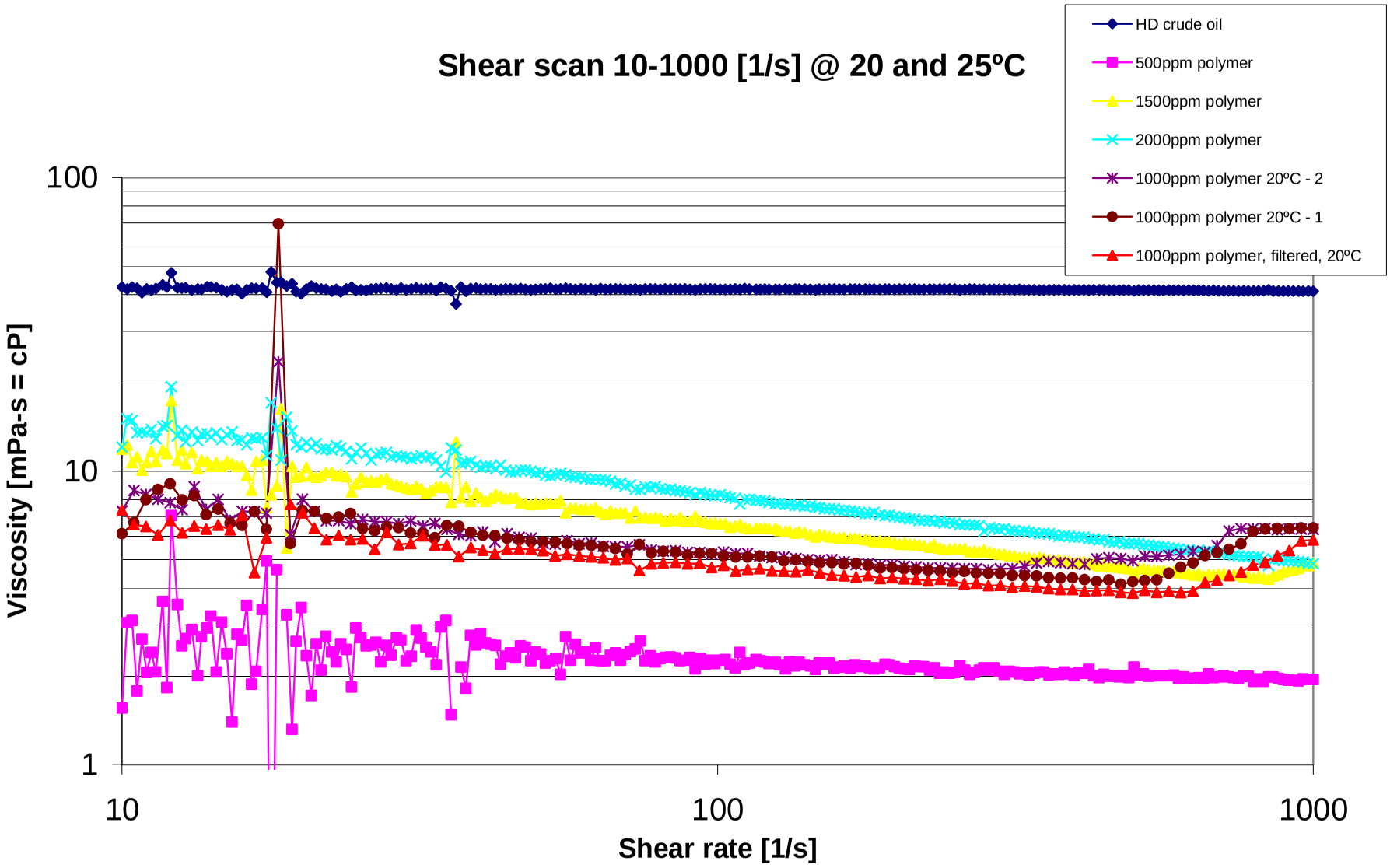
Shear scan 10-1000 [1/s] @ 20 and 25ºC
HD crude oil
500ppm polymer
1500ppm polymer
2000ppm polymer
1000ppm polymer 20ºC - 2
1000ppm polymer 20ºC - 1
1000ppm polymer, filtered, 20ºC
Viscosity [mPa-s = cP]
100
10
1
10
100
1000
Shear rate [1/s]

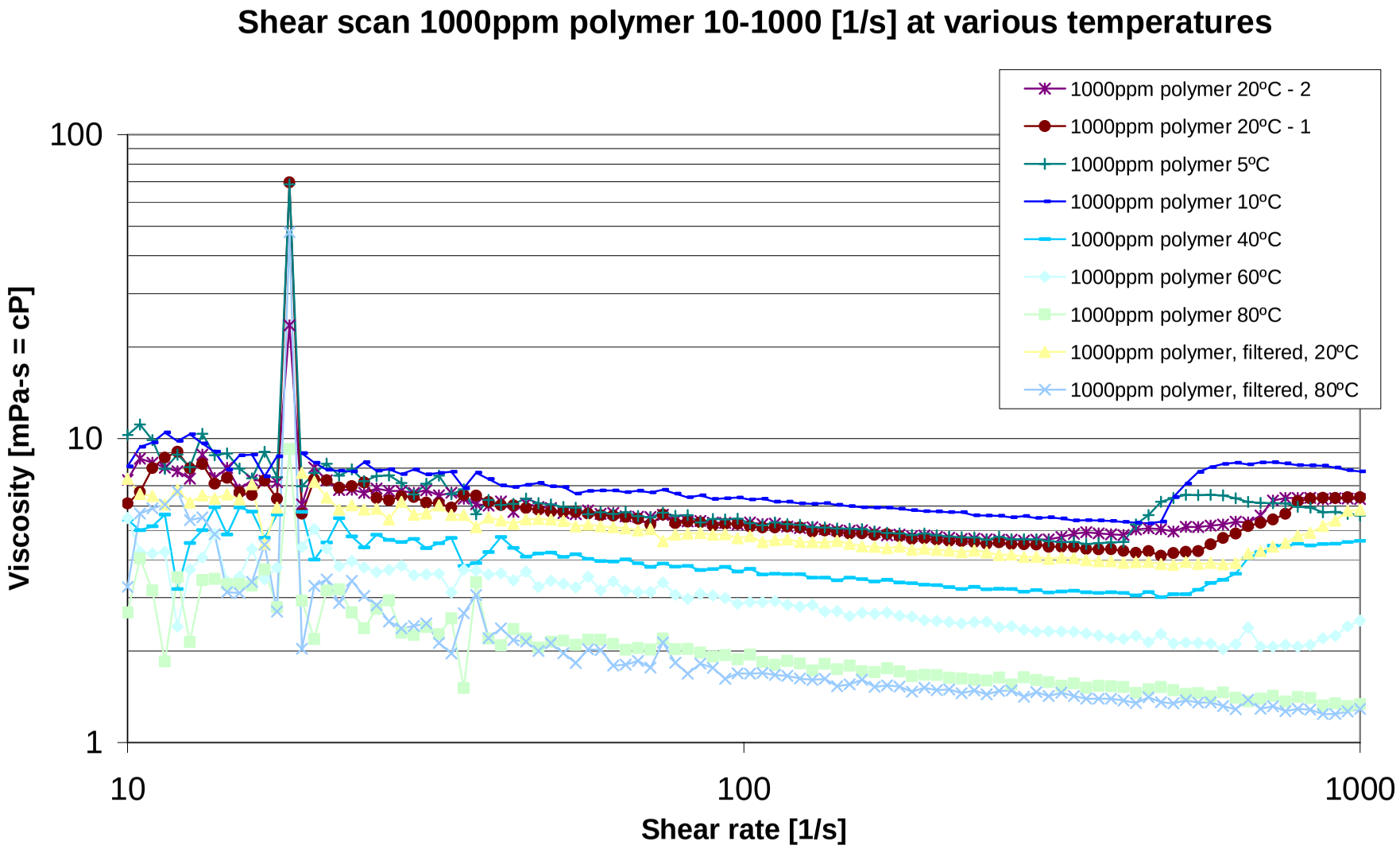
Shear scan 1000ppm polymer 10-1000 [1/s] at various temperatures
1000ppm polymer 20ºC - 2
1000ppm polymer 20ºC - 1
1000ppm polymer 5ºC
1000ppm polymer 10ºC
1000ppm polymer 40ºC
1000ppm polymer 60ºC
1000ppm polymer 80ºC
1000ppm polymer, filtered, 20ºC
1000ppm polymer, filtered, 80ºC
100
10
1
Viscosity [mPa-s = cP]
10
100
1000
Shear rate [1/s]

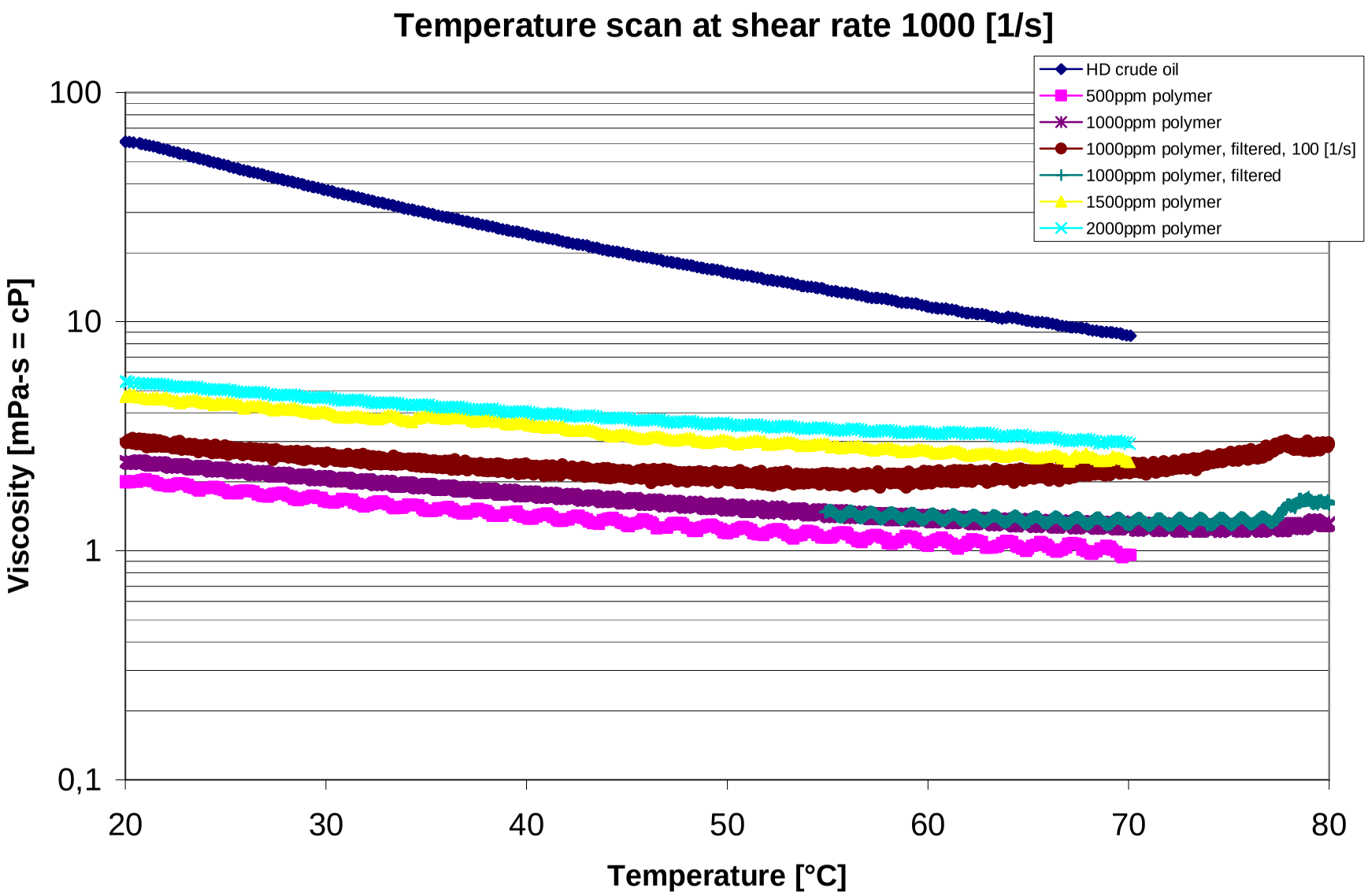
Temperature scan at shear rate 1000 [1/s]
HD crude oil
500ppm polymer
1000ppm polymer
1000ppm polymer, filtered, 100 [1/s]
1000ppm polymer, filtered
1500ppm polymer
2000ppm polymer
Viscosity [mPa-s = cP]
100
10
1
0,1
20
30
40
50
60
70
80
Temperature [°C]

K INTERFACIAL TENSIONS

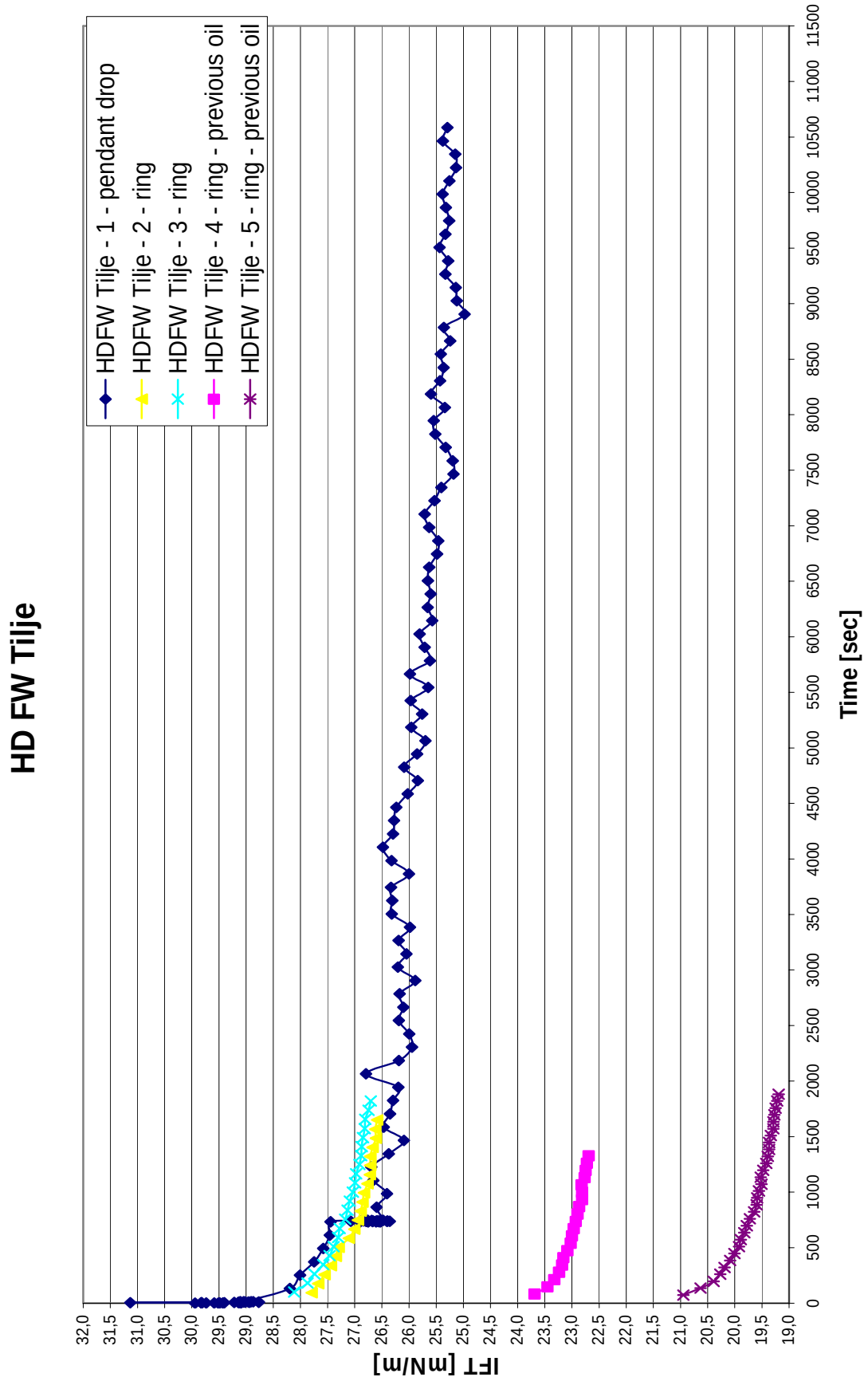

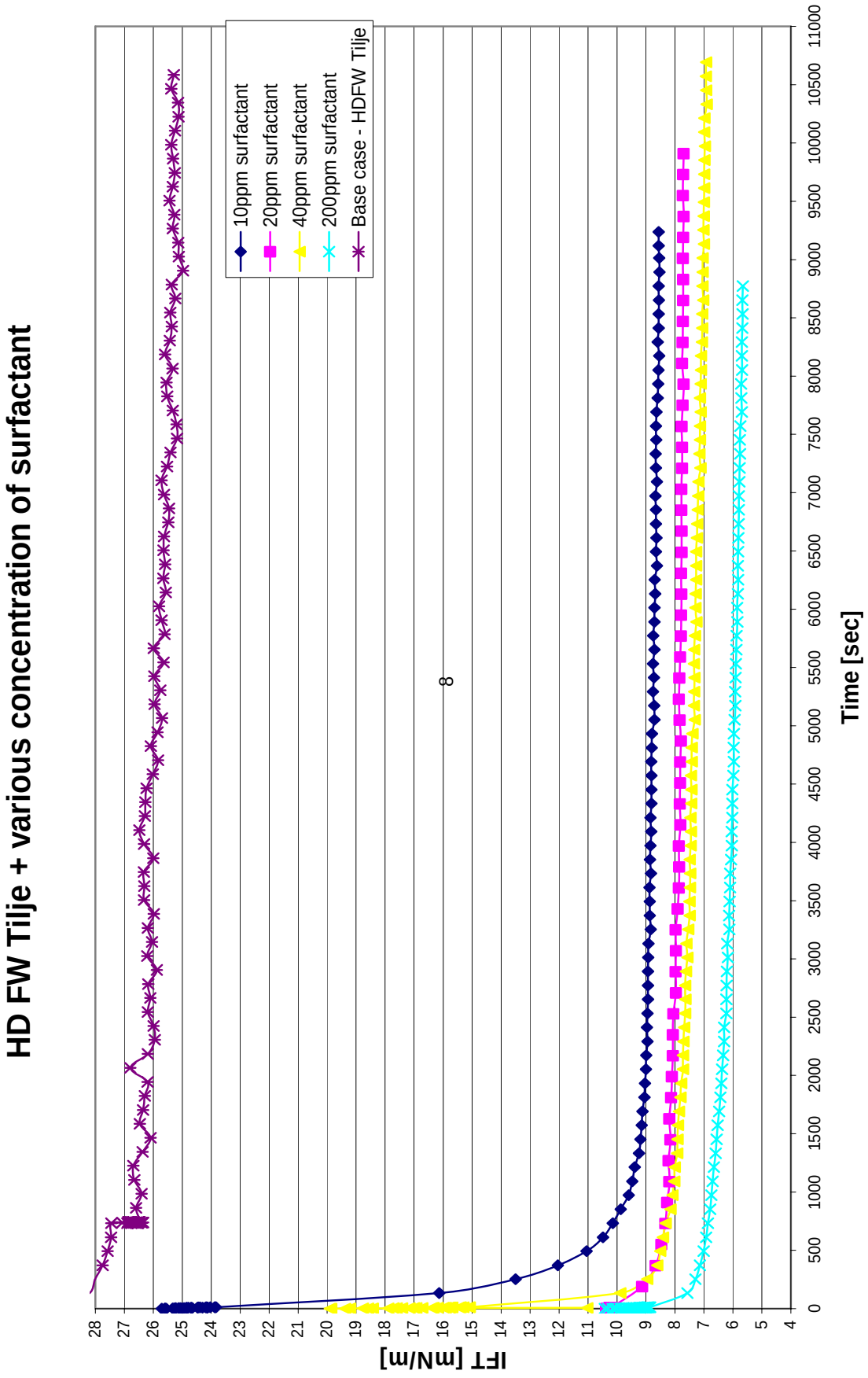
HD FW Tilje + various concentration of surfactant
10ppm surfactant
20ppm surfactant
40ppm surfactant
200ppm surfactant
Base case - HDFW Tilje
IFT [mN/m]
Time [sec]

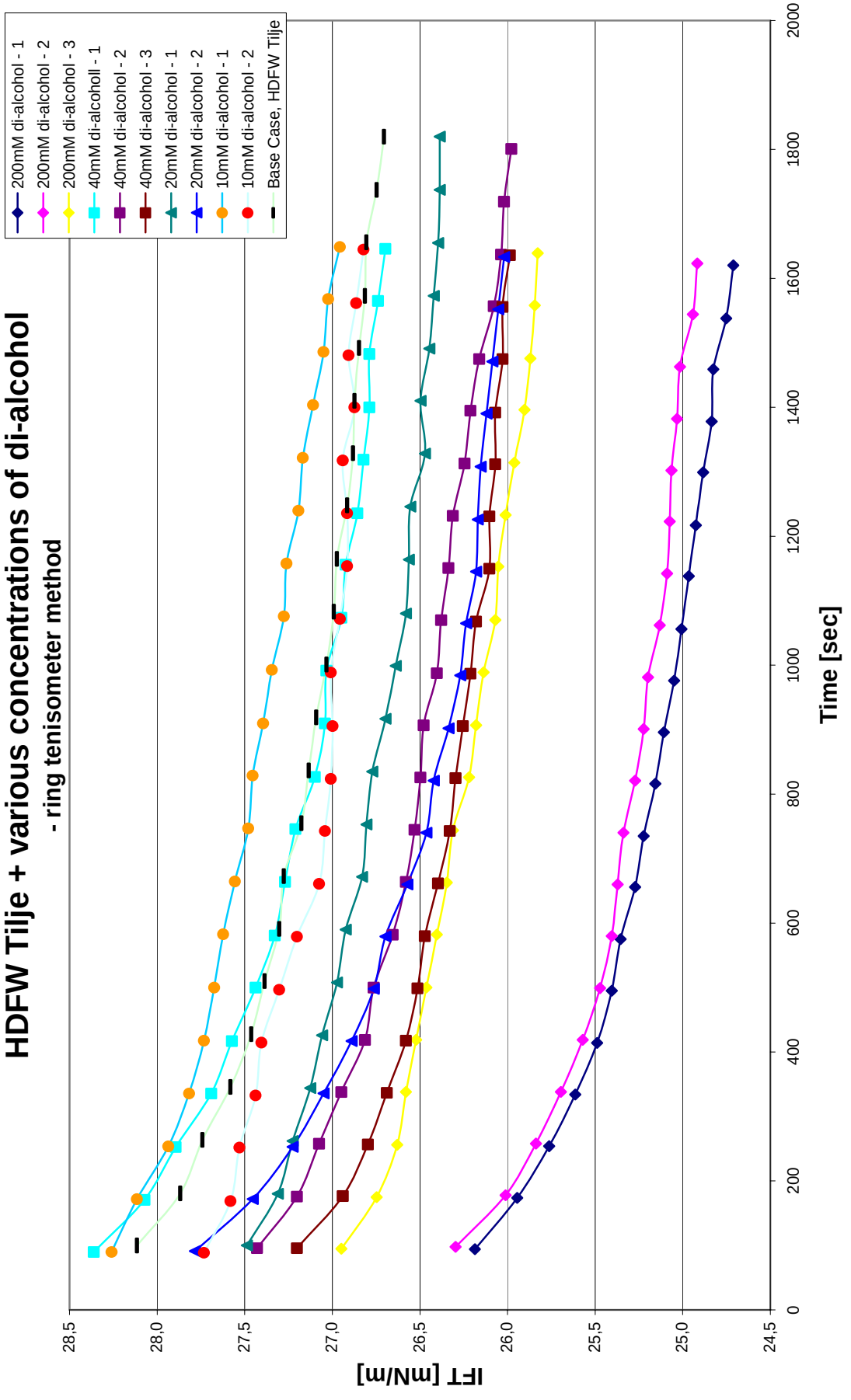
HDFW Tilje + various concentrations of di-alcohol
- ring tenisometer method
200mM di-alcohol - 1
200mM di-alcohol - 2
200mM di-alcohol - 3
40mM di-alcoholl - 1
40mM di-alcohol - 2
40mM di-alcohol - 3
20mM di-alcohol - 1
20mM di-alcohol - 2
10mM di-alcohol - 1
10mM di-alcohol - 2
Base Case, HDFW Tilje
IFT [mN/m]
28,5
28,0
27,5
27,0
26,5
26,0
25,5
25,0
24,5
Time [sec]
0
200
400
600
800
1000
1200
1400
1600
1800
2000

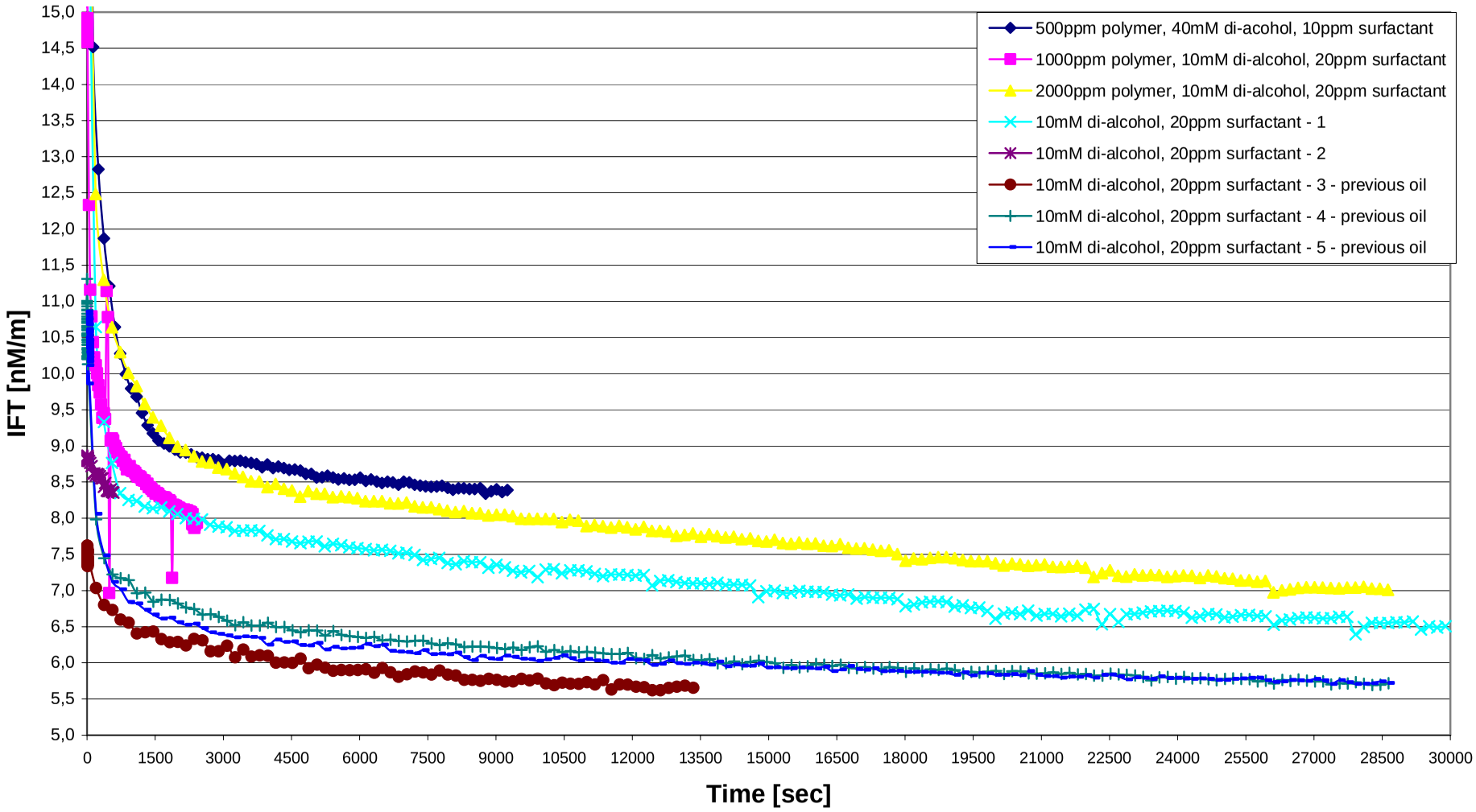
Various concentrations of polymer in HD FW Tilje
with full chemical treatment
IFT [nM/m]
Time [sec]
15,0
14,5
14,0
13,5
13,0
12,5
12,0
11,5
11,0
10,5
10,0
9,5
9,0
8,5
8,0
7,5
7,0
6,5
6,0
5,5
5,0
0
1500
3000
4500
6000
7500
9000
10500
12000
13500
15000
16500
18000
19500
21000
22500
24000
25500
27000
28500
30000
500ppm polymer, 40mM di-acohol, 10ppm surfactant
1000ppm polymer, 10mM di-alcohol, 20ppm surfactant
2000ppm polymer, 10mM di-alcohol, 20ppm surfactant
10mM di-alcohol, 20ppm surfactant - 1
10mM di-alcohol, 20ppm surfactant - 2
10mM di-alcohol, 20ppm surfactant - 3 - previous oil
10mM di-alcohol, 20ppm surfactant - 4 - previous oil
10mM di-alcohol, 20ppm surfactant - 5 - previous oil

HDFW Tilje + 2000ppm polymer with various surfactant and co-surfactant concentrations

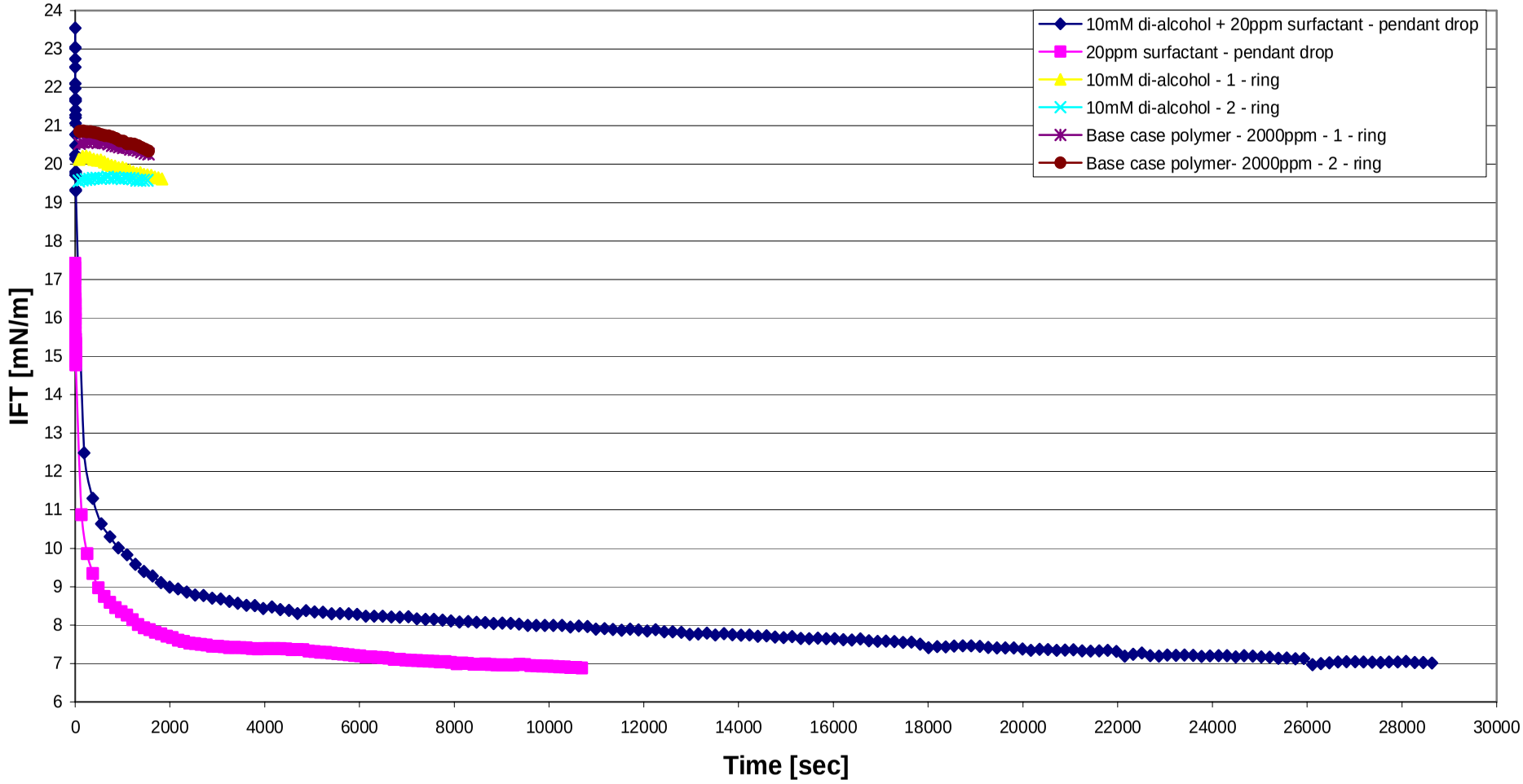

L MOBILITY RATIO

Calculated mobility ratios from two different viscosity measurements.

Mobility ratios	@ 1000 [1/s]		@ 100 [1/s]	
Internal experiment number	**Before**	**After**	**Before**	**After**
	Myo/myd	myo/myd	myo/myd	myo/myd
1	14,8	5,5	14,8	2,9
2	14,8	5,5	14,8	2,9
2*	14,8	5,5	14,8	2,9
3	14,8	5,5	14,8	2,9
4	14,8	5,5	14,8	2,9
5	18,1	6,7	18,1	3,6
6	18,1	3,6	18,1	1,9
7	18,1	3,0	18,1	1,6
8	18,1	3,0	18,1	1,6
9	18,1	3,0	18,1	1,6
10	18,1	3,0	18,1	1,6
11	18,1	9,1	18,1	4,4
12	18,1	6,7	18,1	3,6
M	18,1	-	18,1	-

M COMPATIBILITY TESTS, EMULSION STABILITY OF MAIN TREATMENT SYSTEM

Chemical	Separation time		
	1	2	3
	sec	sec	sec
Destilled water	300 (3,40)	210 (4,70)	210 (4,80)
HDFW Tilje	300 (4,60)	180	60
2000ppm polymer	300	300 (4,30)	
2000ppm polymer + 10mM di-alcohol	300	180 (4,80)	
2000ppm polymer + 20ppm surfactant	300 (4,40)		
2000ppm polymer + 10mM di-alcohol + 20ppm surfactant	300 (3,80)		
1500ppm polymer	300 (4,90)		
1000ppm polymer	120 (5,20)	90	
10mM di-alcohol	90		
10ppm surfactant	80		
20ppm surfactant	80		
10mM di-alcohol + 20ppm surfactant	70	60	

The results are presented as time in seconds it takes to separate the two phases. When a complete separation is not achieved, the volume of free water phase is recorded at the given time when it is stable. This volume is written in parenthesis behind the current time

N CORE PLUG POROSITIES AND MEASURES

Core flood	Plug	Length	Diameter	Cross-section area	Bulk volume	Grain volume	Pore volume	Porosity
		Cm	cm	cm2	cm3	cm3	cm3	%
1	**5**	7,51	3,71	10,78	80,92	62,55	18,38	**22,7**
2	**6**	7,42	3,71	10,79	80,08	61,87	18,21	**22,7**
2*	**2**	7,51	3,71	10,81	81,14	62,96	18,18	**22,4**
3	**7**	7,23	3,70	10,78	77,95	60,38	17,57	**22,5**
4	**8**	7,10	3,71	10,81	76,73	59,66	17,07	**22,3**
5	**B**	7,47	3,77	11,16	83,39	63,70	19,68	**23,6**
6	**C**	7,48	3,77	11,16	83,49	63,87	19,61	**23,5**
7	**D**	7,51	3,77	11,16	83,88	64,10	19,77	**23,6**
8	**G**	7,47	3,77	11,16	83,39	63,46	19,93	**23,9**
9	**F**	7,48	3,77	11,16	83,50	63,72	19,77	**23,7**
10	**J**	7,60	3,77	11,16	84,84	64,56	20,28	**23,9**
M	**E**	7,44	3,77	11,16	83,08	63,66	19,42	**23,4**
11	**I**	7,38	3,77	11,16	82,39	64,33	18,06	**21,9**
12	**A**	7,43	3,77	11,16	82,94	63,35	19,59	**23,6**

O SATURATIONS AND RECOVERIES ACHIEVED AFTER CORE FLOODING AS WATER AND OIL SATURATIONS

Chemical treatment	Internal experiment number	Swi	Movable water	Sor,c	Part of original Sor,w mobilized by chemical
		%	%	%	%
Centre experiment	6	25	32	31	12
Low polymer, low di-alcohol, high surfactant	4	25	37	28	10
Low polymer, low di-alcohol, low surfactant	3	19	35	35	11
Low polymer, high di-alcohol, low surfactant	2*	28	28	30	14
Low polymer, high di-alcohol, high surfactant	1	31	31	24	14
Low polymer, high di-alcohol, high surfactant	2	24	36	30	10
Low polymer, high di-alcohol, high surfactant	5	22	34	34	10
High polymer, low di-alcohol, high surfactant	9	24	30	39	7
High polymer, low di-alcohol, low surfactant	7	25	32	34	9
High polymer, high di-alcohol, low surfactant	8	23	34	32	11
High polymer, high di-alcohol, high surfactant	10	24	38	31	7
500ppm polymer, 40mM di-alcohol, 10ppm surfactant	11	24	32	39	5
1/3 PV: Low polymer, high di-alcohol, high surfactant	12	22	34	40	4

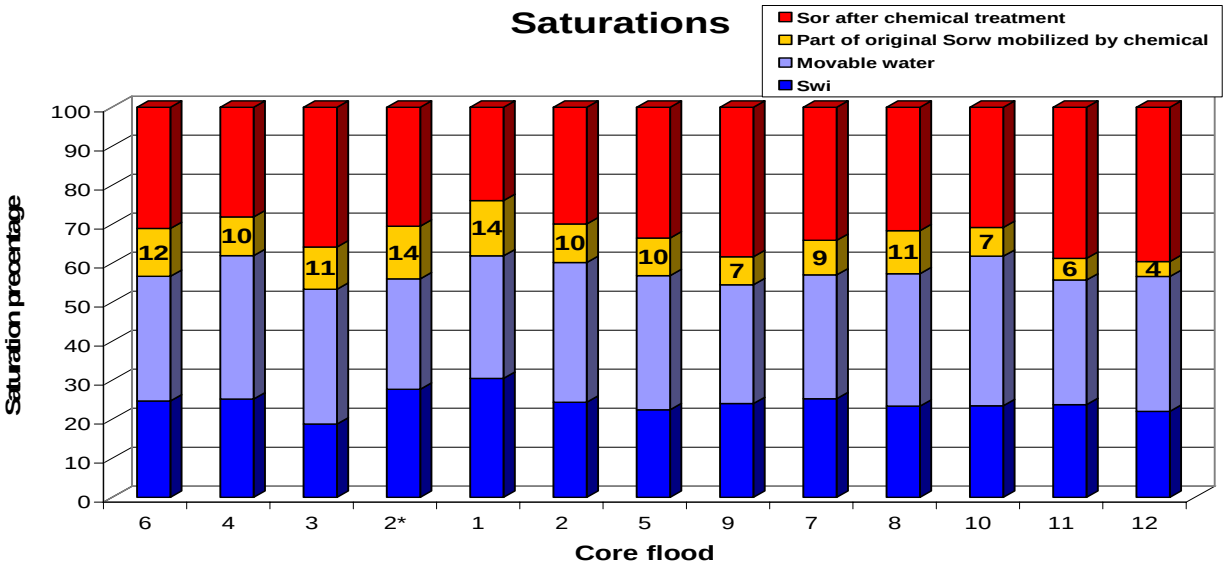

The different core floods are presented in experiment design sequence, but labelled by internal experiment number as seen in the table above.

P CAPILLARY NUMBER

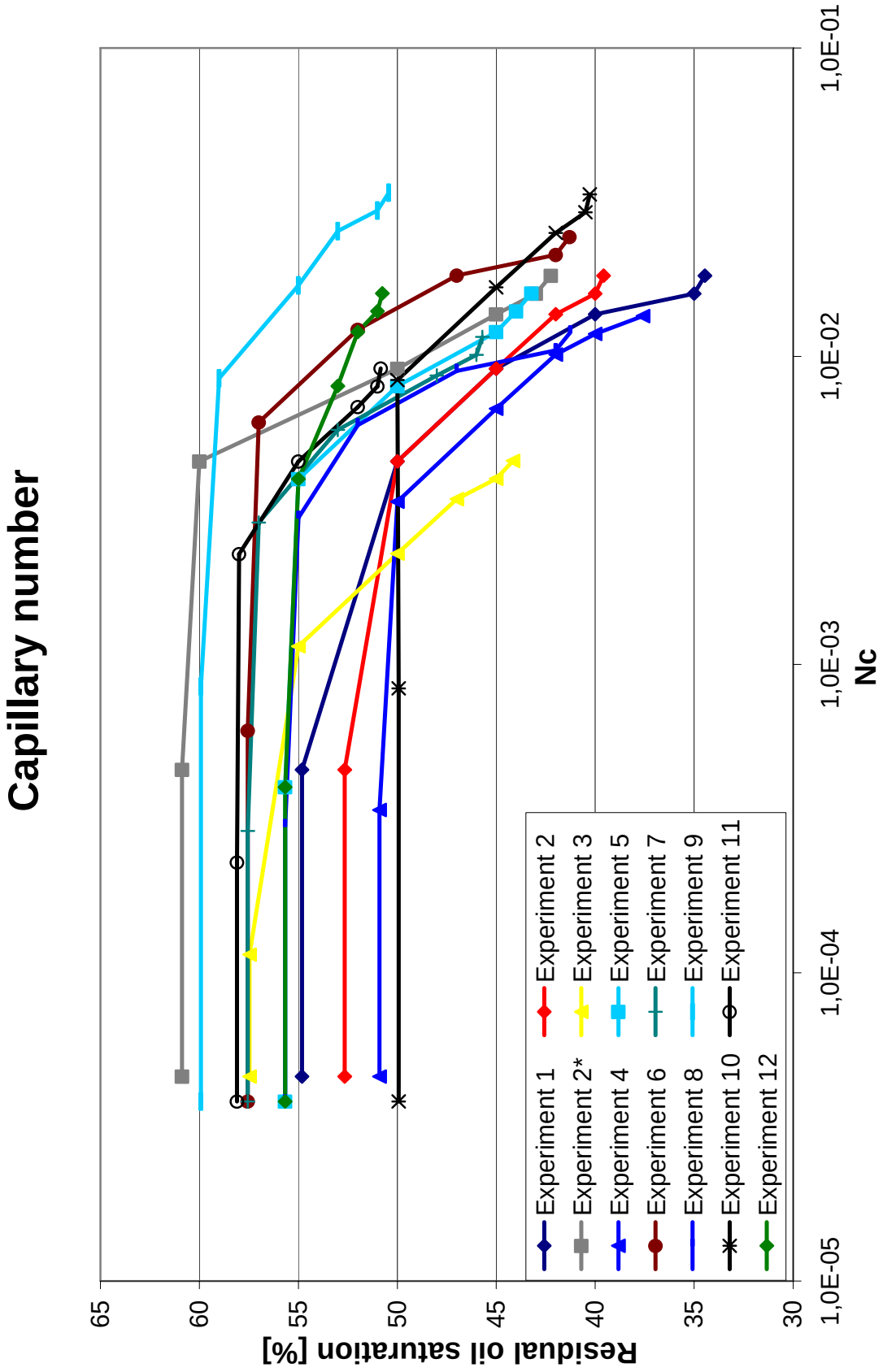

Q PERMEABILITIES

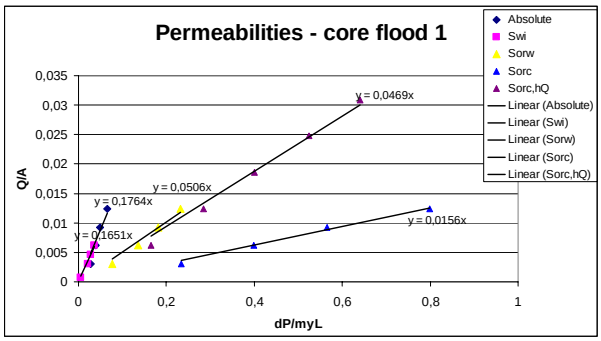

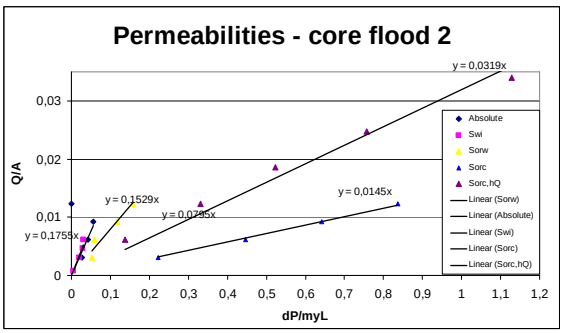

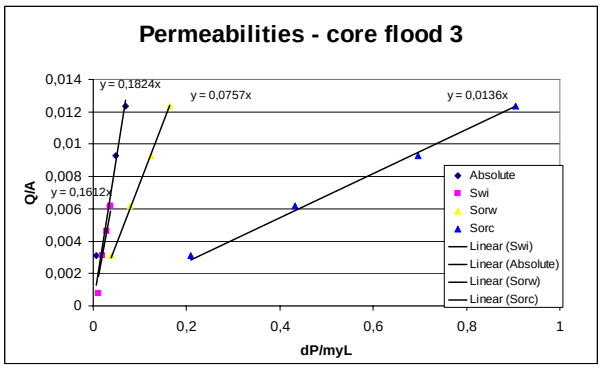

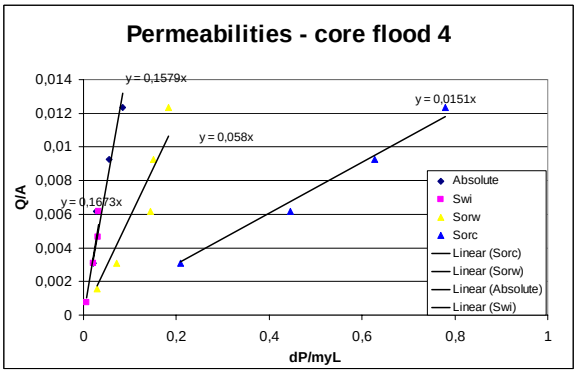

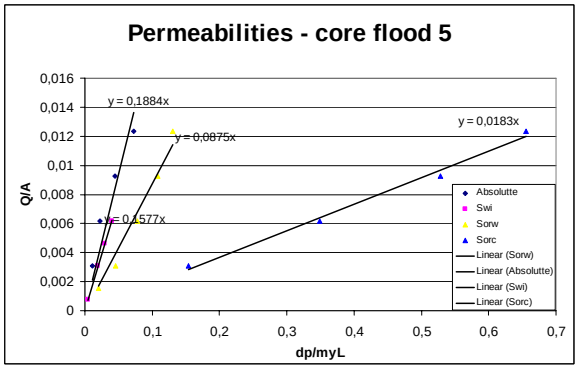

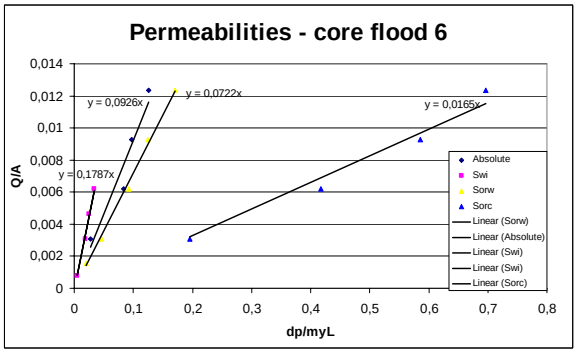

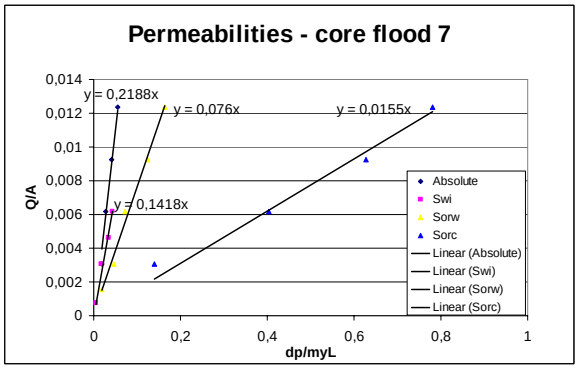

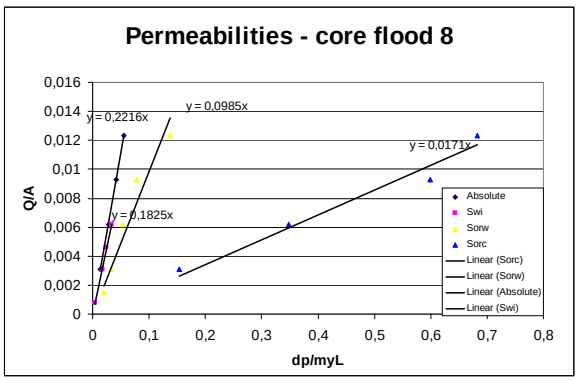

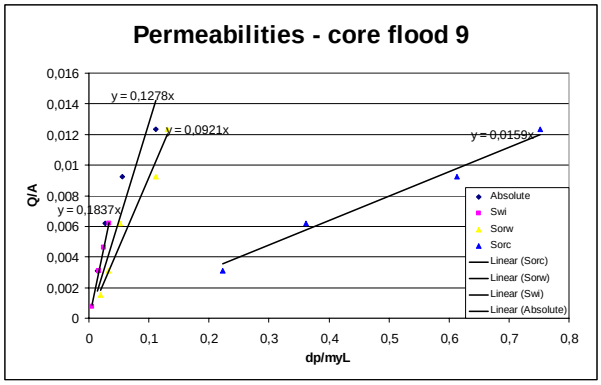
Permeabilities - core flood 9
y = 0,1278x
y = 0,0921x
y = 0,0159x
y = 0,1837x
Q/A
dp/myL
Absolute
Swi
Sorw
Sorc
Linear (Sorc)
Linear (Sorw)
Linear (Swi)
Linear (Absolute)

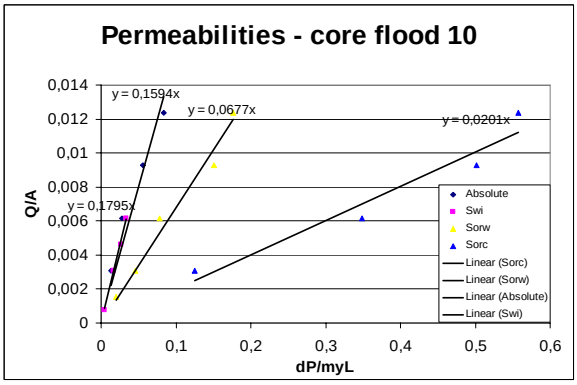
Permeabilities - core flood 10
y = 0,1594x
y = 0,0677x
y = 0,0201x
y = 0,1795x
Q/A
dP/myL
Absolute
Swi
Sorw
Sorc
Linear (Sorc)
Linear (Sorw)
Linear (Absolute)
Linear (Swi)

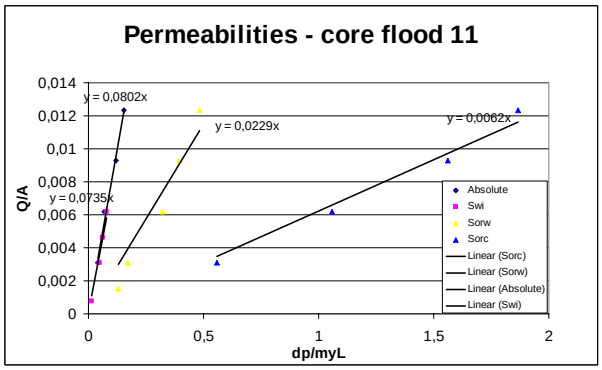
Permeabilities - core flood 11
y = 0,0802x
y = 0,0229x
y = 0,0062x
y = 0,0735x
Q/A
dp/myL
Absolute
Swi
Sorw
Sorc
Linear (Sorc)
Linear (Sorw)
Linear (Absolute)
Linear (Swi)

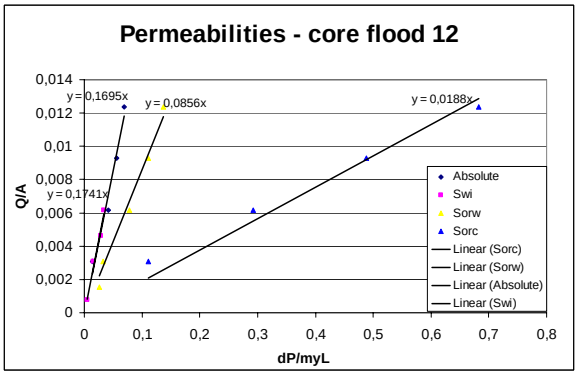
Permeabilities - core flood 12
y = 0,1695x
y = 0,0856x
y = 0,0188x
y = 0,1741x
Q/A
dP/myL
Absolute
Swi
Sorw
Sorc
Linear (Sorc)
Linear (Sorw)
Linear (Absolute)
Linear (Swi)